



Optimizing Radioactive Contamination Screening at Community Reception Centers

Report

December 2023



Science and
Technology





The “Optimizing Radioactive Contamination Screening at Community Reception Centers Report” was prepared by the National Urban Security Technology Laboratory for the Fire Department of the City of New York.

The views and opinions of authors expressed herein do not necessarily reflect those of the U.S. Government.

Reference herein to any specific commercial products, processes, or services by trade name, trademark, manufacturer, or otherwise does not necessarily constitute or imply its endorsement, recommendation, or favoring by the U.S. Government.

The information and statements contained herein shall not be used for the purposes of advertising, nor to imply the endorsement or recommendation of the U.S. Government.

With respect to documentation contained herein, neither the U.S. Government nor any of its employees make any warranty, express or implied, including but not limited to the warranties of merchantability and fitness for a particular purpose. Further, neither the U.S. Government nor any of its employees assume any legal liability or responsibility for the accuracy, completeness, or usefulness of any information, apparatus, product, or process disclosed; nor do they represent that its use would not infringe privately owned rights.

The cover photo and images included herein were provided by the National Urban Security Technology Laboratory.



FOREWORD

The National Urban Security Technology Laboratory (NUSTL) is a federal laboratory organized within the U.S. Department of Homeland Security (DHS) Science and Technology Directorate (S&T). Located in New York City, NUSTL is the only national laboratory focused exclusively on supporting the capabilities of state and local first responders to address the homeland security mission. The laboratory provides first responders with the necessary services, products, and tools to prevent, protect against, mitigate, respond to, and recover from homeland security threats and events.

NUSTL uniquely provides independent technology evaluations and assessments for first responders, thereby enabling informed acquisition and deployment decisions, and helping to ensure that responders have the best technology available to use in homeland security missions.

If there is a radiological release, whether from an accident or from a terrorist act, local response agencies can set up community reception centers (CRCs) to screen the public for radioactive contamination. This “Optimizing Radioactive Contamination Screening at Community Reception Centers Report” was prepared to provide the Fire Department of the City of New York (FDNY) and other emergency response organizations with technical guidance for deploying CRC radiation detection equipment to optimize screening efficiency. The report provides specific recommendations based on the results of NUSTL’s measurements and calculations, including where to position the pedestrian radiation portal monitors used for sensitive whole-body screening and how and where to do prescreening with personal radiation detectors to avoid mistaken alarms and maximize CRC contamination screening throughput. The report includes an introduction to CRCs, describes FDNY’s CRC radiation detection equipment and describes the methods NUSTL used to determine how and where to best use the equipment. Appendices provide full details of NUSTL’s measurements and radiation transport calculations.

Visit the NUSTL website at www.dhs.gov/science-and-technology/national-urban-security-technology-laboratory or contact NUSTL@hq.dhs.gov for more information.



POINT OF CONTACT

National Urban Security Technology Laboratory (NUSTL)
U.S. Department of Homeland Security
Science and Technology Directorate
Office of National Laboratories
201 Varick Street
New York, NY 10014

Email: NUSTL@hq.dhs.gov

Website: www.dhs.gov/science-and-technology/national-urban-security-technology-laboratory

Author:

Paul Goldhagen, Ph.D., NUSTL Physicist

Gladys Klemic, M.S., NUSTL Physicist, managed, designed, and analyzed the first stage of this project.

Norman Chiu, NUSTL Electronics Engineer, was the principal inventor of the remote audible alarm accessory.

The following current and former NUSTL employees and student interns¹ participated in performing measurements for this study and analyzing the measurement data:

Andy Chen, former NUSTL Operations Research Analyst

Shmuel Link, Ph.D., former NUSTL Engineer

Lance Schaefer, former student intern

Carl Schopfer, Ph.D., NUSTL Radiation Safety Officer

Grant Schumock, former student intern

ACKNOWLEDGEMENTS

We thank Timothy Rice, Battalion Chief, FDNY HazMat Operations, and Richard Schlueck, Battalion Chief, FDNY HazMat Battalion (retired), for requesting this work and for many valuable discussions. We also extend our thanks to Dr. Armin Ansari, Lauren Finklea, and Dr. Adela Salame-Alfie of the U.S. Centers for Disease Control and Prevention for valuable discussions. We thank Patrick Brand of Ludlum Measurements, Inc. for supplying custom firmware for the Ludlum Model 52-1-1 radiation portal monitor and for explaining the portal monitor's alarm algorithm. We especially thank Grant Schumock, now a Ph.D. student at the Johns Hopkins Bloomberg School of Public Health, for the Monte Carlo computer code simulating the portal monitor's alarm algorithm.

¹ Through the DHS S&T Office of University Programs Oak Ridge Institute for Science and Education summer internship program, <https://orise.orau.gov/dhseducation>.



EXECUTIVE SUMMARY

Following a radiological release, whether from an accident or a terrorist act, local response agencies can set up community reception centers (CRCs) to screen the public for radioactive contamination. This “Optimizing Radioactive Contamination Screening at Community Reception Centers Report” documents research by the National Urban Security Technology Laboratory (NUSTL) to provide technical advice to the Fire Department of the City of New York (FDNY) for deploying CRC radiation detection equipment following detonation of a radiological dispersal device (RDD). The report includes specific recommendations for positioning and using CRC equipment, and many of the recommendations are applicable to responding to radiological incidents other than an RDD. While the work was performed at the request of FDNY, this report may also be useful to those in other agencies who are planning CRCs.

The main goal of CRCs is to avoid hospitals being overwhelmed by providing a means to reassure tens or hundreds of thousands of people who are not contaminated while finding the relatively few people who will require decontamination and treatment. Because of the large number of people who will need to be screened, it is important to screen them rapidly.

New York City has the equipment and capability to set up several high-throughput CRCs around the city. They would be set up outside the affected area in buildings with a large open space, such as a school with a gymnasium. CRCs will employ personal radiation detectors (PRDs), pedestrian radiation portal monitors (portal monitors, portals), and handheld detectors with pancake Geiger-Mueller probes (pancake-probe detectors) to do prescreening, sensitive whole-body screening, and follow-up screening to locate contamination on people. The FDNY Hazardous Materials (HazMat) Battalion would set up and use the equipment. The U.S. Centers for Disease Control and Prevention (CDC) provides extensive guidance for setting up CRCs but does not address the placement of multiple portal monitors or their proximity to prescreening. Recommendations in this report are intended to supplement, not supersede, CDC guidance.

The leadership of the FDNY HazMat Battalion initially asked NUSTL two questions:

- How far apart should the portal monitors be?
- If radioactive contamination on someone causes a portal monitor to alarm, will handheld screening with a pancake-probe detector be able to find the contamination on the person?

While working to answer the first of these questions, NUSTL determined that the optimal portal spacing and throughput depend critically on prescreening effectiveness in order to avoid *misattributed alarms*—alarms while an uncontaminated person is being screened that are actually caused by radioactivity on someone else. Misattributed alarms could cause confusion and delays, reduce throughput, and undermine public confidence. FDNY then asked NUSTL to evaluate their methods for prescreening, and the lab developed improved prescreening methods and determined optimal locations for prescreening stations. This report documents the results of NUSTL’s investigation of these issues and the methods used to determine those results.

NUSTL was asked to optimize CRC screening with the equipment that FDNY already has. We made measurements and calculations for those instruments; we did not compare that equipment to other brands or models. Even so, many of the results and recommendations in this report may apply to CRCs using different instruments.



The distances to and between prescreening stations that are sufficient to avoid misattributed alarms depend on the amount of radioactivity on the most contaminated people arriving at a CRC, which depends on the activity released by the radiological event. Based on the activity used for National Planning Scenario 11 and in the source that caused a major contamination event in Goiania, Brazil, NUSTL chose an explosive RDD made with 2000 curies (Ci) (74 Terabecquerels) of the radionuclide cesium-137 (Cs-137) as our design-case event. Based on work by others, we estimated the maximum amount of contamination that could be on people who were close to the explosion, but not physically injured, so they could leave the site of the incident on their own and later go to a CRC. We determined prescreening locations that would avoid a disruptive number of misattributed alarms from these highly contaminated people and maintain high CRC throughput. We also considered other threat radionuclides and misattributed alarms from radioactivity in nuclear medicine patients.

To determine the spacing between portal monitors and the prescreening methods and locations required to avoid misattributed alarms, NUSTL made measurements of the sensitivity of FDNY's instruments and performed calculations of the distances from a given amount of Cs-137 and other radionuclides that would cause the instruments to alarm.

The key findings documented in this report are:

- Portal monitors are most sensitive to external radiation from their sides. Consequently, the most important distance between the portal monitors to avoid misattributed portal alarms is the distance between the portal approach lanes.
- With two stages of prescreening using methods we developed, the approach lanes can be 15 feet (4.6 m) apart without having to send people sequentially to non-adjacent portals. This distance depends only on prescreening effectiveness, not on the RDD activity. It applies for clearance around even a single portal.
- First-stage prescreening should be done outside the CRC building 80 feet (24 m) to 250 feet (76 m) from the portal monitors, depending on shielding provided by building materials.
- Second-stage prescreening should be done at least 35 feet from the nearest portal, independent of the activity released in the incident.
- To reduce misattributed prescreening alarms, first-stage prescreening should be done at least 80 feet (24 m) away from the unscreened crowd waiting to enter the CRC.
- The decontamination area for people who trigger prescreening alarms should be as far from the portals as the first-stage prescreening station and at least 80 feet from prescreening stations.
- Misattributed alarms could still occur. Procedures to deal with them are described.
- No changes to the recommended CRC layout or screening procedures would be necessary for an RDD made with gamma- or beta-emitting radionuclides other than Cs-137.
- If external contamination on someone causes a portal monitor alarm, follow-up screening with a pancake-probe detector would be able to find the contamination if the radionuclide emits energetic beta or alpha particles; it might not for radionuclides that emit only gamma and x rays.
- Communication should be maintained between the screening stations.
- Some medical patients who were given therapeutic doses of radioactive materials shortly before the radiological release incident may emit as much radiation as RDD victims. Radionuclide identification devices should be provided at the CRCs to recognize nuclear medicine patients.



TABLE OF CONTENTS

- 1.0 Introduction..... 11
- 2.0 Scope and Applicability 14
 - 2.1 Research Assumptions 14
 - 2.2 FDNY CRC Radiation Detection Equipment..... 15
 - 2.2.1 Personal Radiation Detectors 15
 - 2.2.2 Radiation Portal Monitor..... 17
 - 2.2.3 Pancake-Probe Detector..... 18
 - 2.3 Research Tasks 19
- 3.0 Measurements..... 21
 - 3.1 Measurements of Portal Monitor External Sensitivity and Angular Dependence 22
 - 3.1.1 Angular Dependence of Portal Sensitivity 24
 - 3.1.2 External Source Activity That Could Cause a Misattributed Alarm 24
 - 3.2 Portal Monitor Walk-Beside Tests 26
 - 3.2.1 Walk-beside Tests with Single Cs-137 Sources 26
 - 3.2.2 Walk-beside Tests with Other Radionuclides 27
 - 3.2.3 Walk-beside Tests with Distributed Sources..... 29
 - 3.3 Prescreening Tests 30
 - 3.3.1 First-stage Prescreening..... 31
 - 3.3.2 Second-stage Prescreening..... 32
 - 3.3.3 Prescreening Other Radionuclides 35
 - 3.3.4 Detecting Contamination on Shoes 35
 - 3.4 PRD Sensitivity Measurements 37
 - 3.5 Pancake-Probe Detector Sensitivity Measurements..... 38
- 4.0 Calculations 42
 - 4.1 Distance from Prescreening Stations to Portal Monitors 43
 - 4.1.1 Simulation of Walk-beside Tests..... 43
 - 4.1.2 Distance from First-stage Prescreening to Portal Monitors 44
 - 4.1.3 Distance from Second-Stage Prescreening to Portal Monitors..... 49
 - 4.2 Distances to Avoid Misattributed Prescreening Alarms..... 50
 - 4.2.1 Simulation of PRD Sensitivity Measurements..... 50
 - 4.2.2 Distances to First-stage Prescreening 51
- 5.0 Findings and Recommendations..... 54
 - 5.1 Portal Monitor Spacing..... 54



| | |
|--|----|
| 5.2 Portal Monitor Positioning..... | 55 |
| 5.3 Whole-body Screening Procedures | 56 |
| 5.4 Handheld Screening..... | 57 |
| 5.5 Prescreening Methods | 58 |
| 5.5.1 First-stage Prescreening Method | 59 |
| 5.5.2 Second-stage Prescreening Methods | 60 |
| 5.5.3 Detecting Contamination on Shoes | 61 |
| 5.6 Waiting and Prescreening Locations..... | 62 |
| 5.6.1 Waiting Line | 62 |
| 5.6.2 Prescreening Stations..... | 63 |
| 5.6.3 Distance from Prescreening Stations to Portal Monitors | 63 |
| 5.6.4 Distance to First-stage Prescreening and Between Prescreening Stations..... | 64 |
| 5.6.5 Decontamination Areas | 64 |
| 5.6.6 Diagrams of Prescreening Locations | 64 |
| 5.6.7 Adjustments to prescreening distances | 67 |
| 5.7 Prescreening Flow Control and Communication Between Screening Stations..... | 67 |
| 5.8 Nuclear Medicine Patients..... | 68 |
| 5.9 Radionuclides Other Than Cesium-137 | 68 |
| 6.0 Summary | 69 |
| 7.0 References..... | 70 |
| Appendix A. Detailed Description of Measurements of Portal External Sensitivity | 73 |
| A.1 Materials and Methods | 73 |
| A.2 Analysis and Results..... | 75 |
| A.2.1 Angular Dependence of Portal Sensitivity | 75 |
| A.2.2 External Source Activity That Could Cause a Misattributed Alarm..... | 76 |
| Appendix B. Remote Audible Alarm Accessory..... | 79 |
| Appendix C. Detailed Description of Radiation Transport and Associated Calculations..... | 81 |
| C.1 Distance from Prescreening Stations to Portal Monitors | 82 |
| C.1.1 Simulation of Walk-beside Tests..... | 83 |
| C.1.2 Distance from First-Stage Prescreening Station to Portal Monitors..... | 86 |
| C.1.3 Distance from Second-Stage Prescreening to Portal Monitors..... | 93 |
| C.2 Distance Between Prescreening Stations..... | 93 |
| C.2.1 Simulation of PRD Sensitivity Measurements..... | 93 |
| C.2.2 Distances to First-stage Prescreening | 95 |



| | |
|--|-----|
| C.2.3 Distance Between First-Stage and Second-Stage Prescreening | 98 |
| C.3 Example of MCNP Input | 99 |
| Appendix D. Attaching PRDs to Handles for Second-Stage Prescreening..... | 107 |

LIST OF FIGURES

| | |
|--|----|
| Figure 1-1 Whole-body screening area of a CRC set up for an exercise | 12 |
| Figure 2-1 Thermo Scientific RadEye PRD-ER..... | 16 |
| Figure 2-2 Model 52-1-1 radiation portal monitor | 17 |
| Figure 2-3 Ludlum 26-2 integrated GM pancake detector | 19 |
| Figure 3-1 Setup for measurements of portal external sensitivity and angular dependence | 23 |
| Figure 3-2 Source positions around the portal | 23 |
| Figure 3-3 Angular dependence of portal monitor count-rate sensitivity to Cs-137 | 24 |
| Figure 3-4 Activity of an external Cs-137 source that could cause a misattributed alarm..... | 25 |
| Figure 3-5 Portal monitor walk-beside tests | 27 |
| Figure 3-6 First-stage prescreening with S-shaped path..... | 31 |
| Figure 3-7 Using multiple sources to simulate distributed contamination..... | 33 |
| Figure 3-8 Second-stage prescreening by two screeners using PRDs on long handles | 33 |
| Figure 3-9 Prescreening test with four stationary PRDs..... | 34 |
| Figure 3-10 Prescreening shoes with a PRD under a ramp..... | 36 |
| Figure 3-11 Setup for PRD sensitivity measurements | 37 |
| Figure 3-12 Pancake-probe detector sensitivity measurement..... | 39 |
| Figure 4-1 Distances calculated in order to avoid misattributed alarms..... | 42 |
| Figure 4-2 MCNP model of the walk-beside tests..... | 43 |
| Figure 4-3 Portal monitor counting efficiency vs. energy deposited in a scintillator..... | 44 |
| Figure 4-4 MCNP model of CRC building and person with radioactivity outside | 46 |
| Figure 4-5 Probability for a portal monitor to alarm vs. net count rate in the highest-rate detector ... | 47 |
| Figure 4-6 MCNP model of PRD-ER sensitivity measurements | 50 |
| Figure 4-7 MCNP model of PRD-ER | 50 |
| Figure 4-8 PRD-ER counting efficiency vs. energy deposited in its scintillator | 51 |
| Figure 4-9 MCNP model for calculating distance to first-stage prescreening | 52 |
| Figure 4-10 Details of MCNP model for calculating distance to first-stage prescreening..... | 52 |
| Figure 5-1 Recommended layout of portal monitors in the space of a high-school basketball court .. | 55 |
| Figure 5-2 First-stage prescreening with S-shaped path..... | 59 |



| | |
|---|-----|
| Figure 5-3 Second-stage prescreening by two screeners using PRDs on long handles | 60 |
| Figure 5-4 Distances calculated in order to avoid misattributed alarms..... | 63 |
| Figure 5-5 Distances between screening stations for a CRC in a building with brick walls..... | 65 |
| Figure 5-6 Locations of screening stations on city streets for a CRC in a brick building..... | 65 |
| Figure 5-7 Distances between screening stations for a CRC in a warehouse-like building..... | 66 |
| Figure 5-8 Locations of screening stations on city streets for a CRC in a warehouse-like building..... | 66 |
| Figure 5-9 Distances between screening stations for a CRC on open ground | 67 |
| Figure 7-1 Setup for measurements of portal external sensitivity and angular dependence | 73 |
| Figure 7-2 Source positions around the portal | 74 |
| Figure 7-3 Angular dependence of portal monitor net count rate for Cs-137 | 75 |
| Figure 7-4 Angular dependence of portal monitor net count rate for Am-241..... | 75 |
| Figure 7-5 Activity of an external source that could cause a misattributed alarm..... | 77 |
| Figure 7-6 Prescreening a person standing on the ramped platform | 79 |
| Figure 7-7 Assembled remote alarm accessory box (left) and an opened box (right)..... | 79 |
| Figure 7-8 Remote audible alarm accessory circuit diagram and parts list | 80 |
| Figure 7-9 Distances calculated in order to avoid misattributed alarms..... | 81 |
| Figure 7-10 MCNP model of the walk-beside tests | 83 |
| Figure 7-11 Portal monitor counting efficiency vs. energy deposited in a scintillator | 85 |
| Figure 7-12 MCNP model of CRC building and person with radioactivity outside..... | 87 |
| Figure 7-13 Probability for a portal monitor to alarm vs. net count rate in highest-rate detector | 91 |
| Figure 7-14 MCNP model of PRD-ER sensitivity measurements..... | 93 |
| Figure 7-15 MCNP model of PRD-ER..... | 94 |
| Figure 7-16 PRD-ER counting efficiency vs. energy deposited in its scintillator | 94 |
| Figure 7-17 MCNP model for calculating distance to first-stage prescreening..... | 96 |
| Figure 7-18 Details of MCNP model for calculating distance to first-stage prescreening..... | 96 |
| Figure 7-19 Modified commercial adapter used to attach a PRD to a handle with Acme thread..... | 107 |
| Figure 7-20 Holster method for mounting a PRD on a handle | 108 |

LIST OF TABLES

| | |
|---|----|
| Table 3-1 Photon Emission Energies and Probabilities for Radionuclides Considered in This Work... | 28 |
| Table 4-1 First-stage Prescreening Distance from Portals to Avoid Misattributed Portal Alarms | 48 |
| Table 7-1 First-stage Prescreening Distance from Portals and Portal Alarm Probabilities..... | 92 |
| Table 7-2 Effect of Scattering Material on Calculated PRD Count Rate and Alarm Distance | 98 |



1.0 INTRODUCTION

If there is a radiological release, whether from an accident or from a terrorist radiological dispersal device (RDD, “dirty bomb”), after the initial response to the incident, local response agencies would need to screen the public for radioactive contamination. To do that, New York City (NYC) has developed plans for setting up Community Reception Centers (CRCs) at multiple locations in the city. CRCs would be set up outside the affected area in buildings with a large room or open space, such as a school with a gymnasium or an empty warehouse, or could be set up outdoors in a stadium, field, or parking lot. In NYC, most prospective CRC locations are high schools. The main goal of the CRCs is to avoid hospitals being overwhelmed by providing a means to reassure tens or hundreds of thousands of people who are not contaminated while finding the relatively few people who are and decontaminating and treating them. Because of the large number of people who will need to be screened, it is important to screen them efficiently—rapidly as well as effectively.

CRCs would employ personal radiation detectors (PRDs), pedestrian radiation portal monitors (portal monitors, portals), and handheld detectors with pancake Geiger-Mueller (GM) probes (pancake-probe detectors) to conduct prescreening, sensitive whole-body screening, and follow-up handheld screening to locate contamination on people.

The U.S. Centers for Disease Control and Prevention (CDC) provides extensive guidance for CRCs in its *Population Monitoring in Radiation Emergencies: A Guide for State and Local Public Health Planners* (April 2014), including flow diagrams of sequential stations with various decision points to indicate appropriate measures to address individuals’ varying needs [\[1\]](#). Additional CRC planning tools and resources for setting up and operating CRCs are available on the CDC website [\[2\]](#). Current guidance, however, does not address the placement of multiple portal monitors and their proximity to prescreening stations. Recommendations in this report are intended to supplement, not supersede, CDC guidance.

In NYC, the Hazardous Materials (HazMat) Battalion of the Fire Department of the City of New York (FDNY) would set up and use the radiation detection equipment. The NYC Department of Health and Mental Hygiene, FDNY Emergency Medical Services, and other agencies would perform other CRC functions such as registering people, first aid, crowd control, etc. The leadership of the FDNY HazMat Battalion asked the National Urban Security Technology Laboratory (NUSTL) for technical advice on spacing and positioning the portal monitors to maximize CRC throughput for response to an RDD incident. They also asked whether the pancake-probe detectors would find the minimum amount of contamination that the portals can detect. When NUSTL determined that the optimal portal spacing depends critically on prescreening effectiveness, FDNY asked the lab to evaluate their methods for prescreening, and NUSTL developed and tested improved prescreening methods. This “Optimizing Radioactive Contamination Screening at Community Reception Centers Report” documents NUSTL’s investigation of these issues, including the methods used as well as the results obtained, and makes recommendations based on our findings.

While the work was performed at the request of FDNY, this report is written to also be useful to agencies planning CRCs in other jurisdictions.

Quantities herein are generally given in U.S. units, with the equivalent in international units following in parentheses.



This report assumes the reader is familiar with the basic concepts of radioactivity, radiation, and radiation detection. Those less familiar with the terms, quantities, and units used in the report may want to refer to the CDC's online Radiation Dictionary, [3] which includes a glossary of radiological terms and a primer on radiation measurement.

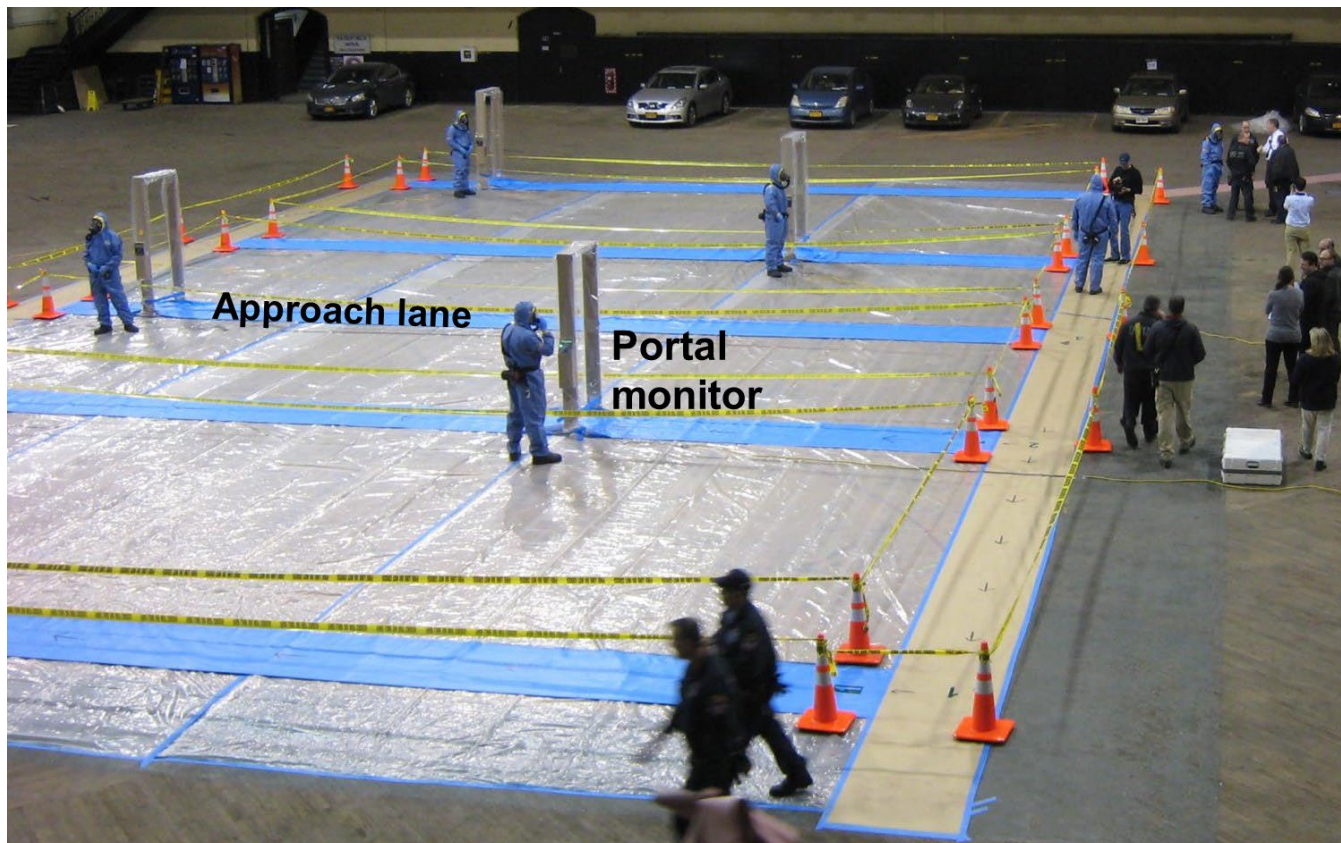


Figure 1-1 Whole-body screening area of a CRC set up for an exercise

[Figure 1-1](#) shows the whole-body screening area of a CRC set up for an exercise by the FDNY in 2015. The portal monitor area is set up in the space of a basketball court and the floor there is covered with plastic sheeting to keep the floor from becoming contaminated. The paths that people walk on to go to the portal monitors, the “approach lanes,” are covered with nonslip material on top of the plastic. People being screened for radioactivity are sent one at a time to walk through one of several portal monitors, which have sensitive radiation detectors in their uprights. If a person has radioactivity on them, the portal alarms: the operator sees a light on the readout panel and may hear an (optional) alarm sound. The portal monitors are spread apart so that radioactivity on a person being screened in one of them is less likely to cause an alarm in a nearby portal, however in this exercise the spacing of the portals and approach lanes was not optimized. It was through this exercise that the need for the research described in this report was identified and the work initiated.

Optimizing contamination screening in a CRC is driven by the need to maximize throughput while avoiding *misattributed alarms*: alarms while an uncontaminated person is being screened that are caused by radioactivity on someone else. Misattributed alarms could cause confusion and delays and undermine public confidence. They can happen because the instruments are sensitive to radiation from all directions and the amounts of radioactivity on some RDD victims could potentially be thousands of times higher than the very small amounts of radioactivity that the instruments can



detect. Some medical patients treated with radioactive material can emit similar levels of radiation. Such individuals could cause many portals to alarm simultaneously from up to hundreds of feet away. They may also cause the background rates in multiple portals to increase, falsely indicating radioactive contamination of the CRC facility. Misattributed portal alarms were first recognized as a problem for CRCs by Kramer et al. in 2006. [4] In a follow-on study, they proposed prescreening as a solution and examined prescreening effectiveness using several different instruments and methods. [5] Much of NUSTL's work is built on their approach.

There are two types of misattributed alarms that responders may encounter—misattributed portal-monitor alarms and misattributed prescreening alarms. To avoid misattributed portal-monitor alarms and elevated background rates, the portals have to be spaced apart and prescreening to divert highly contaminated people must be done at some distance outside the CRC portal room using instruments such as PRDs, which are less sensitive than the portal monitors. Even the PRDs are sensitive enough for misattributed prescreening alarms to occur unless prescreening is done at a considerable distance from the crowd of unscreened people waiting to enter the CRC.

Optimum contamination screening throughput requires maximizing the number of portal monitors in the CRC and minimizing the screening time at each station and the walking time between radioactivity screening stations as well as avoiding misattributed alarms. These goals -generally conflict with each other, so optimum throughput requires trade-offs. For maximum throughput, screening locations need to be separated by distances sufficiently large to avoid a disruptive number of misattributed alarms, but otherwise as close together as possible to minimize walking time between them, to fit more portal monitors into the CRC, and to keep the perimeter of the whole CRC area to a manageable size. Finding the optimum distances between screening stations was a major goal of this work.



2.0 SCOPE AND APPLICABILITY

FDNY asked NUSTL about CRC contamination screening specifically for response to an outdoor explosive RDD. An RDD would be smaller in scale than other major radiological dispersal emergencies such as a release from a damaged nuclear power plant or a nuclear detonation. The amount of radioactivity in an RDD is limited to the activity contained in available and feasibly transportable radionuclide sources, and the radioactive material would be mostly concentrated in a relatively small area—a small part of a city rather than a whole region. These RDD characteristics mean that the vast majority of the population of a city will not be measurably contaminated with radioactivity, while a few people who were close to the explosion will be highly contaminated. An incident involving a ruptured radioactive source or other radioactive spill without an explosion can be similar in these ways to an explosive RDD, and the work in this report may be applicable to CRCs set up in response to such incidents.

In light of the above characteristics of an RDD incident and the FDNY's responsibility for planning contamination screening in CRCs, FDNY brought two questions to NUSTL:

- For response to an RDD, how far apart should CRC portal monitors be spaced?
- If contamination on a person causes a portal to alarm during whole-body screening, will handheld screening with a pancake-probe detector be able to find the contamination on the person?

Answering the first of these questions turned out to be more complicated than expected and led to needing to answer additional questions.

When NUSTL determined that the optimal portal spacing depends critically on prescreening effectiveness, FDNY asked us to evaluate their methods for prescreening. Based on their methods and feedback, we developed and tested improved prescreening methods including a method to prescreen shoes. Much of the work described in this report relates to prescreening—where it should be done as well as how.

Some of the findings and recommendations in this report, including methods for prescreening and the distance between portal approach lanes, should be generally applicable to other types of radiological incidents. In particular, the recommended distance between portal approach lanes depends only on prescreening sensitivity, not on the amount of radioactivity released in the event. Other recommendations, such as where prescreening should be done, do depend on the amount of radioactivity released.

2.1 RESEARCH ASSUMPTIONS

NUSTL's work was performed assuming that CRCs are set up in response to an RDD containing a large amount of a radionuclide that emits energetic gamma rays, x rays, and/or beta particles.² We also assumed that a very large number of people, potentially hundreds of thousands in NYC, might come to the CRCs and that only a small percentage of those people are contaminated.

Most of the work was done for an RDD made with 2000 curies (Ci) (74 Terabecquerels (TBq)) of the radionuclide cesium-137 (Cs-137). This is our design-case event. An activity of 2000 Ci is close to

² If the radionuclide emits only alpha particles (e.g., polonium-210), portal monitors and PRDs would not be effective. In that case, a CRC would employ only handheld screening using thin-window GM detectors.



the activity used for National Planning Scenario 11 [6] and is 1½ times the activity of the Cs-137 radiotherapy source that caused a major contamination event in Goiania, Brazil in 1987. [7]

To guide our research, we needed to estimate the maximum amount of radioactivity on people who might come to a CRC after our design-case RDD incident. We estimated the activity on the most-contaminated ambulatory RDD victims from information in a paper by Smith, Ansari, and Harper. [8] Based on test explosions, they determined the range of contamination on victims injured by an explosive RDD with a “maximum credible” amount of radioactivity (10^3 TBq) and various amounts of explosive. They considered three different radionuclides that are available in high activity sources. Among them, Cs-137 was the worst case for contaminating uninjured people in the vicinity of the explosion because it is in the highly dispersible form of cesium chloride.

We assume that by the time the CRCs are operational, a majority of the most contaminated people would comply with public announcements advising them to change clothing and shower before going to CRCs and that those actions would remove 90% of their contamination. [9] We consider these people our design-case victims and determined the prescreening locations to minimize misattributed alarms from the contamination on them and still maintain high CRC throughput. In addition to our design-case, we also consider two other threat radionuclides from Smith, Ansari, and Harper, cobalt-60 (Co-60) and strontium-90 (Sr-90) to see if a CRC that works for our design case would work for an RDD made with these other radionuclides. [8] In addition, we consider radionuclides emitting lower energy gamma rays, and misattributed alarms from nuclear medicine patients.

NUSTL was asked to optimize CRC screening with the equipment that FDNY already owns. Measurements and calculations were done with and for those instruments. With one exception, we did not compare that equipment to other brands or models. Even so, many of the results and recommendations in this report may apply to CRCs using different instruments if those instruments have similar specifications to the models used by FDNY.

2.2 FDNY CRC RADIATION DETECTION EQUIPMENT

This section describing the radiation detection equipment to be used in NYC CRCs provides context for the measurements and calculations NUSTL performed. It may also be useful for other jurisdictions planning CRCs that would use different equipment, helping them judge whether the results of NUSTL’s study applies to their CRCs.

Full details of NUSTL’s measurements of portal monitor external sensitivity and radiation transport calculations are provided in appendices to aid radiation subject matter experts in other agencies in performing similar measurements and calculations for instruments significantly different than those used by FDNY.

FDNY has Thermo Scientific RadEye PRD-ER PRDs for prescreening, Ludlum M52-1-1 portal monitors for whole-body screening, and Ludlum 26-2 GM “Integrated Frisker” pancake-probe detectors for hand-held screening.

2.2.1 PERSONAL RADIATION DETECTORS

PRDs are pocket-sized alarming instruments with user-readable displays that are usually worn on the body and used to detect radioactive materials that emit gamma rays and to indicate the gamma radiation exposure rate. Because PRDs are small, lightweight, relatively inexpensive, and simple to use, they have become the most commonly deployed instrument used to detect and interdict the



illicit movement of radioactive material. Although they are less sensitive than larger instruments, PRDs can detect and alarm when radiation increases to just a few times higher than background. These properties make them a suitable choice as the instrument for prescreening at CRCs.

The PRD that would be used by FDNY for prescreening is the RadEye PRD-ER from Thermo Scientific. [10] Photographs of the front and back of the PRD-ER are shown in Figure 2-1. The “ER” refers to “extended range.” The RadEye PRD-ER can read exposure rates up to 10 roentgens per hour (10 R/h)—higher than many other PRDs—making it suitable for response as well as interdiction missions.³ Except for the extended range, the RadEye PRD-ER is essentially identical to the RadEye PRD, which is widely used for detection and interdiction missions.

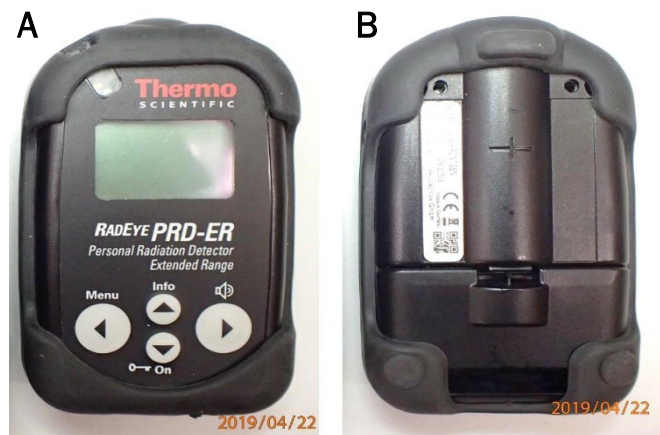


Figure 2-1 Thermo Scientific RadEye PRD-ER
A—Display side B—Detector side

Each instrument measures 4.1 x 2.6 x 1.6 inches (10.4 x 6.7 x 4.1 cm) in its protective rubber sleeve. It is worn using a holster with a belt loop or clip. It is powered by two rechargeable or alkaline AAA batteries and weighs 0.40 pounds (182 g) with batteries and protective sleeve. There is a 2.5 mm miniature audio jack at the bottom of the PRD-ER to send the audio alarm signal to external earphones.

The RadEye PRD-ER uses a sodium iodide (NaI) detector with gamma sensitivity of 1.5 counts per second per microrentgen per hour (cps/(μ R/h)) for Cs-137. Its claimed gamma-ray energy response is 60 kilo electron-Volts (keV) to 1.3 mega electron-Volts (MeV) for dose and dose rate measurement and down to 30 keV for count rate and detection. The time to alarm is typically 1 second. Although the display is usually set to show exposure rate, the detection alarm of the device is based on count rate, not on exposure rate. The PRD-ER incorporates Thermo Scientific’s patented natural background rejection technology that uses measurement of the gamma-ray energy distribution to try to distinguish between naturally occurring radioactive material and radiation from man-made sources. This feature allows the RadEye PRD-ER to have a lower count-rate alarm threshold for “artificial” radiation than for the total count rate.

Alarm thresholds and many other settings can be set by a supervisor using a computer, and some settings, including turning the audible alarm off or on, can be set by the user in the menus of the device. FDNY uses the same alarm threshold settings as the New York City Police Department does for the PRDs it uses for detecting nuclear and radioactive threats as part of the DHS Securing the Cities program.⁴

The one exception to NUSTL’s considering only the instruments FDNY already owns was our brief consideration of the potential impact of using the successor model to the PRD-ER, the RadEye PRD-ER4. [11] The PRD-ER4 has a cesium iodide detector instead of a sodium iodide detector, giving it a

³ Extended range capability is not required for the pre-screening described in this report.

⁴ For more information, contact NUSTL@hq.dhs.gov.



25% higher sensitivity for medium- and high-energy gamma rays. The impact on CRC design is minor, as discussed in [4.2.2](#), at the end of the section on calculations.

2.2.2 RADIATION PORTAL MONITOR

The portable pedestrian radiation portal monitor used by FDNY for whole-body screening in CRCs is the Ludlum Measurements Model 52-1-1. [\[12\]](#) The portal contains four plastic scintillation detectors—two in each vertical panel. Signals from the detectors are counted in an electronics module that is mounted on one vertical panel. A microprocessor uses the count rates in each scintillator to determine whether to trigger a radiation detection alarm. Status indicator lights and a liquid crystal display (LCD) showing the count rates are located on top of the electronics module. An RS-232 port on the bottom of the electronics module allows the instrument to be connected to a printer or computer to record the activity of the instrument. A photograph of the Model 52-1-1 portal monitor is shown in [Figure 2-2](#).

The Model 52-1-1 is designed to be assembled quickly without tools and similarly disassembled for transportation and storage. The portal weighs 70 pounds (32 kg); combined with its wheeled carry case, it weighs 100 pounds (45 kg). The inside dimensions are 32 inches (0.81 m) wide by 81 inches (2.06 m) high. It operates on AC power, external 12 V DC supply, or D-cell batteries – either three or six, user’s choice. Typical battery life using three fresh alkaline batteries 28 hours; using six, 69 hours. FDNY operates the portals using AC power.



Figure 2-2 Model 52-1-1 radiation portal monitor

The portal monitor system may be used in either walk-through or stop-and-count mode. New York City CRC plans would use it in walk-through mode. An occupancy sensor is activated when a person enters the portal and blocks an infrared beam. The microprocessor continually samples the count rate in each detector every 0.2 seconds (0.2 s). In the walk-through mode, the system checks the radiation level every 0.2 s while the portal is occupied, plus 0.2 to 0.4 s before and 0.8 s after occupancy. An alarm occurs when the count rate during this time exceeds the current background rate by a preset factor multiplied by the standard deviation of the background. The standard deviation, sigma, is assumed to be equal to the square root of the number of background counts during a measurement interval. Alarms are indicated by a red LED and an optional audible indicator. Additional LEDs indicate which of the four scintillation detectors alarmed.

During parameter setup, the user can specify one of three options for how the count rates in the four detectors are used to determine whether there is an alarm. If the “individual alarm” option is selected, a high reading on any single detector will cause an alarm. In the “summed alarm” setting, a high reading from the sum of the upper pair or lower pair of detectors triggers the alarm. The third option is “both,” which means either the individual or paired count rates can trigger an alarm. FDNY uses the “both” option.

Other setup parameters that determine the alarm response of the portal include the sigma multiplier (NYC value = factory default value = 4.5), the background averaging time (144 seconds), and the number of 0.2 s measurement samples grouped together for walk-through mode (2 samples = 0.4 s). With those parameter values, when a person walks through the portal, the alarm algorithm



typically makes six overlapping 0.4-second measurements over 1.4 s. In each of those six measurements, if the net counts (measured minus background) in any detector (or the upper or lower pair of detectors) exceeds 4.5 times the square root of the expected background counts in 0.4 s, the portal alarms. The expected background count rate is determined from no-occupancy measurements averaged during the previous 144 seconds.

According to the product's technical manual [\[12\]](#), in walk-through mode with the above default settings the Model 52-1-1 can detect a 1.0 microcurie (μCi) (37 kBq) Cs-137 source in a 10 microrentgen per hour ($\mu\text{R/h}$) background field. This meets the Federal Emergency Management Agency (FEMA) contamination monitoring standard for a portal monitor used for radiological emergency response by state and local governments in response to commercial nuclear power plant accidents, FEMA-REP-21. [\[13\]](#)

Two other parameter settings are worth noting: low-background and high-background warning alarm thresholds. These are the number of counts per 0.2-second interval that the background should not fall below or above in normal operation. The factory default settings, which are used by FDNY, are 20 and 2000, respectively. With these settings, the low-background alarm occurs at about 1/10 of the typical normal background rate of roughly 1000 cps and indicates that a detector has failed or is not connected. The high-background alarm would occur at about 10 times the normal background rate. If either of these alarms happens, the portal cannot be used until the condition is corrected.

Several features of the Ludlum portal monitor Model 52-1-1 differentiate it from some other portable pedestrian radiation portal monitors for use in a CRC: the occupancy sensor, separate alarms for each of the four detectors, openings on the inside faces of the aluminum support structure surrounding the detectors, lack of shielding on the outside of the detectors, and lack of a detector in the base plate of the portal. The occupancy sensor allows the portal to be effectively off when unoccupied, greatly reducing the time when the portal might alarm from radioactivity on people not going through it. The separate alarms for each of the detectors allow the portal to indicate which quadrant of a person's body the radioactivity is on, reducing the time needed for follow-up handheld screening and decontamination. The openings on the inside faces of the portal allow beta-particle radiation through, so the portal can detect radionuclides such as Sr-90 that emit only beta particles. The lack of external lead shielding allows the portal monitor to be relatively lightweight, making it easier and faster to set up, but also making it somewhat more sensitive to gamma radiation from outside the portal. The lack of a radiation detector in the base plate means these portals are not very effective in detecting contamination on people's shoes.

2.2.3 PANCAKE-PROBE DETECTOR

When radioactive contamination is detected on someone during whole-body screening, that person would be sent for follow-up handheld screening to locate where on their body the contamination is, so it can be removed. FDNY uses Ludlum Model 26-2 GM integrated pancake-probe detectors for handheld screening. [\[14\]](#) Traditionally, GM probes have been connected by a cable to a separate, relatively bulky, instrument containing the electronics and display. Modern electronics, however, are so compact that the battery, electronics, and display can be integrated into a GM pancake probe without noticeably increasing its size.

The Ludlum Model 26-2 is such an integrated instrument, and it can be operated with one hand. It weighs 1.0 pound (0.45 kg) including two AA batteries. Battery life is approximately 250 hours. The



detector active area is 2.4 in² (15.5 cm²). The pancake-shaped GM detector itself is essentially identical to the one in the widely used Ludlum M44-9 pancake probe, [15] and the detection efficiencies for all types of radiation are the same for the two instruments.

The 26-2 can be set to read either cps or counts per minute (cpm) on the LCD display. FDNY uses cpm. The range of the instrument is 0.1 cps to 1.99 kcps or 1 cpm to 99.9 kcpm. Above the display are four LEDs, a green LED for “OK” and three red LEDs for three levels of alarm. It has a continuous-tone audible alarm as well. The count rate alarm levels can be set by an authorized user. FDNY sets the first alarm level at 1000 cpm (1.0 kcpm). A photograph of the 26-2 with the first level alarm activated is shown in [Figure 2-3](#).



Figure 2-3 Ludlum 26-2 integrated GM pancake detector

2.3 RESEARCH TASKS

The research tasks NUSTL performed to answer FDNY’s questions and follow-up requests are listed below. The tasks consisted primarily of measurements and calculations. They are listed below in the order of their methodological descriptions in sections [3.0](#) and [4.0](#) of this report. All these tasks except measuring the sensitivity of the pancake-probe detector were essential to answering the first question and related follow-up questions.

- Measure the sensitivity and its angular dependence of the Ludlum Model 52-1-1 portal monitors to external gamma radiation from Cs-137 and other radionuclides.
- Measure the amount of radioactivity on a person that causes an alarm when they walk past an occupied portal at a known distance.
- Determine the minimum separation of the portal monitor approach lanes that will avoid misattributed portal alarms (assuming appropriate prescreening).
- Develop and test methods for prescreening people with PRDs, measuring how small an activity of Cs-137 and other radionuclides can be detected using the RadEye PRD-ER and how quickly.
- Develop and test a method for detecting radioactive contamination on people’s shoes before they enter the CRC building without requiring people to remove their shoes.
- Measure the count-rate sensitivity of the RadEye PRD-ER to gamma radiation from Cs-137 and other radionuclides to enable calculations of minimum distances from prescreening stations required to avoid misattributed PRD alarms and to determine if the distances required for Cs-137 would be sufficient for releases of other radionuclides.
- Measure the sensitivity of the pancake-probe detector used by FDNY for follow-up handheld screening.
- Estimate the maximum amount of radioactive contamination expected to be on someone who is not seriously injured by the explosion of our design-case RDD and could come to a CRC.
- Calculate how far outside different types of CRC buildings initial prescreening should be done to avoid misattributed portal alarms.



- Calculate the minimum distance from people waiting to be prescreened to first-stage prescreening and the distance between prescreening stations required to avoid misattributed PRD alarms during prescreening.
- Determine the optimal positioning of the portal monitors in the space of a high-school basketball court.
- Report other observations and findings related to screening for radioactive contamination at CRCs.



3.0 MEASUREMENTS

NUSTL made numerous measurements of the response of each of the three types of FDNY CRC radiation detection instruments to radiation sources under various circumstances appropriate for radioactive contamination screening at CRCs. The measurements are described in this section and [Appendix A](#). Operational parameters that we could not determine by measurement, such as how far from the CRC building the prescreening needs to be done, were determined by performing detailed radiation transport calculations. The calculations are described in section [4.0](#) and [Appendix C](#).

All tests and measurements involving radioactive sources were performed by personnel trained to work with radioactive materials safely. Procedures were designed to minimize the radiation dose to the people involved and were reviewed and approved by NUSTL's Radiation Safety Officer to ensure radiation doses to personnel would be as low as reasonably achievable and far below regulatory limits.

To determine the minimum distance between portal monitors that will avoid misattributed alarms, the first step was to measure the count rate sensitivity of the portals to radiation from external sources and the angular dependence of the sensitivity. Those measurements and their results are briefly described below in section [3.1](#). A full description of the portal sensitivity measurements and analysis is given in [Appendix A](#).

The angular dependence measurements showed that the maximum sensitivity is directly to the side of the portals. That position is also where people approaching or leaving a portal pass closest to any adjacent portals. So, the situation most likely to cause a misattributed portal alarm is when someone with radioactive contamination passes by the side of a portal monitor while an uncontaminated person is being screened in that portal. Consequently, to avoid misattributed alarms, the most important spacing to consider for portal monitors is the distance between adjacent portal approach lanes. In a CRC with a single portal monitor, the same distance would apply for keeping people away from the portal while they are waiting to be screened.

Our initial portal count-rate sensitivity measurements were conducted using stationary radioactive sources to determine a baseline of approximate activity levels and positions that could potentially cause misattributed portal alarms. For more realistic measurements, we subsequently performed iterative "walk-beside" tests: one of us walked through the portal to trigger the occupancy sensor while a second person walked in parallel a measured distance away while carrying a known source. The walk-beside tests are described in section [3.2](#).

With moderately effective prescreening, misattributed portal alarms can be avoided (at least theoretically) by sending people sequentially to portals that are not adjacent. This essentially doubles the distance from people passing by to the nearest occupied portal, and it is FDNY standard procedure for flow control in the portal area. However, that pattern of pedestrian traffic control potentially limits throughput and can be difficult to maintain with people walking at different speeds and sometimes being delayed at a portal.

For optimal throughput, it might be better to exclude people from the CRC portal area who have enough radioactivity on or in them to cause an alarm if they walked past portals in adjacent lanes. That can be done if the portal approach lanes are far enough apart and appropriate prescreening is performed outside the CRC building. The minimum portal approach-lane spacing that will avoid misattributed alarms depends on both the sensitivity of the portals to radiation from external sources



and the prescreening sensitivity. To avoid misattributed PRD alarms during prescreening it is essential that the PRDs be less sensitive than the portal monitors, which they are, but methods for using them that increase the prescreening sensitivity can allow a smaller portal approach-lane spacing. Minimizing the portal approach-lane spacing is important because more portals can fit in a room if the spacing between them is smaller and having more portals can increase throughput – if misattributed alarms are avoided.

The effectiveness of population prescreening using a PRD depends on detector proximity to contamination on people's bodies, duration of proximity, and body orientation relative to the detector. We therefore measured the sensitivity of different prescreening methods, trying to find effective practical techniques to prescreen people quickly. The NYC goal for CRC throughput, and therefore prescreening speed, is to be able to screen up to 1000 people per hour, or a person every 3.6 seconds, recognizing that this goal might not be achievable. [16] To avoid people tracking radioactive contamination into a CRC or having to remove their shoes, NUSTL developed a method to prescreen people's shoes as part of the prescreening process. The prescreening measurements are described in section 3.3.

Misattributed alarms can occur during prescreening as well as during whole-body screening. To enable calculations to determine the minimum distance between prescreening stations that will avoid misattributed PRD alarms during prescreening, we measured the count-rate sensitivity of the RadEye PRD-ER. These measurements are analogous to the external source count-rate sensitivity measurements of the portals using stationary sources. The PRD sensitivity measurements are described in section 3.4.

FDNY asked NUSTL, "If radioactive contamination on someone causes a portal monitor to alarm, will handheld screening with a pancake-probe detector be able to find the contamination on the person?" If portal screening indicates that a person is contaminated and handheld screening is expected to detect the contamination but doesn't, it could cause confusion and needlessly worry the person being screened. Section 3.5 describes NUSTL's measurements to answer this question.

3.1 MEASUREMENTS OF PORTAL MONITOR EXTERNAL SENSITIVITY AND ANGULAR DEPENDENCE

To determine baseline activity levels and positions that could cause misattributed portal alarms, NUSTL performed laboratory measurements of the count rate sensitivity of the portals to radiation from external sources and the angular dependence of the sensitivity.

The external sensitivity measurements were done by placing a portal in a long open space and placing a radioactive source of known activity at five measured distances from the center of the portal at nine different angles. The source was positioned 1 m above the floor on a movable stand. Rather than move the source to the different angles, the source was kept in place at each distance and the portal was rotated. [Figure 3-1](#) is a photograph of the setup for the measurements.

The selection of radionuclides, vertical positioning of radioactive test sources and the standard laboratory conditions including radiation background levels were consistent with ANSI N42.35 American National Standard for Evaluation and Performance of Radiation Detection Portal Monitors for Use in Homeland Security.⁵ [17]

⁵ ANSI N42.35 describes performance tests for the use of portals to detect the illicit transport of radioactive material but does not address population screening for contamination after an incident.



Two different radionuclide sources were used: Cs-137 and americium-241 (Am-241). Cs-137 was used because an RDD using it could produce high levels of contamination [8] and for consistency with the FEMA-REP-21 standard. [13] Cs-137 decays by beta-particle emission to either stable or metastable barium-137 (Ba-137). The latter quickly decays, usually emitting a gamma-ray photon with an energy of 661.7 keV. The encapsulation of the Cs-137 source used for these tests blocks the beta particles, so the measurements are for gamma radiation only. Since radiation detector efficiency can vary with photon energy, Am-241 was used to test the response to low-energy photons. Am-241 decays by alpha-particle emission (the alpha particles are blocked by the source encapsulation), but 36% of decays also emit a gamma ray with an energy of 59.5 keV. On the dates of NUSTL's measurements, the activity of the Cs-137 source was 127 μCi (4.7 MBq) and the activity of the Am-241 source was 505 μCi (18.7 MBq).

For these measurements, the output of the portal's RS 232 serial port was connected to a laptop computer where software written by NUSTL was used to collect count-rate data every 6.0 seconds from each of the four detectors in the portal for each position of the radioactive source. To enable this, the portal manufacturer provided custom firmware that output data continuously. With standard firmware, the portal monitor outputs data only during an alarm condition. Background counts were collected separately, without the source present. The average background count rate for the four detectors was 1247 cps during the Cs-137 measurements and 1408 cps during the Am-241 measurements.

We specified the source positions in terms of distance, r , and angle. The angle 90 degrees aligns with the direction of transit through the portal, 0 degrees corresponds to the side of the portal with the attached electronics module, and 180 degrees is the other side of the portal. The relative position of the radiation source was varied by rotating the portal (angle) and moving the source to different distances (r). The angle was varied in 22.5-degree increments from 0 to 180 degrees; the distance was varied in 1-m increments from 1 to 5 m; and a constant height of 1 m was maintained, resulting in 45 positions (Figure 3-2).

Typically, 300 seconds of data were collected and totaled to determine the gross count rate in each detector at each position. The procedure was repeated for each of the two radionuclides.

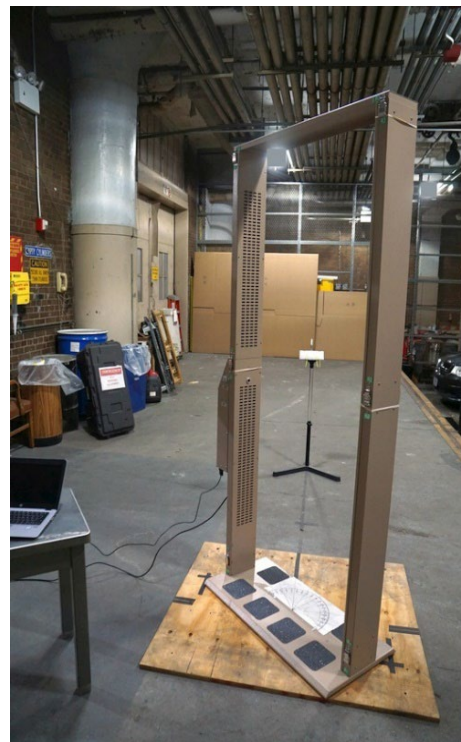


Figure 3-1 Setup for measurements of portal external sensitivity and angular dependence

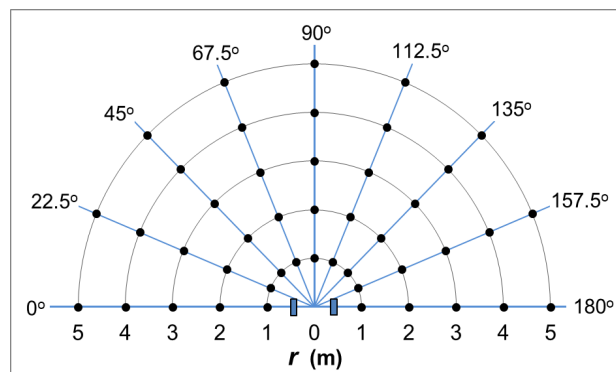


Figure 3-2 Source positions around the portal



3.1.1 ANGULAR DEPENDENCE OF PORTAL SENSITIVITY

To show the angular dependence, for each distance r , we divided the net count rate measured at each angle by that at 90 degrees. The data normalized in this way for each distance are shown in [Figure 3-3](#) for Cs-137. The angular position of the Cs-137 source is plotted on the horizontal axis. The vertical axis shows the count rate relative to that at 90 degrees, expressed as a percentage increase. The data points are connected by lines for ease of viewing. Using this graphing technique, if the portal were equally sensitive in all directions the graph would be all flat horizontal lines at 0%.

The graph of the measurement data shows that the portal is more sensitive to external sources oriented to either side, away from the direction of transit. There are two reasons for this. As the portal is rotated away from 90 degrees, one jamb of the portal moves closer to the source, so the scintillation detectors in that jamb will have higher count rates. This is the most significant effect at distances close to the center of the portal and explains the almost 150% increase in count rate for 0 and 180 degrees at $r = 1$ m. The other reason is that the scintillation material in each detector is wider facing toward and away from the portal center (0 and 180 degrees) than it is facing 90 degrees. Consequently, as the portal is rotated away from 90 degrees, the area of the detectors facing the source increases, intercepting more gamma rays. This effect happens at all distances, so even at a distance of 5 m (16.4 ft) the portal is 32% to 35% more sensitive to either side than it is at 90 degrees. The measurements with Am-241 showed an even larger angular dependence: for Am-241 at a distance of 5 m, the portal is 80% more sensitive to the side than it is on the central axis. Full details of the measurements and analyses for both radionuclides are given in [Appendix A](#).

The measurement results show that the portal monitor sensitivity to external gamma-ray sources is highest directly to the side of the portal. That position is also where people approaching or walking away from a portal pass most closely to the portals in adjacent approach lanes. For optimal throughput, then, it would be best to identify people who have enough radioactivity on or in them to cause an alarm as they walked past portals in adjacent lanes and divert them for decontamination before they enter the CRC portal area.

3.1.2 EXTERNAL SOURCE ACTIVITY THAT COULD CAUSE A MISATTRIBUTED ALARM

NUSTL's team also analyzed the measurements described above to determine the approximate source activity that could cause a misattributed portal alarm at a particular distance and angle: the activity that would cause the portal's net count rate, N , to reach its alarm threshold rate, N_{al} .⁶

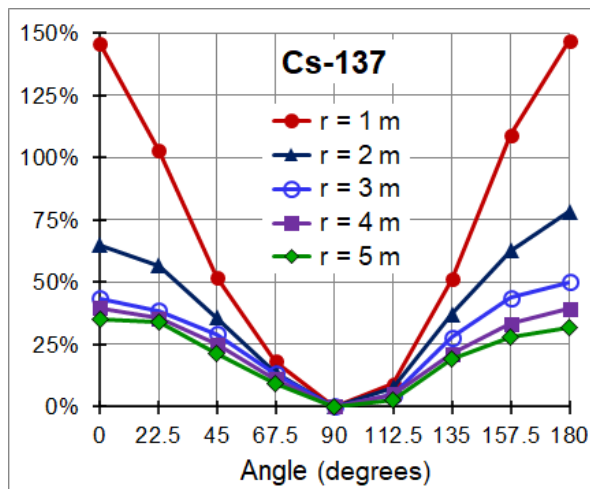


Figure 3-3 Angular dependence of portal monitor count-rate sensitivity to Cs-137

⁶ The actual number of counts in a measurement is randomly spread around its average value. In a series of real measurements, if the average count rate is N_{al} , the portal will alarm in half of the measurements, because the actual count rate will be above the average half of the time and below the average half of the time.



The portal's sensitivity, S , to a source at a given position is defined as the net count rate per unit source activity, $S = N/A$, where A is the source activity. The measurements determined S for Cs-137 and Am-241. Knowing S , the activity that would produce a given count rate N at a given position is:

$$(3-1) \quad A = N/S .$$

The activity that would produce the alarm threshold count rate is:

$$(3-2) \quad A_{al} = N_{al}/S.$$

The next step is to determine what net count rate causes an alarm. The Ludlum portal monitor alarm algorithm involves multiple short measurements during a span of 1.4 seconds and is effective for the dynamic situation of a person walking through the portal. NUSTL was initially unaware of the complexity of the portal alarm algorithm, and for analysis of the static laboratory measurements, we approximated the alarm condition using a single measurement 1 second long. If there were one alarm-test measurement 1 second long, the alarm threshold would be $N_{al} = 4.5\sqrt{B}$, where B is the rate of background counts per second. Using this value for N_{al} , Equation 3-2 becomes:

$$(3-3) \quad A_{al} = 4.5\sqrt{B}/S .$$

The points plotted in [Figure 3-4](#) show the alarm threshold activity, A_{al} , in microcuries determined from the Cs-137 measurements and Equation 3-3. For each fixed angle from 0 to 90 degrees, a line connects the data points for $r = 1, 2, 3, 4,$ and 5 m. These results show the expected consistency with the analysis in [Figure 3-3](#) in that the portal is more sensitive towards the side (0 degrees); that is, it would alarm to a weaker source. For example, at a distance of 5 m (16.4 ft), a 38 μCi (1.4 MBq) source to the side could cause an alarm vs. 51 μCi (1.9 MBq) in the direction of transit.

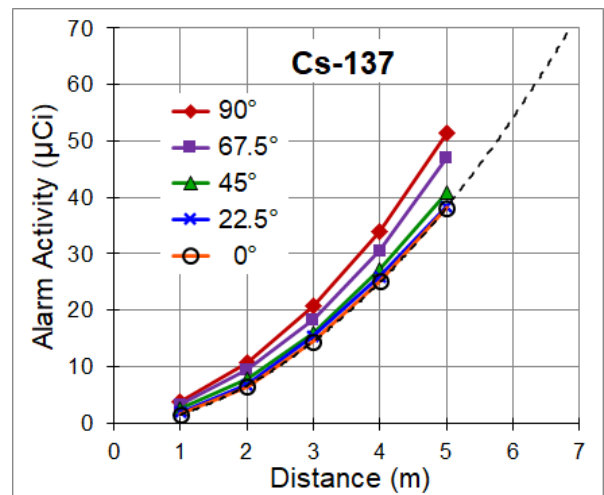


Figure 3-4 Activity of an external Cs-137 source that could cause a misattributed alarm at various distances and angles

The dashed line in [Figure 3-4](#) shows the quadratic function that best fits the data for the most sensitive orientation (0 degrees). The fit provides values of the external source activity that could cause an alarm for distances between the measurements. For example, a 23 μCi (0.85 MBq) Cs-137 source could cause a misattributed alarm half of the time at a distance of 12.5 feet (3.8 m) to the side of a portal that is screening someone. The fit can also be used to extrapolate beyond the distances and source activity used in the measurements, though with increasing uncertainty as the distance increases. Based on this uncertain extrapolation, if the portal screening area of a CRC is 90feet (27 m) long, a person entering the CRC with 1 millicurie (1 mCi, 37 MBq) of Cs-137 contamination on them could cause every portal in use in that CRC to alarm.

The measurements with stationary sources have limited usefulness because they differ in several important ways from the situation in a CRC when a person with radioactivity on them walks near a portal while another person is being screened in that portal. In the stationary source measurements, the radioactivity was in an isolated point source, the portal was empty, the radiation was constant, the background rate had a particular value, and the analysis was done for single 1-second-long measurements. In a real case, radioactivity is likely to be spread out on the body of the person being



screened and their body back-scatters some radiation toward the portal; there is also a person in or near the portal scattering some radiation into the detectors and blocking some background radiation; both people are moving, so the radiation changes throughout the 1.4-second screening window; the background rate can have different values; and the portal alarms if any of six 0.4-second measurements in any of the four detectors or the upper or lower pairs of detectors reaches the alarm threshold. Nevertheless, the measurements with stationary sources provided valuable initial target values for the amount of radioactivity that prescreening must be able to detect in order to divert people to avoid misattributed alarms from people passing a given distance from the portals. The static measurements also provided the starting values for source strengths and distances NUSTL used for the more realistic “walk-beside” measurements described in the next section.

3.2 PORTAL MONITOR WALK-BESIDE TESTS

Using the measurements described above, NUSTL determined the approximate activity of a stationary Cs-137 or Am-241 source expected to cause a portal monitor to alarm at a given distance. However, these measurements did not test whether a person with that much activity on them actually causes an alarm when they walk past an occupied portal at that distance—the situation in a CRC that would cause a misattributed portal monitor alarm. To simulate that situation, we performed “walk-beside” tests: one person walked through the portal to trigger the occupancy sensor while a second person walked in parallel beside them a measured distance away carrying a known source. We performed 17 sets of walk-beside measurements with sources having various activities of three different radionuclides, carrying the sources past the test portal at different distances and walking speeds.

3.2.1 WALK-BESIDE TESTS WITH SINGLE CS-137 SOURCES

To minimize scattering of radiation from the ceiling and walls during the walk-beside tests staged at NUSTL, we performed the measurements in a relatively empty area that has a 13.7-ft (4.2-m) high ceiling. The source was carried in a small plastic container and held 1 m above the floor.

NUSTL used results from an early analysis of the stationary-source measurements as the starting point for the source activities and distances to use in the walk-beside measurements and began with a 23 μCi (0.85 MBq) Cs-137 source. This was an activity of sources we had, and our other tests had shown that prescreening people with PRDs could detect it.

Carrying the source 12.5 feet (3.8 m) from the center of the test portal produced 10 alarms in 10 trials walking at a leisurely pace of 2.2 miles per hour (1 m/s) and 5 alarms in 5 trials walking at a brisk 3.4 miles per hour (1.5 m/s). These tests showed that a CRC portal approach-lane spacing of 12.5 feet is too small to meet the goal of avoiding misattributed alarms without needing to send people sequentially to portals that are not adjacent. Carrying the source 14.76 feet (4.5 m) from the center of the test portal produced an alarm about half of the time—11 alarms in 20 trials.



Most of the walk-beside tests were done at NUSTL, but a few of them were done at an FDNY CRC training facility set up in an empty NYC warehouse (Figure 3-5, bottom). We repeated the run of 14.76-foot (4.5-m) trials made at NUSTL in the more realistic large space of the training facility to see if radiation scattered from the walls in the NUSTL test area had affected the initial measurements. The same 23 μCi Cs-137 source carried at the same distance caused 8 alarms in 20 trials—not significantly different from the measurements at NUSTL.

These results mean that if the maximum amount of contamination on people who pass prescreening were a single 23 μCi Cs-137 source on the middle of the person, 15 feet would be a suitable spacing between portal approach lanes. It would be sufficient to avoid misattributed portal alarms because it would be rare for anyone to have almost exactly the maximum activity on them that prescreening would miss. Appropriate methods of prescreening (see 3.3.2) can actually detect considerably less than 23 μCi of Cs-137 contamination concentrated in one spot on the middle of a person.

3.2.2 WALK-BESIDE TESTS WITH OTHER RADIONUCLIDES

NUSTL also performed walk-beside tests with two other radionuclides, Am-241 and barium-133 (Ba-133), which emit lower energy gamma-ray and x-ray photons than Cs-137 does. Doing measurements with these other radionuclides is important for several reasons. One reason is that an RDD might be made with a low-energy-emitting radionuclide, including Am-241 itself. Another reason is that Ba-133 emits gamma rays with energies similar to the gamma rays emitted by iodine-131, which is used medically. Some patients who have been given therapeutic doses of iodine-131 for thyroid conditions can retain significant amounts of radioactivity for several weeks, and if there is a radiological incident, might come to a CRC and might cause the portals and PRDs to alarm from far away.

Finally, measuring the sensitivity of a portal monitor to low energy photons from radionuclides enables calculations of the portal's response to radiation that has scattered, lowering its energy. This is important because much of the radiation reaching a portal monitor from a distant source is low-energy scattered radiation.

We did not perform portal sensitivity measurements or walk-beside tests with Co-60, which emits high-energy gamma rays, because we did not have a suitable Co-60 source. As a substitute, we did a calculation. The calculation is described at the end of sections 4.1.1 and C.1.1.

To compare the portal's sensitivity to radiation from different radionuclides one has to take into account how many photons are emitted in each decay of each nuclide. For the radionuclides



Figure 3-5 Portal monitor walk-beside tests
Top—at NUSTL
Bottom—at NYC CRC training facility



considered, [Table 3-1](#) summarizes the photon energies, E, emitted and the emission intensities, I, the percentage of decays emitting a gamma ray or x ray. [18]

Table 3-1 Photon Emission Energies and Probabilities for Radionuclides Considered in This Work

| Cs-137 (Ba-137m) | | Am-241 | | Ba-133 | | I-131 | | Co-60 | |
|----------------------|-------------------------|----------------------|-------------|----------------------|--------------------------|----------------------|--------------------------|----------------------|--------------|
| E _γ (keV) | I (%) | E _γ (keV) | I (%) | E _γ (keV) | I (%) | E _γ (keV) | I (%) | E _γ (keV) | I (%) |
| 661.7 | 85.1 | 59.54 | 35.9 | 53.2 | 2.2 | 80.2 | 2.6 | 1173.2 | 100.0 |
| | | | | 79.6 | 2.6 | 284.3 | 6.1 | 1332.5 | 100.0 |
| | | | | 81.0 | 34.1 | 364.5 | 81.7 | | |
| | | | | 276.4 | 7.1 | 637.0 | 7.2 | | |
| | | | | 302.9 | 18.3 | 722.9 | 1.8 | | |
| | | | | 356.0 | 62.1 | | | | |
| | | | | 383.9 | 8.9 | | | | |
| Total γ | 85.1 | Total γ | 35.9 | Total γ | 136.5^b | Total γ | 100.8^b | Total γ | 200.0 |
| X-ray E (keV) | I (%) | | | X-ray E (keV) | I (%) | X-ray E (keV) | I (%) | | |
| 31.82 | 2.0 | | | 30.63 | 34.9 | 29.46 | 1.4 | | |
| 32.19 | 3.8 | | | 30.97 | 64.5 | 29.78 | 2.6 | | |
| | | | | 34.92 | 6.0 | | | | |
| | | | | 34.99 | 11.6 | | | | |
| | | | | 35.82 | 3.6 | | | | |
| Total x-ray | 5.8 | | | Total x-ray | 121.4^b | Total x-ray | 4.8^b | | |
| Total / | 92.2^b | Total / | 35.9 | Total / | 257.9^b | Total / | 105.6^b | Total / | 200.0 |

^a Only photon energies above 25 keV with emission intensities greater than 1% are shown in this table.

^b The total gamma- and x-ray emission intensities shown include additional photons with emission intensities as low as 0.02%, so these total intensities are greater than the sum of the intensities of the listed photons.

A Cs-137 source emits 0.922 x-ray and gamma-ray photons per decay, of which 0.851 are the 661.7-keV gamma ray, while Am-241 emits 0.36 59.54-keV gamma rays per decay. If the portal responded equally to photons of these energies, an Am-241 source would have to have $0.851/0.36 = 2.36$ times as much activity as a Cs-137 source to produce the same count rate. To produce the same count rate as a 23 μCi Cs-137 source, an Am-241 source would have to be 54 μCi.⁷

Ba-133 emits 2.579 photons per decay. Of those, 1.365 are gamma rays with energies above 53 keV, and 1.214 are x rays with energies from 30 to 36 keV. 62% of Ba-133 decays emit a 356-keV gamma ray. Most of the x rays are absorbed in the source encapsulation, source holder, and the aluminum surrounding the portal's scintillators. Without the x rays, a Ba-133 source would need to have 0.62 times as much activity as a Cs-137 source to produce the same count rate, and a Ba-133 source would have to be about 14.3 μCi to produce the count rate of a 23 μCi Cs-137 source – if the portal responded equally to photons of all energies above 53 keV.

⁷ In sections 3.2 and 3.3, the source activities in μCi are not repeated in international units. 1 μCi = 37 kBq.



We performed walk-beside measurements at NUSTL with Ba-133 sources of several activities that we had available. The sources were carried past the test portal at a distance of 14.76 feet (4.5 m). With 10.1 μCi of Ba-133 (≈ 16.2 μCi of Cs-137), there was 1 alarm in 6 trials. With 15.5 μCi of Ba-133 (≈ 24.9 μCi of Cs-137), there were 10 alarms in 15 trials. With 17.9 μCi of Ba-133 (≈ 28.7 μCi of Cs-137), there were 4 alarms in 4 trials. Comparing these results to the results of the walk-beside measurements with Cs-137, we conclude that the portal is about as sensitive to the gamma rays from Ba-133 (and therefore to those from iodine-131) as it is to the Cs-137 662 keV gamma ray.

Walk-beside measurements with Am-241 sources at NUSTL and at the NYC CRC training facility were conducted with 50 μCi and 104 μCi Am-241 sources the lab had available. With the 50 μCi Am-241 source (≈ 21.2 μCi of Cs-137), there were 0 alarms in 5 trials at a distance of 14.76 feet (4.5 m) and 0 alarms in 5 trials at 10.9 feet (3.32 m). With the 104 μCi Am-241 source (≈ 44 μCi of Cs-137), there were 2 alarms in 10 trials at 12.5 feet (3.81 m) and 5 alarms in 5 trials at 10.9 feet (3.32 m). At 12.0 feet (3.66 m), there were 8 alarms in 18 trials (44%) at NUSTL and 3 alarms in 14 trials (21%) at the CRC training center. We conclude that, for external sources, the portals are less than half as sensitive to the 60-keV photons from Am-241 as they are to the 662-keV photons from Cs-137.

The results of these measurements show that misattributed alarms should be less of a problem for RDDs made with radionuclides that emit low-energy photon radiation—if the PRDs used for prescreening are at least as sensitive to low energy photons as the portals. Diagram 11-3 in the operating instructions book that comes with the PRD-ER [\[10\]](#) shows a graph of the relative count-rate response of the PRD-ER as a function of incident photon energy. The PRDs are actually 8 times *more* sensitive to 60 keV photons than they are to the 662 keV photons from Cs-137. We conclude that a CRC designed to avoid misattributed alarms for Cs-137 contamination will also avoid misattributed alarms for contamination with radionuclides that emit lower energy photon radiation.

3.2.3 WALK-BESIDE TESTS WITH DISTRIBUTED SOURCES

All the walk-beside measurements described above were done with a single source held at 1 m above the floor as it was carried past the test portal. 23 μCi of Cs-137 contamination concentrated in one spot on the middle of a person would be easy to detect in prescreening, but contamination on a person exposed to an RDD debris cloud is likely to be spread out over the person's body and might be mostly on one side. For this reason, NUSTL developed a prescreening method that can detect as little as 21.6 μCi of Cs-137 distributed over a person's body (see [3.3.2](#)) by scanning PRDs vertically along the front and back of a person. Consequently, the hardest plausible distribution for that method of prescreening to detect is if it were evenly spread out from head to foot along the sides of the body. If the contamination is all on one side, it would be closest to an adjacent portal as the person walks by and most likely to cause a misattributed alarm.

As a person walks on a path a given distance from a portal, one side of their body is closer to the portal by half the width of their body. We took the width of a person to be 1.5 feet (0.46 m)⁸, [\[19\]](#) so if they walk 15 feet from a portal and their contamination is on one side, the distance from their radioactive side is 14.25 feet (4.34 m). The walk-beside measurements described in [3.2.1](#) determined the activity of a single Cs-137 source that would cause a portal monitor to alarm at

⁸ According to [\[19\]](#), the width across the shoulders of a 50th percentile American man and of a 99th percentile American woman is 1.5 ft, so this width is larger than the width of about 74% of the U.S. adult population.



various distances. At a distance of 14.25 feet, 23 μCi of Cs-137 would be just enough to trigger an alarm. That is, if a person walked past a portal 15 feet away many times with a single 23 μCi Cs-137 source on their side, the portal would alarm about half the time.

NUSTL simulated spread-out radioactivity for walk-beside portal tests using several 4.3 μCi Cs-137 sources attached to one side of a NUSTL scientist. Wearing 6 sources totaling 25.8 μCi , there were 2 alarms in 10 trials when he walked on a line 16 feet (4.88 m) from the center of the test portal and 6 alarms in 7 trials when he walked 15 feet (4.57 m) from the portal. When he wore 5 sources totaling 21.6 μCi , there were no alarms in 10 trials when he walked 15 feet from the portal⁹ and 4 alarms in 10 trials when he walked 14 feet (4.27 m) from the portal. Thus, the portals are about as sensitive or slightly less sensitive to external sources spread-out on someone than they are to a single concentrated source.

We conclude that if prescreening can detect as little as 23 μCi of Cs-137 on someone and send them for decontamination before they enter the portal-monitor whole-body screening room, then almost no misattributed portal alarms will be caused by people walking past adjacent portals with a portal approach-lane spacing of 15 feet.

An approach-lane spacing of 15 feet or less is a significant threshold for NYC CRCs because it will allow more portal monitors to be used in many of the City's potential CRC buildings. Many of the potential locations are high schools, where the portals would be located in the gymnasium. Many NYC high-school gymnasiums have an open floor area not much bigger than their basketball court, which is 84 feet (25.6 m) long by 50 feet (15.2 m) wide.¹⁰ If the portal lane spacing had to be much larger than 15 feet to avoid misattributed alarms, only five portals would fit. If the lane spacing can be 15 feet or less, six portals can fit, and throughput could increase by up to 20%.

3.3 PRESCREENING TESTS

When NUSTL determined that the optimal portal spacing depends critically on prescreening effectiveness, FDNY asked us to evaluate their methods for prescreening, and we developed and tested improved prescreening methods. FDNY would do prescreening using Thermo Scientific RadEye PRD-ER personal radiation detectors (described in [2.1.1](#)). FDNY asked NUSTL to evaluate methods for prescreening by two screeners working separately in two stages outside the CRC building. In their original plan, one screener would wear the PRD on or near their belt and either walk along the line of people waiting to be screened ("clients") or have the line of clients walk by the screener. Closer to the CRC building, the second screener would hold the PRD in their hand and pass it near each client from shoulder to knee height and back up. In both stages, the screeners would not need to look at the PRD display unless there is an alarm.

NUSTL tested the effectiveness of these two prescreening techniques, measuring how small an activity of Cs-137 and other radionuclides could be detected and how quickly. We found that the concept of having two stages of prescreening is very useful, and, together with FDNY, we developed improved versions of the methods for both stages that are just as fast, easier to perform, and can reliably detect smaller activities.

⁹ With only 10 trials, no observed alarms at 15 feet means the true alarm frequency might be as high as 30%.

¹⁰ A high-school basketball court is 10 feet shorter than a U.S. college or professional basketball court.



3.3.1 FIRST-STAGE PRESCREENING

NUSTL tested the detection sensitivity for a screener wearing a PRD-ER walking past a test client with a Cs-137 source attached to their body or having the test client walk past the screener. We found better and more consistent sensitivity if the client walked past the screener, so the orientation of the client's body could be controlled.

A PRD on a screener at waist height can easily detect radioactivity on a client walking past if the contamination is near the client's waist on the side facing toward the PRD. NUSTL tested cases simulating radioactive contamination on parts of the body where it would be more difficult to detect: head, feet, half on the head and half on the feet, and the side facing away from the PRD. The head and feet are the parts of the body farthest from the PRD and the radiation might have to pass through the head or foot to reach the PRD. Radiation from radioactivity on the far side of someone is attenuated (scattered and/or absorbed) by their body before it reaches the PRD.

We determined that it would be best if the clients turned as they walked past the screener so that different sides of their body face toward the PRD. It could be difficult to communicate to each client that they must stop and turn all the way around; their stopping and turning around would also take too much time. Instead, the clients can walk toward the screener and turn 180 degrees as they walk past without stopping. Then they turn 180 degrees again, moving along an S-shaped path, as shown in [Figure 3-6](#). The path can be delimited by portable barriers. People are used to walking through such S-shaped paths in queues like those at airports.

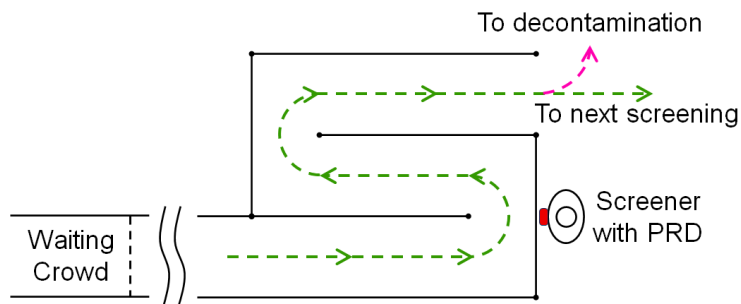


Figure 3-6 First-stage prescreening with S-shaped path

This prescreening method not only reduces the problem of shielding by people's bodies, but the serpentine path also directs clients toward the screener a second time. If radioactivity on someone causes the PRD to alarm, the screener can re-scan the clients who just went past, identify the contaminated person or persons, and direct them to decontamination.

This method can prescreen people very quickly when there are few alarms. Even if clients are spaced 10 feet (3 m) apart and walk at a leisurely pace of 3.3 feet (1 m) per second, a client passes the screener every 3 seconds, so the method could screen up to 1,200 people per hour. This is a higher throughput than the other screening stages are likely to achieve, so it should not be maintained, or a line of clients will build up at second-stage prescreening.

This method can prescreen people very quickly when there are few alarms. Even if clients are spaced 10 feet (3 m) apart and walk at a leisurely pace of 3.3 feet (1 m) per second, a client passes the screener every 3 seconds, so the method could screen up to 1,200 people per hour. This is a higher throughput than the other screening stages are likely to achieve, so it should not be maintained, or a line of clients will build up at second-stage prescreening.

Highly contaminated people in the line of clients waiting to be prescreened can cause misattributed PRD alarms at the first stage of prescreening unless the front of the waiting line is a considerable distance from the first prescreening station—up to 80 feet (24 m).¹¹ NUSTL did not test whether it is better to send people from the front of the waiting line to the first-stage prescreening station spaced out one at a time or in groups with pauses between the groups. Kramer et al. [5] found that grouping

¹¹ Calculations of the required distance are described in section 4.2.2 and Appendix C.2.2.



could be advantageous. They concluded that the best method would depend on the percentage of clients who trigger an alarm and could be determined during actual CRC operations.

The lab tested the sensitivity of the S-path prescreening method using two Cs-137 sources with different activities held near various parts of the body of a test client. The activity of each of the two sources was several tens of μCi .¹² The PRD alarmed with the weaker source on most locations of the body, but only with the stronger source when the source was on the far side of the body (i.e., facing away from the screener during the turn) and the far side of the feet. The PRD count rate did not quite reach the alarm threshold with the stronger source on the far side of the head, but we calculated that it would with a slightly stronger source. The S-path prescreening method can rapidly identify people with several tens of μCi of Cs-137 on them, but it is not sensitive enough to identify those with 23 μCi of spread-out contamination on their person.

3.3.2 SECOND-STAGE PRESCREENING

The goal in developing methods for second-stage prescreening was to find a high-throughput method that can reliably detect 23 μCi or less of Cs-137 contamination anywhere on a client's body so that people with that much contamination can be sent to decontamination before approaching the portal monitors and the portal approach lanes can be positioned 15 feet (4.6 m) apart (as explained in [3.2.3](#)).

NUSTL tested the sensitivity of several methods for second-stage prescreening and how much time each method took to perform. For tests of methods where a PRD is scanned near a person, we tried to keep the PRD 6 to 12 inches (15 to 30 cm) from the test client's body. We started with FDNY's original proposed method: having the screener hold the PRD in their hand and scan it vertically near each client from shoulder height to knee height and back up. Passing a PRD down the front of a client from shoulder height to knee height can sensitively detect radioactivity located on their chest, abdomen, or the front of their thighs, but is less sensitive to radiation on their back, head, or feet, so we put Cs-137 sources in those harder-to-detect places for our tests. With a 23 μCi Cs-137 source on the test client's back, the PRD did not reliably alarm unless we scanned along the client's back or side as well as their front.

We tried having the test client stand still with a 23 μCi Cs-137 source between his feet or near his back while the screener scanned the PRD down the client's front, stepped around the client and scanned the PRD up the client's back. The PRD reliably alarmed, but the screener's movements were awkward to perform and took over 3.5 seconds, not including the time for the client to walk up to the screener and walk away.

Because prescreeners will need to screen thousands of clients per shift, optimizing the physical ease of the prescreening method is important. To avoid the screener's having to crouch and step around the client, the lab tried having the screener sit and the client walk toward the screener, place their feet in a marked outline on the floor, turn 90 degrees and walk away. As the client puts their feet into the outline, the screener does a shoulder to knee scan. As the client turns and departs, the screener scans upward along their back. Since the front and back of the client are closely scanned in this method, we tested it with 12 μCi of Cs-137 on the test client's head and 11 μCi on his feet.¹³ The

¹² For more information, contact NUSTL@hq.dhs.gov.

¹³ The split-source arrangement is a difficult case for prescreening, but it is a realistic one. People exposed to the dust cloud from an exploded Cs-137 RDD could have contamination settle on their heads where it might be difficult to remove from their hair, and they could get radioactive dust on their shoes walking across pavement covered with it.



PRD alarmed in 10 out of 10 trials. The scanning took 3 seconds not including the client's walking time and 6 seconds total with the client approaching from 8 feet away. Hence, this method could prescreen up to 600 clients per hour if there are few alarms. A disadvantage of this method is that the client would be walking away by the time the PRD alarms and might have to be chased after. Also, the method still requires the screener to bend over to some extent to reach the clients' knees.

When a NUSTL scientist expressed concern about the potential for repetitive motion injury from screeners bending their backs thousands of times per shift, FDNY suggested attaching the PRD to the end of a stick used as a long handle. This suggestion led to our recommended method for second-stage prescreening. The general method is to have the clients wait about 10 feet from the screening spot, walk one at a time in a straight line and stop with their feet in a marked outline on the floor. The screener stands to the side of the client's path and holds the stick angled downward in front of the client with the PRD at shin level. As soon as the client stops, the screener scans the PRD up the front of the client to over their head, allowing the client to pass under the handle and walk away. The same screener can scan the PRD down the back of the client before the client is told to go, but it is faster to have a second screener simultaneously scan down the client's back. The two-screener version of the method for second-stage prescreening is illustrated in [Figure 3-7](#).



Figure 3-7 Second-stage prescreening by two screeners using PRDs on long handles

We first tested the one-screener version of the method, using just the upward frontal scan with 11 μCi of Cs-137 on the test client's head and 12 μCi on his feet. The PRD always alarmed, and the total time was about 4 seconds including the client's walking time. If the scan down the client's back is performed by a second screener while the first screener scans the client's front, the whole operation, including the client's walking time, can be completed in less than 4.5 seconds and the method can screen up to 800 people per hour if there are few alarms and the screeners are not fatigued. [20]. The actual scanning is so easy to do that there is a tendency to do it too quickly. To maintain the required sensitivity, it is essential to take at least a full second, and preferably 1.5 seconds, to perform each scan.

With the PRD scanning up and down a client's front and back, the location of radioactivity on the client's body that is most difficult to detect is evenly spread out along the client's side. We simulated spread-out radioactive contamination using several 4.3 μCi Cs-137 sources attached to the side of the test client's body as shown in [Figure 3-8](#). We screened a test client with three different total activities distributed on his side, scanning up the client's front for half the trials and down his back for the other half of the trials,



Figure 3-8 Using multiple sources to simulate distributed contamination



taking a little over 1 second for each scan. With 4 sources totaling 17.3 μCi , the PRD alarmed 22 times in 45 trials, or about half the time. With 6 sources totaling 25.8 μCi , the PRD alarmed 10 times in 10 trials. With 5 sources totaling 21.6 μCi , as seen in [Figure 3-8](#), the PRD alarmed 14 times in 20 trials, or 70% of the time (48% to 86% with 95% confidence). We conclude that the sensitivity of this method meets our goal for second-stage prescreening.

We tried various lengths and kinds of long handles and found that a 4-foot (1.2-m) long dowel or broom/mop handle was the most effective. We attached the PRD to the handle by first attaching the PRD's holster to the handle and inserting the PRD into the holster. The orientation of the PRD influences the sensitivity of the screening method. The PRD was inserted into the holster with its detector side ([Figure 2-1 B](#)) facing away from the handle and scanning was done with the detector side facing the client. This minimizes the amount of material that can partially block radiation coming from the client before it reaches the detector. The holster was attached to the handle so that the long dimension of the PRD was parallel to the handle and consequently close to horizontal during most of the scan. This orientation maximizes sensitivity because it presents a larger area of the detector to radiation coming from the client's feet and head at the beginning and end of each scan.

At a CRC, there may be a line of clients who have passed first-stage prescreening and are waiting to go through second-stage prescreening. NUSTL tested how far the nearest of those clients should stand from the PRDs used for second-stage prescreening to avoid PRD alarms caused by contamination on those who are waiting. After passing first-stage prescreening, clients can get as close as 6 feet to a PRD without causing it to alarm. To allow for the position of the second screener and for clients occasionally starting to walk forward too soon, we recommend having the front of the line be 10 feet from where they stand during second-stage prescreening.

FDNY also asked NUSTL to test the effectiveness of prescreening with a stationary portal-like arrangement of four PRDs fastened to upright supports that people would walk between. To perform the test, we set the PRDs in pairs 32 inches (81 cm) apart horizontally with one pair 18 inches (46 cm) above the floor and the other pair 54 inches (137 cm) above the floor. We tested this arrangement with a pair of Cs-137 sources totaling 23 μCi on a test client's body, first together as a single source 3 feet above the floor, then split, with one source fastened to his shoe and the other source placed on top of his head ([Figure 3-9](#)).

The stationary portal-like arrangement of PRDs worked well for a single source 3 feet above the floor, alarming 9 times in 10 trials with a client walking at a normal walking speed of 2.9 miles/h (1.3 m/s). The arrangement worked poorly, however, with the sources on the head and foot, alarming 3 times in 10 trials when the client was walking at 2.2 miles/h (1 m/s). Changing the height of the pairs of PRDs did not significantly improve the detection sensitivity.

NUSTL concluded that prescreening people walking through a stationary portal-like arrangement of PRDs is not as effective as the method where two screeners sweep PRDs on handles up and down the front and back of people standing still for 1 second. It is possible that the methods could be effective if combined, reducing the number of staff needed for second-stage prescreening, but we have not tested that.



Figure 3-9 Prescreening test with four stationary PRDs



3.3.3 PRESCREENING OTHER RADIONUCLIDES

The laboratory also did some simple prescreening tests with Am-241 and Ba-133 sources to determine if RDDs made with radionuclides that emit low-energy photon radiation would be more challenging or less challenging for misattributed portal alarms than Cs-137. As described in section [3.2.2](#), NUSTL determined that the portal monitors are less than half as sensitive to the 60-keV photons from Am-241 as they are to the 662-keV photons from Cs-137, which is good for avoiding misattributed alarms. We tested whether the PRD-ER can detect the 104- μ Ci Am-241 source that caused walk-beside portal alarms only 44% of the time at 12 feet from the portal. We placed the 104- μ Ci Am-241 source on the floor and scanned downward with a PRD on a long handle. The PRD alarmed at 20 inches (0.5 m) above the source when the PRD was oriented with its long dimension vertical (which points the PRD's scintillation crystal end-on to the source) and 36 inches (0.9 m) above the source when the PRD's long dimension was oriented horizontally.

We performed a similar measurement with a 7.8- μ Ci Ba-133 source (equivalent to between 13 μ Ci and 22 μ Ci of Cs-137) and got similar, though less dramatic, results. With the Ba-133 source on the floor, the PRD alarmed reliably with a down and up scan that reached 20 inches (0.5 m) above the floor with the long axis of the PRD horizontal, but the scan had to reach down to 17 inches (0.43 m) from the floor to alarm when the PRD was kept with its long axis vertical. We conclude that a CRC designed to avoid misattributed alarms for Cs-137 contamination will not have a problem with misattributed alarms for contamination with radionuclides that emit lower energy photon radiation. We also conclude that the orientation of the PRD is important during prescreening, especially for low-energy-emitting radionuclides. For maximum sensitivity, the long dimension of the PRD should be perpendicular to the client's body and near horizontal at the bottom and top of a prescreening sweep from shin to overhead. It is at least as important for the PRD to be oriented with its detector side facing the client's body. With its axis horizontal, the PRD alarmed over 36 inches (0.9 m) away from the Am-241 source with its detector side facing down toward the source, but it had to be within 6 inches (0.15 m) of the source to alarm with the detector side facing away from the source.

3.3.4 DETECTING CONTAMINATION ON SHOES

There is concern that radioactive contamination on clients' shoes could be tracked into the CRC and contaminate the facility's floor, which could shut down CRC operations until the contamination is removed. FDNY planned to have clients remove their shoes before entering the CRC building and carry their shoes with them during whole-body screening. The process was tested during a CRC exercise, and it did not impact CRC throughput. However, NUSTL recommends against having people remove and carry their shoes because they might contaminate their hands and clothing in the process and walking through the CRC without shoes increases the chance of injuries. Instead, NUSTL developed a method to prescreen clients' shoes during second-stage prescreening.

Second-stage prescreening using the methods described in the previous section is not sensitive enough by itself to detect a few microcuries of Cs-137 on the soles of clients' shoes because the PRDs are brought no lower than shin height. Bringing the PRDs into near contact with clients' shoes would add time and effort to prescreening.

We investigated placing a PRD on the floor to screen clients' shoes as they stepped over it. To protect the PRD, we used sections of a commercial cable protector with a wheelchair ramp over the

cable protector¹⁴ to prevent it from being a trip hazard. The arrangement is shown in [Figure 3-10](#). For maximum sensitivity to radiation from above, the PRD was placed with its detector side up (display side down). The PRD under the central flat area of the ramp alarmed when a 4 μCi (148 kBq) Cs-137 source was held a few inches above it. We attached the same source to one shoe of a test client. The PRD did not alarm when the test client walked across the ramp with his source shoe stepping over the center of the ramp. The PRD did alarm when the test client's source shoe stepped onto the flat area in the center of the ramp. It alarmed every time when the test client placed both feet onto the center of the ramp for a moment before walking off. The lab also did a follow-up test with a 1 μCi (37 kBq) Cs-137 source attached to the bottom of a running shoe. The PRD alarmed 9 times in 10 trials when the source was placed on the ramp for 1 second within 2.5 inches (6 cm) of the point directly over the PRD. We conclude that our method for prescreening shoes can reliably detect less than 2 μCi (74 kBq) of Cs-137 on the soles of clients' shoes. Calculations show that this method would detect even smaller activities of Am-241 or Co-60 on shoe soles.

If second-stage prescreening with PRDs on handles is done while clients stand over a PRD on the floor, the clients' shoes can be screened without slowing the prescreening process at all. (See [Figure 3-7](#) and [Figure 7-6](#) for images of the ramp in use.) The center of the ramp is marked to show clients where to place their feet; the feet should be close together so both feet will be close to the PRD underneath.

The ramp need not be the one we used so long as it has space underneath it for the PRD, though it must not be much higher than the PRD nor be a trip hazard. To avoid blocking radiation, the area over the PRD should be made of relatively thin and light material such as plywood, fiberboard, or plastic less than 1/2 inch (12 mm) thick, or thin aluminum.

Because the PRD is hidden beneath the platform, the PRD's alarm light cannot be seen and prescreening personnel must rely on the PRD's audible alarm. Unfortunately, the ramp muffles the alarm sound, and the use of HazMat personal protective equipment can make it even harder to hear the alarm sound. At the request of FDNY, NUSTL developed a remote audible alarm accessory to amplify the alarm sound from the PRD underneath the ramp. The remote alarm accessory box is placed on the ground just outside the ramp and connected to the PRD's audio output jack with an audio cable. The accessory provides a loud alarm sound that can be easily heard even through the headgear of HazMat personal protective equipment, and it does so without the use of batteries or external power. A detailed description of the remote audible alarm accessory is given in [Appendix B](#).



Figure 3-10 Prescreening shoes with a PRD under a ramp
Top—client standing on ramp
Bottom—PRD between ramp supports

¹⁴ Ultra-Sidewinder Large and Ultra-Sidewinder Ramp, large; <https://www.spillcontainment.com/products/sidewinders-cable-protection/>.



3.4 PRD SENSITIVITY MEASUREMENTS

Misattributed alarms can occur during prescreening as well as during whole-body screening. To avoid misattributed PRD alarms during prescreening, waiting lines of unscreened people need to be kept at a considerable distance from the prescreening stations. To determine the required distance, we used detailed radiation transport calculations (see section 4.2 and Appendix C.2) because we could not perform appropriate measurements with high-activity radiation sources at large distances. To calibrate the calculations, we measured the count-rate sensitivity of the RadEye PRD-ER in the laboratory by exposing it to smaller sources of known activity at a measured distance, then did calculations simulating the laboratory measurements.

Figure 3-11 shows the basic setup for the PRD sensitivity measurements. The PRD and the gamma-ray source were mounted on plastic containers filled with water. This was done so the measurement would include reduced-energy backscattered photons similar to photons backscattered from the bodies of the screener and the radioactive client in actual first-stage prescreening. The PRD was mounted inside its holster with the detector side facing the source, as it should be used during prescreening. The measurements were done on a cart with wire shelves to minimize scattering from other materials such as a table top. For the same reason, the measurements were performed in a large room with a high ceiling (the same room used for the walk-beside measurements).¹⁵ The distance from the center of the source to the center of the scintillator crystal was 75.5 ± 0.3 cm. The dimensions of all items involved, including the sources, water containers, cart uprights and wire shelves, and the room itself, were carefully measured so they could be modeled in calculations. (Figure 3-11 may be compared with a diagram of the model of the measurements used in the calculations simulating the measurements, which is shown in Figure 4-6.)

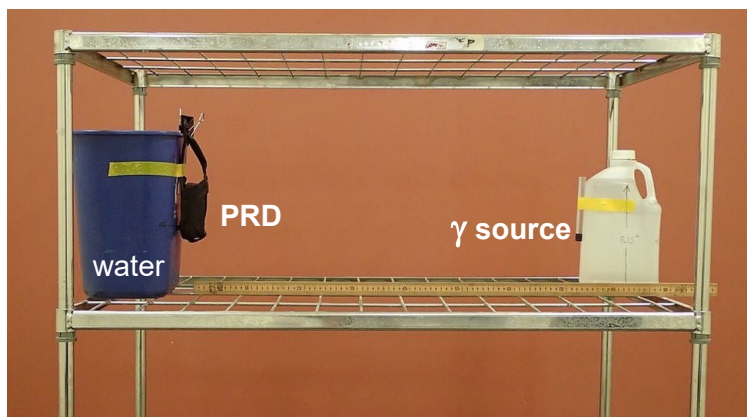


Figure 3-11 Setup for PRD sensitivity measurements

We made measurements with radionuclides that have different photon emission energy spectra to test how the PRD's sensitivity varied with photon energy. We used Cs-137 and Ba-133, the latter with its low-energy x-rays present and with the x-rays filtered out. The photon radiations emitted by these are given in Table 3-1. Note that almost half of the photons emitted by Ba-133 are x-rays with energies from 30 to 36 keV.

Doing measurements with Ba-133 as well as Cs-137 was important for two main reasons. First, measuring the sensitivity of the PRD-ER to low energy photons, including the x-rays from Ba-133, enabled calculations of the PRD's response to radiation that has scattered, lowering its energy. Much of the radiation reaching detectors from distant sources has scattered. Second, Ba-133 emits gamma rays with energies similar to the gamma rays emitted by iodine-131 (I-131), which is used medically. Patients who have been given therapeutic doses of I-131 can retain millicuries of it for

¹⁵ To show the components of the measurements clearly, the photograph in Figure 3-11 was taken of a mock-up in front of a blank background rather than the actual measurement in the large room.



several weeks. [21] Knowing the response of the PRD to I-131 photons enabled accurate calculation of the distance that patients treated with that nuclide need to be kept from prescreening stations to avoid misattributed PRD alarms.

The source shown in [Figure 3-11](#) is the Cs-137 source, which was an Eckert & Ziegler Isotope Products model GF-137-R2 plastic rod source with a diameter of 0.5 inches (12.7 mm) and an activity of 122.0 μCi (4.51 MBq) $\pm 3.0\%$ (99% confidence) on the date of the measurements. The Ba-133 source was a planar array of three portal monitor test sources designed by the National Institute of Standards and Technology (NIST) [22] with a total activity of 27.4 μCi (1.014 MBq) $\pm 4.0\%$ (95% confidence) on the date of the measurements. The Ba-133 material in each source is encapsulated between two stainless steel discs, each 0.01 inch (0.25 mm) thick and 1.5 inches (38.1 mm) in diameter. The discs are welded together and mounted in an aluminum holder. The encapsulation is thin enough to transmit about 1/3 of the x-rays with energies from 30 to 36 keV. To do measurements without the x rays, the sources were covered by a sheet of steel 0.035 inches (0.89 mm) thick.

Three 10-minute PRD-ER count-rate measurements were taken for background, Cs-137, and Ba-133 with and without the steel x-ray filter. The mean background count rate was 12.71 counts per second (cps). The mean rate for the Cs-137 source was 229.23 cps. The mean rate for the Ba-133 sources was 135.03 cps including the x-rays and 124.27 cps with the x rays filtered out. These rates are the benchmarks that the calculations simulating the measurements had to reproduce to verify that the response of the PRD-ER was accurately modeled. (See section [4.2.1](#).)

3.5 PANCAKE-PROBE DETECTOR SENSITIVITY MEASUREMENTS

One of the questions FDNY asked NUSTL was “If radioactive contamination on someone causes a portal monitor to alarm, will handheld screening with a pancake-probe detector be able to find the contamination on the person?” To enable an objective answer, we recast the last part of this question to “will the contamination also cause the pancake-probe detector to alarm during subsequent handheld screening?” NUSTL was able to answer this question for external contamination (*on* the body or clothes of someone, rather than inside their body). The question relates to the lowest amount of radioactive contamination that the portals can detect and the case in which that very small amount of contamination is spread out over a person’s body, making it harder to detect with a handheld detector. If portal screening indicates that a person is contaminated but handheld screening cannot find the contamination when it is expected to, it could cause confusion and needlessly worry the person being screened.

To answer the question, we performed two series of measurements, one for beta particles and the other for gamma rays. Most radionuclides available in high-activity sources emit energetic beta particles, which a GM pancake probe is highly efficient at detecting. Examples of beta-emitting radionuclides include the four radionuclides most widely available in high-activity sources, Cs-137, Co-60, Sr-90, and Iridium-192. However, some radionuclides decay by electron capture, the inverse of beta decay. Instead of emitting an electron, the nucleus of the atom absorbs one of the electrons orbiting around it. These radionuclides emit gamma rays, but no beta particles. Examples include Ba-133 and Iodine-125. The pancake probe’s efficiency for detecting gamma rays is lower than its efficiency for detecting beta particles.

For the beta-particle measurements, we scanned an FDNY Ludlum Model 26-2 pancake-probe detector at various measured speeds and distances over a weak Cs-137 source representing a



fraction of the contamination on a person. A portal alarms when a 1 μCi gamma-ray source of Cs-137 passes through its center; NUSTL estimated that it should alarm on roughly that much activity if it is spread over part of the surface of a person's body or clothing. The first source we used for our beta-particle handheld screening tests was a 0.21 μCi (7.8 kBq) Cs-137 plastic disk check source with a thin window on one side to allow beta particles to escape. The plastic disk was 0.125 inches (3.2 mm) thick with the radioactivity in a well at its center. To perform the tests scanning at a constant distance from the surface with the source on it, we used a fixture made from a 2-foot x 1-foot (60-cm x 30-cm) piece of plastic foam 2.2 inches (5.6 cm) thick with a 2.25-inch x 15-inch (5.7-cm x 38-cm) slot cut out of it. The fixture was placed on a table and the source was placed in the center of the slot. The pancake-probe detector was passed along the slot at measured speeds from 1 to 8 inches/s. [Figure 3-12](#) is a photograph of the pancake-probe detector sensitivity measurement. We also made a similar 1-inch thick fixture that could be used separately or added on top of the first fixture to increase the scanning distance to 3.2 inches.



Figure 3-12 Pancake-probe detector sensitivity measurement

CDC guidance for handheld screening [\[23\]](#) calls for holding the probe $\frac{1}{2}$ inch to 1 inch from the surface of the person being screened and scanning the probe at 1 inch per second (in/s). We found that the Model 26-2 pancake-probe detector alarmed when scanned past the 0.21 μCi test source at speeds up to 6 in/s when held 2.2 inches above the surface and at up to 3 in/s when held 3.2 inches above the surface. We deduce that the instrument would alarm on as little as 0.02 μCi (740 Bq) of Cs-137 contamination in an area of 10 square inches (65 cm^2) when scanned in the recommended manner and therefore would alarm when screening a person with 1 μCi of Cs-137 contamination on them spread over an area of 500 square inches (0.32 m^2), or about one third of the surface area of one side of a person's body.

NUSTL later obtained a 1-inch diameter 0.050 μCi (1,850 kBq) technetium-99 (Tc-99) beta particle source. (Tc-99 is a pure beta-particle emitter. It is different from the Tc-99m frequently used in nuclear medicine, which is a short half-life gamma-ray emitter.) We used the low-activity Tc-99 beta source to perform a more precise test of the pancake probe detector's lower limit of detection. Scanned past the Tc-99 source at 1 in/s held 1 inch above the source, the detector measured a net count rate of over 2 kcpm, twice the alarm threshold, so the detector will alarm on as little as 0.025 μCi of Tc-99. The efficiency of the probe for detecting Tc-99 beta particles is given by the manufacturer as 18%, while the efficiency for the higher energy beta particles emitted by Cs-137 is roughly 24%. [\[14\]](#) [\[15\]](#) Therefore, the detector should alarm on as little as 0.019 μCi of Cs-137. This test confirms the extrapolated results of the tests with the 0.21 μCi Cs-137 beta source.

NUSTL would like to point out that 1 inch per second is very slow—much slower than shown in the CDC video that is intended to demonstrate the recommended scanning method. [\[23\]](#) Screeners are likely to initially scan the probe at a higher speed, and it may be appropriate to do so, slowing to the recommended 1 in/s for a second scan if the quicker scan does not find the contamination indicated by whole-body screening.

For external contamination with radionuclides that emit energetic beta particles, including all four of the radionuclides available in high-activity sources considered by Smith et al., the answer to FDNY's



question—“If radioactive contamination on someone causes a portal monitor to alarm, will the contamination also cause the pancake-probe detector to alarm during subsequent handheld screening?”— is essentially “yes.”

However, even for these beta emitters, there are some cases where the pancake-probe detector might not alarm. One situation is if 1 μCi of contamination is spread out extremely evenly over most of a person’s body, which is unlikely. Another is if the slight contamination is spread out evenly over a moderate area of a person’s skin beneath uncontaminated clothing that blocks the beta particles. The solution in that case is to have the person remove the clothing.

We measured the efficiency for detecting gamma rays compared to the efficiency for detecting beta particles by holding the pancake probe still over the Cs-137 check source and comparing the count rate with the source’s thin window down to the count rate with the window up. With the window down, the check source’s plastic absorbed the beta particles headed upward and only the gamma rays emerged upward toward the detector. With the window up, both beta particles and gamma rays emerged upward. The measured background count rate was 25 ± 2 cpm. At 2.2 inches above the table surface, the net count rate above background per microcurie with the window up was $20,216 \pm 191$ cpm, and with the window down it was 542 ± 25 cpm. Correcting for 0.851 gamma rays emitted per decay, the net count rate in the detector per Cs-137 gamma ray was only 3.3% of the rate per Cs-137 beta particle. The measured count rate for the gamma rays included gamma rays that originally emerged downward into the thick wood tabletop and were scattered upward to the detector, approximately simulating the scattering from the body of a person with contamination on them.

The pancake probe’s detection efficiency for both beta particles and gamma rays changes with energy. The efficiency of the Ludlum Model 26-2 for detecting beta particles with different energies is given in the instrument’s user’s manual. [\[14\]](#) The beta detection efficiency rises with energy and varies from 2% for beta particles from carbon-14 (average energy of 49 keV), to 32% for the betas from phosphorus-32 (average energy of 565 keV). The GM detector in the Model 26-2 is essentially identical to the detector in the Ludlum Model 44-9 GM pancake probe. A graph on the 44-9 product web page [\[15\]](#) gives the probe’s efficiency for detecting gamma rays with different energies relative to its efficiency for detecting Cs-137 gamma rays. As gamma-ray energy increases, the detection efficiency relative to 662 keV Cs-137 gammas rises, falls, then rises again, spanning values from 0.6 to 6. At most, the gamma detection efficiency is 20% of the efficiency for detecting Cs-137 beta particles.

For external contamination with radionuclides that emit only gamma rays, the answer to FDNY’s question is essentially “no” – the pancake probe detector might not alarm during handheld screening for the minimal amount of contamination on a person that can cause a portal alarm during whole-body screening. At 1 inch from the body surface, the pancake probe detector will alarm if the contamination is concentrated in a small area, so most of the radiation emitted outward hits the probe as it passes over that area, but not if the contamination is spread out over the body, so most of its radiation misses the probe.

Generally, personnel doing handheld screening should rely on the alarm and not attempt to read the numeric display. If there is no alarm during handheld screening performed according to guidance, the screener can try to locate the contamination that caused the portal to alarm by scanning again



while listening to the audio beeps or clicks and reading the numeric display to look for elevated count rates.

NUSTL did not test the effectiveness of the pancake probe for detecting surface contamination with radionuclides that emit alpha particles, but the efficiency of the pancake probe for detecting alpha particles is similar to its efficiency for detecting beta particles. Specifications for the Ludlum Model 26-2 give its efficiency for detecting alpha particles from plutonium-239 as 11%. [\[14\]](#) Because alpha particles can be stopped by a few inches of air, it is especially important to scan the probe less than 1 inch from the surface of the person being screened. If used in the recommended manner, the pancake probe detector should be able to find external contamination of alpha-emitting radionuclides with activities sufficient to trigger a portal alarm from their gamma-ray emission.

Our tests did not determine what level of *internal* contamination handheld screening can detect, for example if a person inhaled radioactive dust and afterwards washed off their external contamination. Even if the contamination cannot be located by handheld screening, people with a confirmed alarm during whole-body screening should be sent to decontamination, where they can be assessed for internal contamination.

4.0 CALCULATIONS

The portal monitor and prescreening measurements allowed us to determine the minimum spacing between portal approach lanes required to avoid misattributed portal alarms during whole-body screening of prescreened people. However, the measurements don't tell us how much radiation reaches the instruments in various situations and the resulting count rates. Therefore, the measurements are not sufficient by themselves to determine minimum distances to and between the prescreening stations required to avoid misattributed portal and PRD alarms from radioactivity on clients waiting to be prescreened. To determine these distances, we performed detailed radiation transport calculations. We calculated values for four distances:

1. From the portals to first-stage prescreening
2. From the portals to second-stage prescreening
3. Between the first-stage and second-stage prescreening stations
4. From first-stage prescreening to the front of the line of people waiting to be prescreened

These distances are diagrammed in [Figure 4-1](#). Increasing distances 1 and 2 reduces misattributed portal alarms during whole-body screening. Increasing distance 3 reduces misattributed PRD alarms at second-stage prescreening. Increasing distance 4 reduces misattributed PRD alarms at first-stage

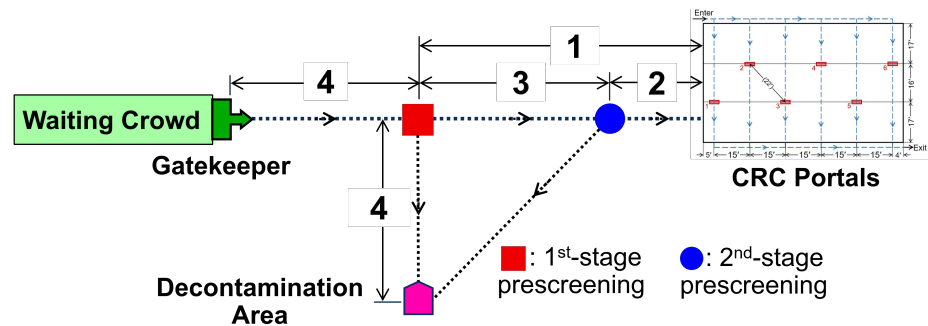


Figure 4-1 Distances calculated in order to avoid misattributed alarms

prescreening. The distance from the decontamination area to first-stage prescreening should be at least as large as distance 4. The calculations we performed to determine minimum values for these distances are described below and described in more detail in [Appendix C](#).

Minimum values for these distances depend on the count-rate sensitivity and alarm threshold of the portals and PRDs, how much radioactivity might be on people who come to a CRC, and what fraction of the emitted radiation reaches the instrument detectors and produces a count. The instrument count-rate sensitivities were determined from the measurements described in sections [3.2](#) and [3.4](#). We estimated how much radioactivity might be on RDD victims and nuclear medicine patients from published papers and books. [\[8\]](#) [\[21\]](#) We determined how much radiation reaches the instruments in various situations and the count rates it produces by performing calculations using the Monte Carlo N-Particle (MCNP) radiation transport computer code. [\[24\]](#) [\[25\]](#) MCNP is a widely used general purpose radiation transport computer code developed by the Los Alamos National Laboratory.

To set up an MCNP calculation of the count rate in a detector exposed to a radiation source, the user creates an input file that describes the radiation source; where the source, detector, and other material objects are; the composition of the materials; and the response of the detector. The code performs the calculation by simulating what happens to each radiation particle step-by-step as it is emitted from the source and interacts with materials that it hits. The answer for the count rate in the



detector is determined by calculating what happens on average to a large number of particles. The precision of the answer generally depends on the square root of the number of particles that are followed. Our calculations typically followed 200 million to 2 billion particles to reduce the statistical uncertainty in the calculated count rate to less than 1%.

4.1 DISTANCE FROM PRESCREENING STATIONS TO PORTAL MONITORS

Before we calculated how far away from the portals the first-stage and second-stage prescreening stations need to be to avoid misattributed portal alarms (distances 1 and 2 in [Figure 4-1](#)), we verified that we could calculate correct portal monitor count rates for a known situation with a portal exposed to external radiation—the count rates we measured during the portal walk-beside tests.

4.1.1 SIMULATION OF WALK-BESIDE TESTS

The calculated count rate in a portal monitor detector exposed to a gamma-ray source is the product of the source activity in decays per second times the number of photons emitted per decay of the radionuclide times the calculated fraction of emitted photons that hit the detector and produce a count. For the walk-beside portal sensitivity measurements, we know the activities and the number of photons emitted per decay of each of the sources we used. We calculated the fraction of photons reaching the portal scintillators and the energy each photon deposits by simulating the portal walk-beside measurements using MCNP.

[Figure 4-2](#) is diagram showing our MCNP model of the walk-beside tests that were done with single sources of Cs-137, Am-241, and Ba-133. The MCNP simulation includes the details of the source encapsulation and holder, the portal monitor, and the room. The objects labeled “phantom” are simple geometric stand-ins for the bodies of the

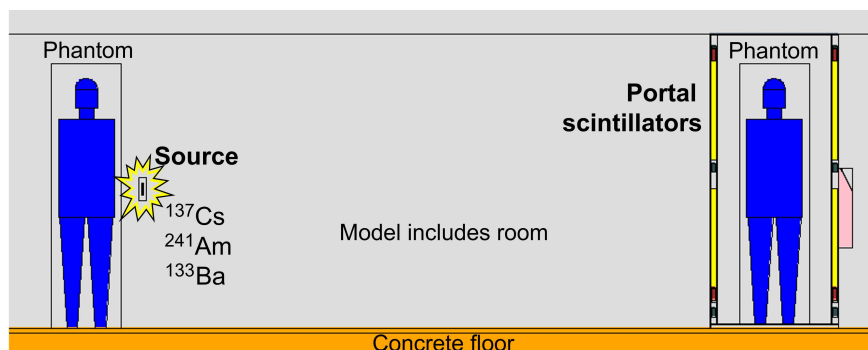


Figure 4-2 MCNP model of the walk-beside tests

person walking through the portal and the person carrying the source. Radiation that is initially going away from the portal can scatter toward the portal when it hits the phantoms and the floor, ceiling, and walls of the room, so they are significant parts of the calculation.

To determine if a photon that deposits a certain energy in a portal scintillator produces a count, it is necessary to know the portal’s counting efficiency at that energy. Initially, we did not know the portal’s counting efficiency at low energies. All we knew to start with was that the efficiency was likely to be near 100% for deposited energies above about 30 keV and 0% below some lower energy. We determined the portal’s low-energy response by comparing the calculated count rates with the measured count rates, adjusting the portal’s low-energy response curve to get the best agreement.



The result is shown in [Figure 4-3](#): the portal counting efficiency gradually decreases from 100% for energy deposits above 30 keV to 0% below 5 keV. Using this portal counting efficiency curve, the calculated count rates averaged for the portal's four detectors were within 1% of the measured count rates for the walk-beside measurements with Cs-137 and Am-241 and within 2% for Ba-133. This agreement means we modeled the portal monitor's count-rate response correctly and gives us confidence in the results of our calculations of the count rates in a portal in a CRC with a contaminated person at a prescreening station outside to determine the minimum distance from the prescreening stations to the portals in the CRC that will avoid misattributed portal alarms.

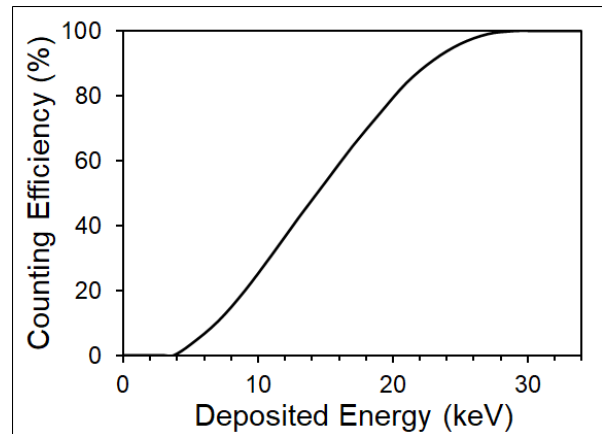


Figure 4-3 Portal monitor counting efficiency vs. energy deposited in a scintillator

The technical manual for the Ludlum Model 52 series portal monitors [\[12\]](#) gives the energy response range of the portal as 30 keV to 3 MeV, but these values are for the energies of photons that the portal is specified to be able to detect. The low-energy counting efficiency curve we determined is for the energy deposited within the scintillators.

Calculations simulating the walk-beside tests were useful in another way. We wanted to do portal and PRD measurements with Co-60, which emits high-energy gamma rays, because we were concerned that the count-rate sensitivity of the portal monitors might decrease for high-energy gamma rays less than the sensitivity of the PRDs used for prescreening decreases. If that were so, the 15-foot separation of the portal approach lanes that is sufficient to avoid misattributed portal alarms for Cs-137 contamination would not be sufficient for Co-60. That said, we did not perform portal sensitivity measurements or walk-beside tests with Co-60 because we did not have a suitable Co-60 source. As a substitute for measurements, we did calculations. To determine the relative sensitivity of the portal monitors to photons from the two radionuclides, we performed MCNP calculations simulating a contaminated person walking in parallel with a person going through a portal, first with Cs-137 contamination and then with Co-60. The result showed the portal is 88% as sensitive to Co-60 gamma rays as it is to Cs-137 photons. When we calculated the relative sensitivity of the PRDs to photons from Co-60 and Cs-137 (see last paragraph of [4.2.1](#)), the result was a similar decrease, so a portal approach-lane spacing that works for Cs-137 will also work for Co-60.

4.1.2 DISTANCE FROM FIRST-STAGE PRESCREENING TO PORTAL MONITORS

The first-stage prescreening station is the place where unscreened people who might be highly contaminated would get closest to the portal monitors in a CRC. To calculate how far the first-stage prescreening station needs to be from the portal monitors inside a CRC to avoid misattributed portal alarms (distance 1 in [Figure 4-1](#)), we estimated how much radioactivity might be on the most contaminated RDD victims who might come to a CRC ([4.1.2.1](#)) and calculated the count rates in the portal's detectors using MCNP to model a portal monitor in a CRC building with such a contaminated person outside ([4.1.2.2](#)). We modeled different kinds of buildings that may house CRCs and tried various distances to the contaminated person, looking for the distance that resulted in calculated count rates that would produce a portal alarm probability of about 0.5. We determined what count



rates in the portal's four detectors would cause the portal to alarm by writing a short Monte Carlo computer code that simulates the portal's alarm algorithm (4.1.2.3). Results for the recommended distances from the first-stage prescreening station to the CRC portal monitors in four types of buildings are given in 4.1.2.4, along with advice for how to use the results.

4.1.2.1 RADIOACTIVITY ON RDD VICTIMS

The count rate in the portal monitors, and consequently the minimum distance from the first-stage prescreening station to the portal monitors that will avoid misattributed alarms, depends on how much radioactivity is on people who might come to a CRC.

We estimated the activity on the most-contaminated RDD victims from information in a paper by Smith, Ansari, and Harper. [8] Based on test explosions, they determined the range of surface contamination on victims injured by an explosive RDD with a "maximum credible" amount of radioactivity (10^6 GBq, 27,027 Ci)¹⁶ and various amounts of explosive. They considered three different radionuclides that are available in high activity sources: Cs-137, Co-60, and Sr-90. Cs-137 is the worst case for contaminating uninjured victims because it is in the form of cesium chloride, which is highly dispersible. Based on their work, we determined the maximum contamination on an uninjured person for the 2000 Ci (74,000 GBq) Cs-137 RDD used as the design-case incident in our work. While smaller than Smith et al.'s maximum credible event, 2000 Ci is a very high activity close to the activity used for National Planning Scenario 11 [6] and 1½ times the activity of the Cs-137 radiotherapy source that caused a major contamination event in Goiania Brazil [7].

While an RDD using a large amount of explosive would cause the most injuries, damage, and widespread contamination, Table 1 of Smith et al. [8] shows that an RDD with a smaller amount of explosive would maximize the contamination on people who are just outside the range of injury from the explosion. These heavily contaminated yet uninjured people could leave the scene of the incident on their own and later go to a CRC; thus, an RDD with a relatively small amount of explosive could potentially cause the most misattributed alarms at CRCs. Table 1 of Smith et al. gives the minimum surface contamination on an injured victim of an RDD made with 10^6 GBq (27,027 Ci) of Cs-137 and 10 kg of high explosive as 33 GBq/m² (900 mCi/m²). We took the minimum contamination on an injured victim to be equal to the maximum contamination on an uninjured victim. Using 1 m² as the area of one side of a person's body and an RDD source activity of 2,000 Ci, the Cs-137 activity on the most-contaminated uninjured victim is 67 mCi (2.46 GBq).

We assumed that by the time the CRCs would be operational, many of the most-contaminated RDD victims would have complied with public announcements advising them to change clothing and shower before going to CRCs and that those actions would remove 90% of their contamination, [9] leaving 10%, or about 7 mCi (0.25 GBq), on a majority of the most contaminated people likely to come to a CRC. We performed our calculations of the minimum distance to keep unscreened people from the CRC portal monitors and prescreening stations using this activity as our design case. However, some of the most-contaminated uninjured RDD victims might be homeless or otherwise unable or unwilling to go home to change clothes and shower. Such victims of our design-case incident might arrive at a CRC with more than our design-case activity, potentially triggering some

¹⁶ To indicate the range of uncertainty, Smith, Ansari, and Harper gave their source activity as "on the order of 10^6 GBq (10^5 Ci)". 10^6 GBq is actually equivalent to 27,027 Ci. Calculations in this report are based on 10^6 GBq, resulting in the highest victim contamination activities for our 2000 Ci RDD design incident. Had we used 10^5 Ci for the Smith et al. source, the contamination activity for our design case would have been 27% of the activity we used.



misattributed alarms. Procedures to deal with misattributed alarms during whole-body screening are described in section 5.3.

4.1.2.2 PORTAL COUNT RATE FROM RADIOACTIVITY ON PEOPLE OUTSIDE A CRC

Since many potential NYC CRC locations are high schools, our basic MCNP input file describes the materials in a portal monitor in a high school basketball court in a gymnasium inside a notional high school building. Figure 4-4 is a pair of diagrams showing top and front views of our MCNP model.

The person with radioactivity on them and a person being screened inside a portal are represented by simple phantoms. The diagrams are to scale, so the phantoms and the portal appear tiny in the main diagrams—practically just points in the top view.¹⁷ A jagged halo emphasizes the location of the person with radioactivity outside the building. Magnified insets

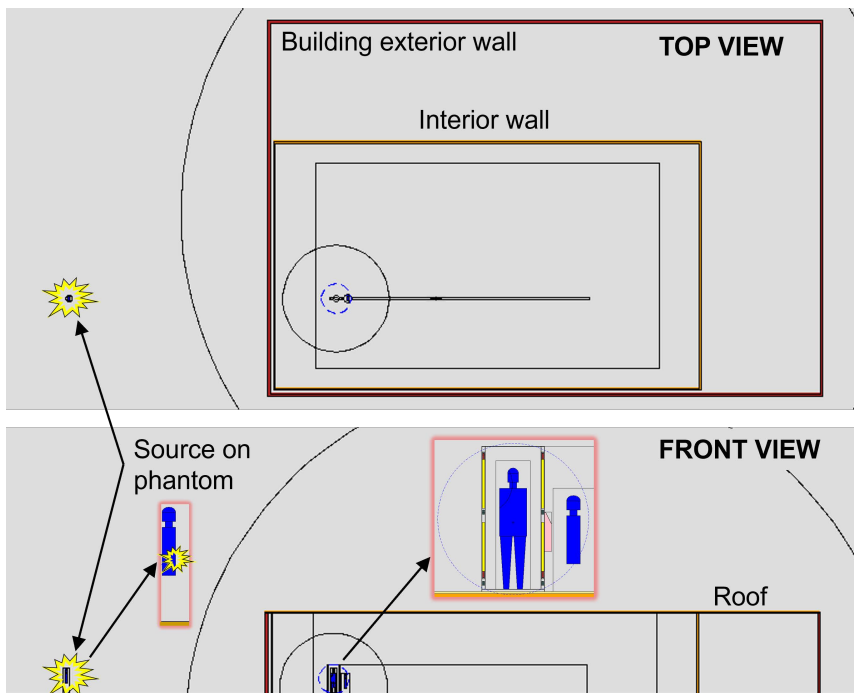


Figure 4-4 MCNP model of CRC building and person with radioactivity outside

show details of the phantom with the radioactive source and the portal monitor and the phantoms in and near it. We used a single point source 1 m above the ground on the surface of the outdoor phantom. We included a third phantom representing the portal operator reading the display.¹⁸

We modeled four basic kinds of potential CRC buildings:

1. No building, e.g., an open field, parking lot, or outdoor stadium
2. A warehouse with a 4-inch (10-cm) thick concrete block exterior wall and an insubstantial roof¹⁹
3. A building representing a NYC school, with an 8-inch (20-cm) thick brick exterior wall, one 4-inch (10-cm) thick concrete block interior wall surrounding the gymnasium, and an insubstantial roof
4. The same brick school building, but with a 3-inch (8-cm) thick concrete roof

We used the low-energy response determined from the simulations of the walk-beside measurements. We made several trial calculations for each type of building, putting the radioactive person at different distances to find the distance at which the portal would alarm with 50% probability.

¹⁷ The circles and arcs around the portal scintillator and building are spherical surfaces used for variance reduction to reduce the calculation time (see Appendix C).

¹⁸ The legs of the phantoms shown in profile are not visible in the figure because the view shown is a cross-section slice down the middle between their legs.

¹⁹ Thin enough so that it does not significantly attenuate gamma rays.



4.1.2.3 PORTAL COUNT RATE ALARM THRESHOLD

Using MCNP, we calculated the average count rate in each of a portal's four scintillator detectors at a given distance from a radioactive source, but to determine the minimum distance that will avoid misattributed portal alarms, we need to know what count rate in the detectors would cause a portal to alarm. Or, rather, we need to know the probability that the portal will alarm at a given count rate. Whether a portal alarms when someone walks through it depends on the count rate in its detectors, the background count rate, and the alarm algorithm of the portal's microprocessor.

As described in [2.2.2](#) and [C.1.2.3](#), the Ludlum portal monitor alarm algorithm compares combinations of short measurements of the count rate in each detector to an alarm threshold based on the square root of the background count rate. The portal monitor's microprocessor continually samples the count rate in each detector every 0.2 seconds. In walk-through mode with the FDNY values of the portal setup parameters, the alarm algorithm combines the 0.2-second sample measurements in pairs and tallies the counts in six overlapping 0.4-second measurements over 1.4 seconds. In each of those six measurements, if the net counts in any detector or the sum of the upper pair or lower pair of detectors exceeds 4.5 times the square root of the expected background counts, the portal alarms.

The complexity of the alarm algorithm makes it difficult to determine the probability that the portal will alarm using standard statistical formulas. The solution was to write a computer program that duplicates the alarm test algorithm of the portal monitor's microprocessor, substituting code-generated random numbers for the number of counts in each portal detector. Details of the alarm algorithm simulation code are given in [C.1.2.3](#).

Since the alarm criterion depends on the background-radiation count rate, we need to choose a background rate for our analysis. Average background rates in each scintillator during all of our portal monitor measurements ranged from 988 to 1444 cps. Since a portal will alarm at lower net count rates for lower background rates, we decided to use a low, but not unusual, background rate for our alarm analysis to make sure we put the prescreening stations far enough from the portals. We chose a background rate of 1000 cps.

[Figure 4-5](#) shows a graph of the output of the alarm algorithm simulation code: the probability for a portal to alarm as a function of the average net count rate in the detector with the highest count rate. The graph shows plots of the outputs for the ratios of detector net count rates from the MCNP calculations with a Cs-137 source for the four building types. The four curves are all very similar. The count rate in the highest-rate detector that gives an alarm probability of 50% is 114 cps for open ground, 116 cps for the brick building with a concrete roof, and 113 cps for the other two building types.

The alarm probability code also gives the probability of a *false* alarm just from random fluctuations in the background. For a background rate of 1000 cps, setting the net count rate to zero gives a detector

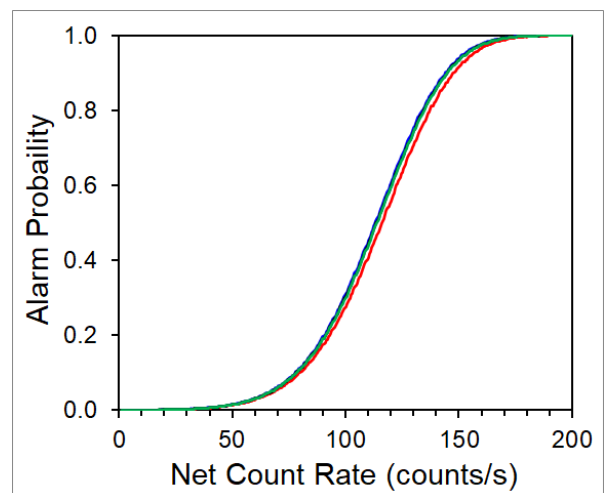


Figure 4-5 Probability for a portal monitor to alarm vs. net count rate in the highest-rate detector



alarm probability of 2×10^{-4} , or 2 portal false alarms in 10,000 screenings. In a CRC with multiple portals screening people as fast as they arrive from prescreening—800 people per hour—there will be an average of about 1 false alarm every 6 hours. Screeners should be made aware that there will be occasional false alarms as well as misattributed alarms and procedures should include methods to deal with them.

4.1.2.4 RESULTS OF CALCULATIONS FOR THE FOUR BUILDING TYPES

[Table 4-1](#) gives the results of our calculations of the minimum distance from the first-stage prescreening station to the nearest portal in a CRC that will avoid most misattributed portal alarms when our design-case RDD victim is prescreened outside each of the four types of CRC buildings. The distances in the table are a few feet greater than the calculated minimum required distance to allow for clients to move a few feet toward the portals before turning toward the decontamination area. If there is no building to provide shielding, the first-stage prescreener should be 250 feet (76 m) from the center of the nearest portal, so if a CRC is set up on the field of a sports stadium, the portals and first prescreening station should be near opposite ends of the field. If the CRC is in a building such as a NYC high school with a structural brick exterior wall and a concrete-block interior wall around the gymnasium with the portal monitors, the minimum distance to the first prescreening station depends some on the shielding effectiveness of the roof over the gymnasium: if the roof is thin, the distance is 90 feet (27 m); if the roof is 3-inch-thick concrete or there are building floors above the gymnasium, the distance can be 80 feet (24 m). It might seem that the roof would be unimportant, but with thick walls shielding the portals from radiation coming directly from the source and no shielding by the roof, a noticeable amount of the radiation reaching the portals would be radiation that had scattered downward from the air above.

Table 4-1 First-stage Prescreening Distance from Portals to Avoid Misattributed Portal Alarms

| CRC building type | Distance from prescreening to nearest portal |
|---|--|
| No building (open field, parking lot, stadium) | 250 feet (76 m) |
| 4" concrete-block exterior wall, thin roof (warehouse) | 180 feet (55 m) |
| Brick exterior wall, 4" concrete-block interior wall, thin roof | 90 feet (27 m) |
| Brick exterior wall, 4" concrete-block interior wall, concrete roof | 80 feet (24 m) |

The distances in [Table 4-1](#) are for our design-case RDD scenario. These distances should be taken as starting values and adjusted according to the nature of the event and the layout of the area around the CRC. Some practical applications of how these measures might be adjusted include:

- If the most practical locations for prescreening are at larger distances than those in the table, use those locations.
- If the activity released in the event is known to be greater than 2000 Ci, use larger distances.



- If the activity is known to be less than 200 Ci, the starting distance from prescreening to the portals can be cut in half without increasing misattributed alarms.
- If no misattributed alarms or elevated background rates are observed during CRC operations, the prescreening locations can be moved closer to the portal area if it is convenient and useful to do so.

The same flexibility applies to the distance between prescreening stations discussed in section [4.2.2](#).

In addition to Cs-137, NUSTL also considered two other threat radionuclides discussed by Smith, Ansari, and Harper: strontium-90 (Sr-90) and Co-60. [8] The calculated distances for preventing misattributed alarms would suffice for these other radionuclides, though for very different reasons. Sr-90 emits only beta particle radiation, which is far less penetrating than gamma radiation of similar energy, so distances that prevent misattributed alarms for Cs-137 would be more than sufficient for an RDD made with Sr-90. This is so even though beta particles can generate x rays when they slow down in matter. Co-60 emits two high-energy gamma rays per decay, so distances that prevent misattributed alarms for Cs-137 would not be adequate for the same activity of Co-60 on a victim. At the same 80-foot distance from portals in the brick building, Co-60 could cause a portal alarm with only 23% as much activity as Cs-137. However, because the Co-60 in high activity sources is in pieces of solid cobalt metal, exploding a Co-60 source produces mostly large fragments that injure victims rather than contaminating them with radioactive dust. Consequently, the maximum activity on an uninjured victim of an RDD made with 2000 Ci of Co-60 is only 15% of the maximum activity on an uninjured victim of a similar Cs-137 RDD. Because of this lower maximum activity, distances that prevent misattributed alarms for Cs-137 would be sufficient for an RDD made with a similar activity of Co-60. The same applies for the distance between prescreening stations discussed in section [4.2](#).

4.1.3 DISTANCE FROM SECOND-STAGE PRESCREENING TO PORTAL MONITORS

The second-stage prescreening station is the place where people who have had only first-stage prescreening would come closest to the portal monitors in a CRC. NUSTL did MCNP calculations to determine how far the second-stage prescreening station should be from the portal monitors to avoid misattributed portal alarms (distance 2 in [Figure 4-1](#)). The source we used in the calculations was the maximum activity that could be on people who reach the second-stage prescreening station, which is the largest activity that might be missed by first-stage prescreening. This activity depends on the detection sensitivity of first-stage prescreening, not on the activity released in the incident. We modeled the portal and source with phantoms as we did in the calculations for the minimum distance to the first-stage prescreening station, but we allowed the second-stage prescreening station to be inside the building, with no intervening walls to provide shielding. For the maximum activity that could be missed by first-stage prescreening, the distance that results in a 50% probability of causing a misattributed portal alarm is 30 feet (9 m). Allowing an extra 5 feet for a client to possibly walk closer to the portal before turning to go to decontamination, the second-stage prescreening station should be located at least 35 feet (11 m) from the nearest portal. The 30-foot distance with no shielding can be decreased to 20 feet (6 m) if there is an intervening masonry or brick wall, in which case the second-stage prescreening station can be located as close as 25 feet (8 m) from the nearest portal.



The 30-foot distance from the portals required to avoid misattributed alarms for people with close to the maximum activity that could be missed by first-stage prescreening is twice the 15-foot distance we determined for the optimal portal approach-lane spacing after second-stage prescreening. If second-stage prescreening is not performed, the S-path prescreening method described in [3.3.1](#) would be adequate to avoid misattributed alarms during whole-body screening if the portal approach lanes are spaced 30 feet apart or they are spaced 15 feet apart and people are sent sequentially to portals that are not adjacent.

4.2 DISTANCES TO AVOID MISATTRIBUTED PRESCREENING ALARMS

Misattributed alarms can occur during prescreening as well as during whole-body screening. NUSTL performed calculations to determine the minimum distance from the front of the line of unscreened people to the first-stage prescreening station and between the first-stage and second-stage prescreening stations that will avoid misattributed PRD alarms during prescreening (distances 4 and 3 in [Figure 4-1](#)). As we did for the portal count-rate calculations, we first determined the low-energy counting efficiency of the PRD-ER and verified that we could calculate accurate count rates for the device in a known situation.

4.2.1 SIMULATION OF PRD SENSITIVITY MEASUREMENTS

To test and calibrate the prescreening station distance calculations, we simulated our count-rate sensitivity measurements of the RadEye PRD-ER (see [3.4](#)). A diagram of our MCNP model of the PRD sensitivity measurements is shown in [Figure 4-6](#), which may be compared with the photograph of the measurement setup shown in [Figure 3-11](#).

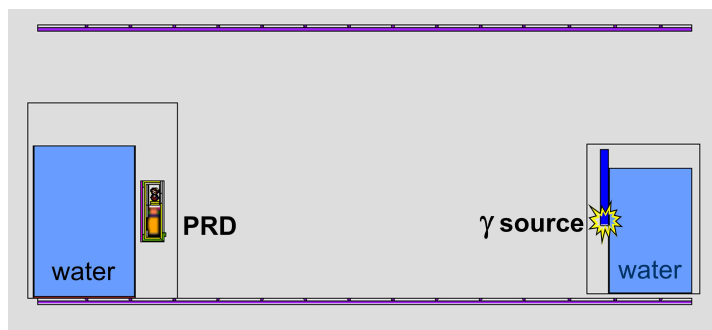


Figure 4-6 MCNP model of PRD-ER sensitivity measurements

The most important part of modeling the PRD sensitivity measurements is modeling the PRD-ER itself. We determined the dimensions of the significant components of the PRD by taking apart a damaged RadEye PRD and measuring each component, including the sodium iodide crystal scintillator. [Figure 4-7](#) shows cross-sectional diagrams of our MCNP model of the PRD-ER viewed from the top, front, and side. Details of the PRD's crystal have been blurred in the figure to obscure proprietary information.

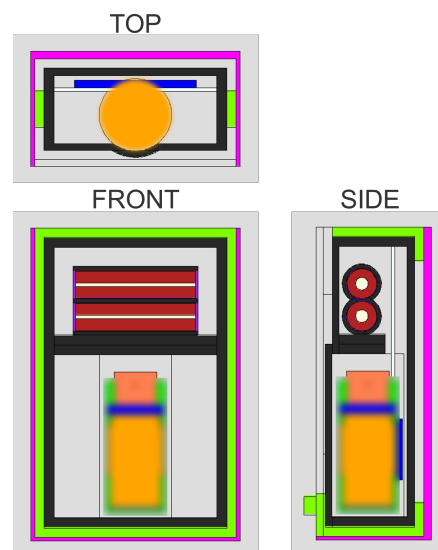


Figure 4-7 MCNP model of PRD-ER

In order to determine if the simulation could reproduce the measured count rate over a range of photon energies, especially low energies, we took PRD sensitivity measurements with different radionuclides (Cs-137 and Ba-133) and with containers of water behind the source and PRD, and then simulated the measurements with MCNP. Low energies are important because many of the photons reaching the PRD from distant sources have scattered down to low energy.



To determine if a photon that deposits a certain energy in the PRD's crystal produces a count, it is necessary to know the PRD's counting efficiency at that energy. In the operating instructions book that comes with the PRD-ER [10], diagram 11-3 shows a graph of the relative count-rate response of the PRD-ER as a function of incident photon energy. We converted values of relative response versus photon energy taken from that graph to counting efficiency versus energy deposited in the crystal by performing MCNP simulations of the type of measurements the manufacturer made to obtain the photon response data. Figure 4-8 shows a graph of the resulting counting efficiency as a function of deposited energy.

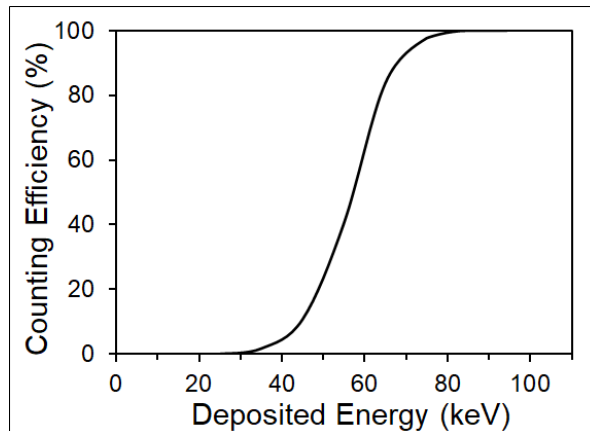


Figure 4-8 PRD-ER counting efficiency vs. energy deposited in its scintillator

The MCNP simulations of our PRD count-rate sensitivity measurements with a Cs-137 source and with Ba-133 sources with and without filters to remove the low-energy x-rays produced calculated count rates that matched the three measured count rates to within 0.2%, 3%, and 2% respectively. This agreement means NUSTL modeled the PRD-ER and its low-energy response correctly and gives us confidence in the results of our calculations to determine the minimum distance from unshielded people to prescreening stations that will avoid misattributed PRD alarms during prescreening.

As mentioned in the last paragraph of section 4.1.1, we did not have a suitable Co-60 source to do measurements but were concerned that the count-rate sensitivity of the PRDs might decrease for high-energy Co-60 gamma rays more than the sensitivity of the portal monitors would decrease. If that were so, the 15-foot (4.6-m) separation of the portal approach lanes that is sufficient to avoid misattributed portal alarms for Cs-137 contamination would not be sufficient for Co-60. To determine the relative sensitivity of the PRD to photons from the two radionuclides, we performed MCNP calculations simulating second-stage prescreening for Cs-137 and Co-60 contamination on the side of a person. The result showed that the PRD is 89% as sensitive to Co-60 gamma rays as it is to Cs-137 photons. When we calculated the relative sensitivity of the portal monitors to the two radionuclides, we found that the portal is 88% as sensitive to Co-60 gamma rays as it is to Cs-137 photons—almost the same—so: the portal approach-lane spacing that avoids misattributed alarms for Cs-137 contamination will also work for Co-60.

4.2.2 DISTANCES TO FIRST-STAGE PRESCREENING

There are two places where unshielded people who might be highly contaminated would come closest to PRDs being used to prescreen someone else and, thus, might cause a misattributed prescreening alarm: at the front of the line of people waiting to be prescreened, where they stand some distance from the first-stage prescreening station just before their turn to approach it, and at the first-stage prescreening station, where they need to be a similar distance away from the second-stage prescreening station. These distances are labeled “4” and “3” in Figure 4-1. Using MCNP, we calculated minimum values of these two distances that will avoid a disruptive number of misattributed PRD alarms from contamination on our design-case RDD victims and from I-131 possibly remaining in certain nuclear medicine patients. (While few patients recently given



therapeutic doses of I-131 are likely to come to CRCs, we performed calculations to see if those who do might cause misattributed alarms.)

Our MCNP model for calculating both distances is similar: a phantom representing an RDD victim or a nuclear medicine patient with radioactivity on or in them standing on a sidewalk near city buildings and a second phantom at some distance representing either a screener wearing a PRD (first-stage prescreening) or a client with the PRD about 9 inches

(23 cm) from them (second-stage prescreening). NUSTL made trial calculations at different distances to find the distance that produced a PRD count rate at the alarm threshold. [Figure 4-9](#) is a pair of diagrams showing two views of our MCNP model for calculating the minimum distance to the first-stage prescreening station (distance “4”). The diagrams are to scale, so the phantoms appear tiny, and the PRD is invisible. (The circles centered around the PRD are spherical surfaces used for variance reduction to reduce the calculation time (see [Appendix C](#))). As indicated in [Figures 4-9](#) and [4-10](#), the answer for the distance required to avoid misattributed PRD alarms from the design-case contaminated RDD victim is 80 feet (24 m) from the first-stage screener.

[Figure 4-10](#) shows close-up side views of the phantom with the source and the phantom representing the screener with the PRD.²⁰ The phantom with the source (left) is now more detailed and is shown with two possible sources: one for an RDD victim and one for a nuclear medicine patient treated with I-131. The screener phantom (right) is the same one we used for the portal calculations.

For the radioactive source on an RDD victim, we used the same design-case activity of Cs-137 that we used to calculate the distance from the first-stage prescreening station to the nearest portal.

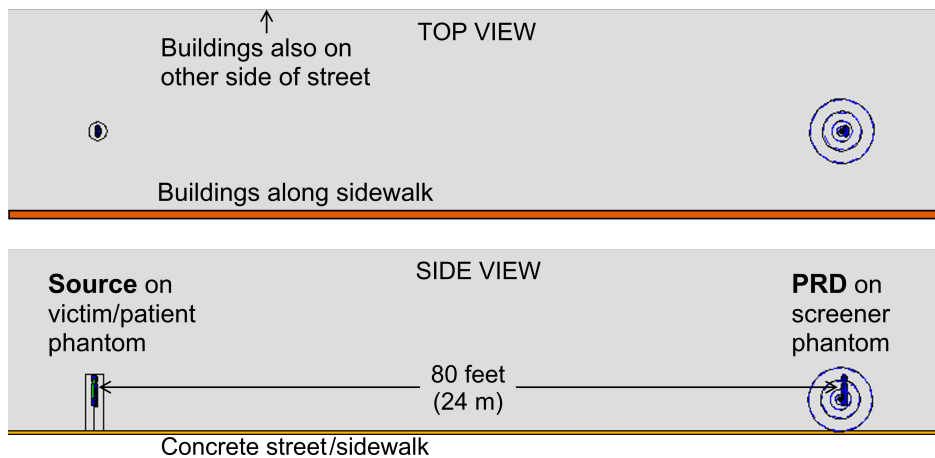


Figure 4-9 MCNP model for calculating distance to first-stage prescreening

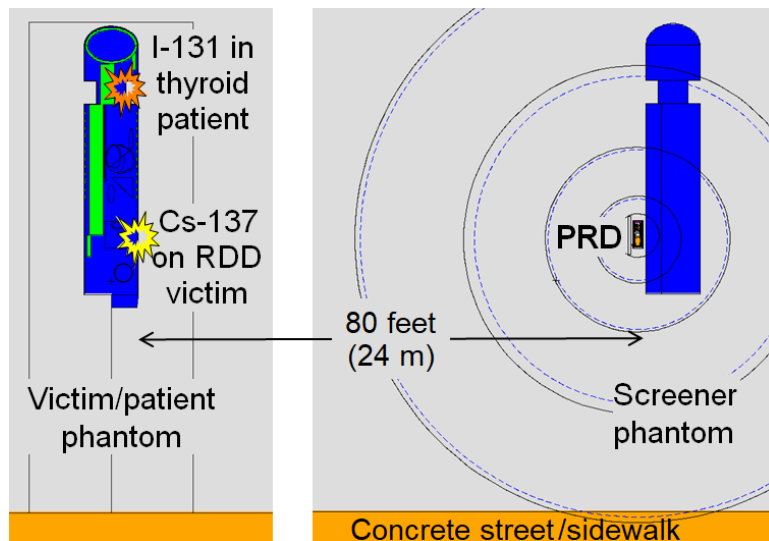


Figure 4-10 Details of MCNP model for calculating distance to first-stage prescreening

²⁰ The legs of the phantoms are not visible in the figure because the profile view shown is a slice down the middle between their legs.



For a medical patient who might cause misattributed alarms at large distances, we repeated the calculation at a distance of 80 feet, but with I-131 in the thyroid gland of the source phantom instead of Cs-137 near the navel of the phantom. We looked in the medical literature for how much I-131 could be in the thyroid gland of someone after receiving a therapeutic dose of I-131. [21] We found that the amount of I-131 typically remaining in the thyroid 10 days after a patient is treated for hyperthyroidism could cause a PRD to alarm 80 feet away. That is, up to 10 days after treatment, these nuclear medicine patients can retain enough radioactivity to cause misattributed alarms at even larger distances than our design-case RDD victim.

Other nuclear medicine procedures can leave patients with sufficient radioactivity to trigger CRC alarms when the patient is screened that can be confused with alarms from contamination. We recommend that CRCs have radionuclide identification devices (also called radioisotope identification devices or RIIDs) at the decontamination area and the handheld screening area to recognize nuclear medicine patients and determine whether they might also be contaminated by the radiological incident.

For calculating the distance between the first-stage and second-stage prescreening stations (distance “3” in [Figure 4-1](#)), the only difference is that the PRD in second-stage prescreening is approximately 9 inches (23 cm) away from a person undergoing second-stage prescreening rather than being worn by the first-stage screener. The calculated distance at which the contamination on the design-case RDD victim would cause a PRD to alarm during second-stage prescreening on a city sidewalk is 75 feet (23 m). For simplicity, we recommend that the distance between the two prescreening stations be the same as the distance from the front of the line of people waiting to be prescreened to the first-stage prescreening station: 80 feet.

After most of the work for this report was done, NUSTL learned that Thermo Scientific is replacing the PRD-ER with a new model, the RadEye PRD-ER4. [11] The PRD-ER4 has a cesium iodide detector instead of a sodium iodide detector, giving it a 25% higher sensitivity for medium- and high-energy gamma rays. NUSTL wanted to know if the CRC prescreening and portal locations we determined using the PRD-ER would still work for a CRC where prescreening would be done using the PRD-ER4. Since the ER4 has a higher sensitivity, we thought perhaps distances 4 and 3 would need to be increased to avoid misattributed PRD alarms during prescreening. We repeated the calculation of the count rate in the PRD on the first-stage prescreener for a Cs-137 source on a phantom 80 feet (24 m) away (distance “4”), this time replacing the sodium iodide detector with a cesium iodide detector. The net count rate was 9% higher, but the background count rate and alarm threshold for the ER4 are also higher, so the required distance to avoid misattributed alarms is still 80 feet. (The net count rate is only 9% higher instead of 25% because most of the radiation reaching the PRD from the distant source on the RDD-victim phantom has scattered and has low energy.) The cesium iodide detector of the ER4 has a higher sensitivity for high-energy gamma rays, but the sodium iodide detector in the PRD-ER is already maximally efficient for detecting low-energy photons. Therefore, distances “4” and “3” would not need to be changed if prescreening uses the newer PRD-ER4.

For Cs-137 and other radionuclides that emit high-energy gamma rays, prescreening with PRD-ER4s can detect lower amounts of contamination than prescreening with PRD-ERs. However, those who want to plan CRCs using PRD-ER4s and a single layout for the portals should not decrease the 15-foot distance between portal approach lanes. An RDD might be made with a radionuclide such as Am-241 that emits low-energy gamma-ray photons, for which the detection efficiency of the PRD-ER4 is no higher than that of the PRD-ER.



5.0 FINDINGS AND RECOMMENDATIONS

This section gives recommendations and findings for radioactive contamination screening based on the results of NUSTL's measurements and calculations described in sections 3 and 4.

Recommendations and core findings are marked with a bullet (●). Additional information provides context and gives reasons for the recommendations.

This is not a comprehensive list of instructions for how to operate a CRC safely, effectively, and efficiently. Each recommendation should be considered together with possible supplemental planning and operations needed to support the recommendation.

While someone is being screened at a CRC, a radiation detection alarm can be caused by radioactivity on or in that person (a true alarm), random fluctuations in the background reading of the device (a false alarm), or radioactivity on someone or something else nearby. For alarms that occur while an uncontaminated person is being screened that are actually caused by radioactivity on someone else, we use the term "misattributed alarms". [4] [5] Misattributed alarms could cause confusion and delays, reduce throughput, and undermine public confidence. At CRCs, misattributed alarms could happen in the pedestrian radiation portal monitors used for whole body screening and in the PRDs used for prescreening.

Optimum CRC throughput requires minimizing misattributed alarms and the delays they cause as well as minimizing the screening time at each station and the walking time between radioactivity screening stations. These goals conflict with each other, so optimum throughput requires trade-offs. For maximum CRC throughput, screening locations need to be separated by distances sufficiently large to avoid a lot of misattributed alarms, but otherwise as close together as possible to minimize walking time between them and keep the area of the whole CRC operation to a manageable size.

If a CRC is set up in NYC, FDNY would conduct sensitive whole-body screening using Ludlum model 5-1-1 pedestrian radiation portal monitors. Because the portal monitors will alarm in response to external radiation sources with relatively low activity,

- It is essential to prescreen people outside the CRC portal area using less-sensitive instruments such as PRDs and divert highly and moderately contaminated people for decontamination before they approach the portal monitors.

5.1 PORTAL MONITOR SPACING

FDNY asked NUSTL how far apart the portals should be spaced. To determine the minimum distance between portal monitors that will avoid misattributed alarms, NUSTL measured the count rate sensitivity of a Ludlum model 5-1-1 portal monitor to radiation from sources outside the portal and the angular dependence of the sensitivity. The measurement results showed that the maximum sensitivity is directly to the side of the portals. That position is also where people approaching or leaving a portal in a CRC would pass most closely to adjacent portals. Consequently:

- The most important spacing between the portal monitors to avoid misattributed portal alarms is the spacing between the portal approach lanes.

In addition to the portal monitor count-rate sensitivity measurements with stationary sources, NUSTL performed "walk-beside" tests: one person walked through the portal to trigger the occupancy sensor while a second person walked in parallel at a measured distance away while carrying a known



source. The walk-beside measurements determined the amount of radioactivity that will cause a portal monitor to alarm at a given distance. A person with 22 μCi of Cs-137 contamination on them will produce a count rate just below the alarm level when they walk past a portal on a path 15 feet from the center of the portal. Together with measurements showing that two-stage prescreening can detect 22 μCi of spread-out Cs-137 contamination, this provided the answer to FDNY's initial question about how far apart the portals should be spaced:

- The spacing between portal approach lanes should be 15 feet (4.6 m).
- The optimal portal approach-lane spacing does not depend on the radionuclide²¹ or the amount of radioactivity released in an RDD incident. It depends only on the prescreening sensitivity.
- The 15-foot portal approach-lane spacing is also appropriate for CRCs set up in response to radiological emergencies other than an RDD.
- Even CRCs with just one portal monitor should keep people waiting to be screened at least 15 feet away from the portal.

5.2 PORTAL MONITOR POSITIONING

In NYC, most prospective CRC locations are high schools, where the portal monitors for whole-body screening would be in the gymnasium. FDNY asked NUSTL to determine the optimal layout of the portal monitors in a space the size of a high-school basketball court.

- [Figure 5-1](#) is a drawing of the recommended layout of portal monitors in the space of a high-school basketball court.

The six small, numbered rectangles in the figure represent the portal monitors, and the dashed lines are the paths people would follow to go through the portals one at a time. Dimensions are given in feet.

The approach-lane spacing is 15 ft. The portal locations are staggered so contaminated people who may be rescreened or otherwise delayed at a portal would be even farther (22 ft) from adjacent portals where others would continue being screened. The walking paths leading to and from the portal approach lanes are outside the side lines of the court, providing sufficient distance to avoid alarms from people walking along them even if the second-stage prescreening described in [5.5.2](#) cannot be performed.

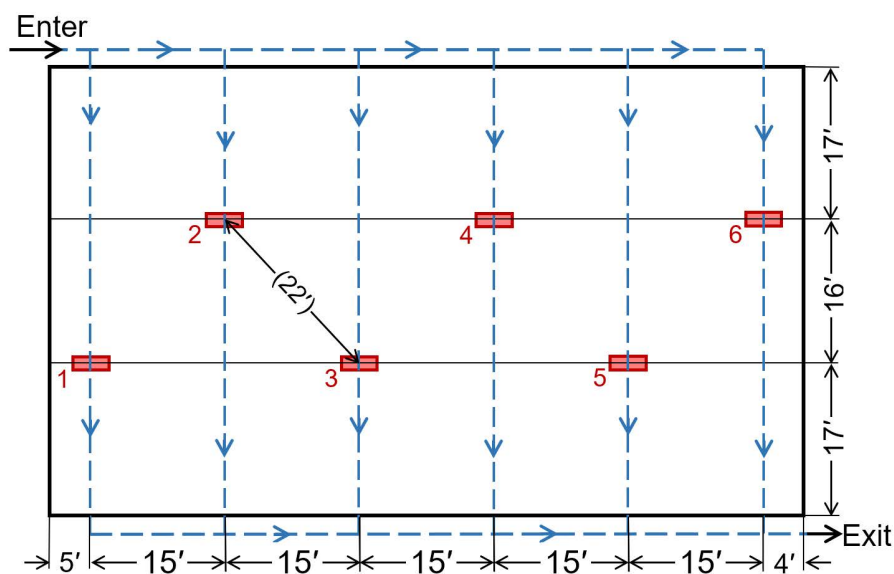


Figure 5-1 Recommended layout of portal monitors in the space of a high-school basketball court

²¹ For radionuclides that emit energetic gamma rays, x rays, and/or beta particles.



Using this layout in a gymnasium not much longer than its basketball court depends on having doors at diagonally opposite corners of the room or near the centers of each end so potentially contaminated clients do not walk close to the portals at the ends. If more than six portal monitors are available and the room is sufficiently long, more portals can be added using the same spacing pattern with the portal approach lanes 15 feet apart.

- If clients go through the first-stage and second-stage prescreening procedures described in [5.5.1](#) and [5.5.2](#), the layout in [Figure 5-1](#) will avoid misattributed portal alarms from contamination on clients in the room regardless of the order in which people are sent to each portal.
- If sufficient personnel are not available to do second-stage prescreening, the recommended layout will be effective with just first-stage prescreening if clients are sent sequentially to non-adjacent portals.

5.3 WHOLE-BODY SCREENING PROCEDURES

FDNY has full procedures for whole-body screening, including having portal operators give people a form showing whether they triggered an alarm and, for those who do, which of the portal's four detectors alarmed. The suggestions below may be useful to other agencies and as a supplement to FDNY's procedures to help recognize and address false and misattributed alarms.

FDNY flow-control procedures for whole-body screening send people sequentially to non-adjacent portals, for example, to portal numbers 1, 3, 5, 2, 4, 6 in [Figure 5-1](#). This practice is recommended when there are no delays or interruptions at any of the portals. However, that pattern of pedestrian traffic control can be difficult to maintain with people walking at different speeds and sometimes being delayed at a portal. With the recommended layout and prescreening procedures, people may be sent in any order to any portal that is available.

- When there is a portal alarm, the portal operator should send the person being screened back through the portal, perhaps twice, to determine if the alarm was caused by radioactivity on/in that person or might be a false or misattributed alarm.
- If just one portal has alarmed and the person triggers an alarm on their second pass through the portal, the person should be sent for follow-up handheld screening and decontamination.
- If just one portal has alarmed and the person does not trigger an alarm on the second and third pass through the portal, the original alarm was most likely a false alarm. The person can be considered as not contaminated and should be reassured that false alarms occasionally occur. (Calculations predict an average of about 1 false portal alarm per 5,000 screenings.)
- If two or more portals in the CRC alarm at nearly the same time, one or more of them may be a misattributed alarm. Pause portal screening and have the clients at the alarming portals return to the sideline path. Then, check the portal background readings and communicate with staff at upstream prescreening stations to learn if they have just observed unusually high radiation levels that may indicate the presence and location of a highly contaminated person or other source of radiation. When the person or source of the high radiation levels has been decontaminated or removed, or if there are no high readings, have the clients who seemed to cause an alarm go through their portals again one at a time.

The delay that would be caused by this procedure to find out who is actually contaminated if multiple portals alarm is one reason the screening procedures recommended in this report were designed to minimize the number of misattributed alarms.



5.4 HANDHELD SCREENING

When radioactive contamination is detected on someone during whole-body screening, that person should be sent for follow-up handheld screening to locate where on their body the contamination is, so it can be removed. FDNY would use Ludlum 26-2 integrated pancake-probe detectors for handheld screening.

One of the initial questions FDNY asked NUSTL was “If radioactive contamination on someone causes a portal monitor to alarm, will handheld screening with a pancake-probe detector be able to find the contamination on the person?” NUSTL was able to answer this question for external contamination (*on* the body or clothes of someone, rather than inside their body). The answer depends on the type of radiation the radionuclide emits: pancake probe detectors are more efficient for detecting beta and alpha particles than for detecting gamma rays.

- If contamination with a radionuclide that emits energetic beta or alpha particles on someone causes a portal monitor to alarm, handheld screening performed according to CDC guidance [23] will almost always be able to locate the contamination.²²
- For contamination with radionuclides that emit only gamma rays, the pancake probe detector might not alarm during handheld screening for the minimal amount of contamination on a person that can cause a portal alarm. At 1 inch from the body’s surface, the pancake probe detector will alarm if the contamination is concentrated in a small area, but not if it is spread out over the body.
- If the RDD radionuclide emits only gamma rays, inform personnel performing handheld screening that they may not be able to locate small amounts of such contamination and prepare them to reassure clients when this occurs.

Even for beta and alpha emitters, there are some cases where the pancake-probe detector might not alarm. One situation is if 1 μCi of contamination is spread out extremely evenly over most of a person’s body, so it has no specific location. Another is if the slight contamination is spread out over a moderate area of a person’s skin beneath uncontaminated clothing that blocks the particles.

- Generally, personnel doing handheld screening can rely on the alarm and not attempt to read the numeric display while scanning.
- If there is no alarm during handheld screening of someone whose contamination caused a portal alarm, the screener can try to locate the contamination by scanning again while listening to the audio beeps or clicks and reading the numeric display to look for elevated count rates.
- If the contamination still cannot be located, have the person remove their outer clothing and scan again.

Detecting small amounts of contamination in follow-up handheld screening is not essential. Decontamination can proceed without this information.

Our tests did not determine what level of *internal* contamination handheld screening can detect, for example if a person inhaled radioactive dust and afterwards washed off their external contamination.

²² CDC guidance for handheld screening calls for holding the probe $\frac{1}{2}$ inch to 1 inch from the surface of the person being screened and scanning the probe at 1 inch per second.



- Even if the contamination cannot be located by handheld screening, people with a confirmed alarm during whole-body screening should be sent to decontamination, where they can be assessed for internal contamination.

5.5 PRESCREENING METHODS

The section on CRC operations in the CDC's *Population Monitoring in Radiation Emergencies* [1] includes a recommendation that one or more staff members with radiation detection equipment perform initial sorting. That is, they should walk the line of people waiting to be screened in order to identify people in need of priority care or services, such as those who are highly contaminated, have small children, might have medical problems, etc. The prescreening methods developed by NUSTL are not intended to replace such initial sorting, but rather to supplement it in the case of an RDD or similar concentrated radiological incident.

With the prescreening methods described below, initial sorters do not need to deliberately search for contaminated people, just wear a PRD while they walk near waiting people to perform their other tasks. If their instrument alarms, they can attempt to find the person who caused the alarm and send or escort them to the decontamination area. The exposure rate at 3.3 feet (1 m) from people with enough contamination to cause misattributed alarms when they reach the front of the line for prescreening would be over 2 mR/h, which is enough to trigger a typical *second-level* alarm on a PRD. In addition, crowd control personnel equipped with PRDs could also assist in detecting highly contaminated people waiting in line.

FDNY would perform prescreening using Thermo Scientific RadEye PRD-ER personal radiation detectors. Working with FDNY, NUSTL developed methods for two stages of prescreening and measured the minimum amount of Cs-137 contamination each method can detect as well as how fast it can screen people. In both stages, prescreening can rely on the PRD's alarm.

- Screeners do not need to look at the PRD display during prescreening unless there is an alarm.

To avoid interrupting the staff doing the prescreening (screeners) and maintain throughput, if sufficient staff are available,

- Another staff person, whom we will call a "conductor," should be present at each prescreening station to maintain communication with other CRC staff, assist in resolving alarms, reassure people who trigger an alarm, and perhaps escort those individuals to the decontamination area.



5.5.1 FIRST-STAGE PRESCREENING METHOD

- The recommended method for first-stage prescreening is illustrated in [Figure 5-2](#).

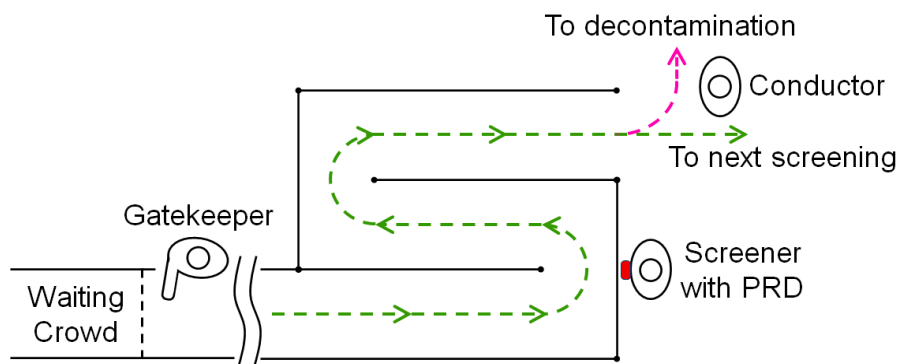


Figure 5-2 First-stage prescreening with S-shaped path

People being screened (clients) would walk toward the screener, turn 180 degrees as they walk past without stopping, then turn 180 degrees again, moving along an S-shaped path. The path can be delimited by portable barriers. The serpentine path serves the purpose of directing clients who have just been screened back toward the screener. If radioactivity on someone causes the PRD to alarm, the screener can then re-scan the clients who just went past, identify the contaminated person, and direct them to the decontamination area. In the event that it is raining or snowing during CRC operation, this method would work with people holding umbrellas.

The S-path prescreening method is not sensitive enough to be the only prescreening to avoid misattributed portal monitor alarms inside a CRC unless strict traffic control to send people sequentially to non-adjacent portals is constantly maintained.

The S-path prescreening method can prescreen up to 1,200 people per hour if there are few alarms. This is a higher throughput than the other screening stages are likely to achieve, so the rate of clients being sent to first-stage prescreening should be controlled to be roughly the same as the throughput of the slower second-stage prescreening in order to minimize the number of people waiting to pass through the next station. To maintain the optimum throughput,

- Have a staff person (gatekeeper) at the front of the line of people waiting to be screened to control when each person or group starts walking toward the first-stage prescreening station.

Highly contaminated people in the line of clients waiting to enter the CRC can cause misattributed PRD alarms at the first stage of prescreening unless the front of the queue is a considerable distance—up to 80 feet (24 m)—from the first prescreening station (see [5.6.4](#)). NUSTL did not test whether it is better to send people from the front of the queue to the first-stage prescreening station one at a time or in groups with pauses between the groups. The best method will depend on the percentage of clients who trigger an alarm; it can and should be determined during actual CRC operation. [\[5\]](#)

- A first-stage prescreening alarm might be caused by radioactivity on any of the clients approaching the S-path as well as those already in the "S".
- When there is a first-stage prescreening alarm, the gatekeeper must pause client traffic from the front of the line. Then, the screener, assisted by the first-stage conductor, determines which



person or persons triggered the alarm by reading the display of the PRD while rescanning the people who were just screened and screening the clients who were walking toward the S-path.

- Even for response organizations planning CRCs with very limited available personnel, PRDs, and portals, first-stage prescreening is strongly recommended for radiological incidents where people could be contaminated with activities above 100 μCi (3.7 MBq) or in which the RDD activity is more than about 2 Ci (74 GBq).
- If there are insufficient resources to do second-stage prescreening, first-stage prescreening using the S-path method would be sufficient to avoid misattributed portal alarms if the portal approach lanes are spaced 30 feet apart or if they are spaced 15 feet apart (as shown in [Figure 5-1](#)) with strict client traffic control to send people sequentially to non-adjacent portals.

5.5.2 SECOND-STAGE PRESCREENING METHODS

- Recommended methods for second-stage prescreening involve at least one screener using a PRD on a long handle to scan upward from shin level to overhead in front of each client. The back of the client must also be scanned.
- The PRD should be 6 to 12 inches (15 to 30 cm) from the client's body while scanning, and the vertical scan should take 1 to 1.5 seconds.

The general second-stage prescreening method is to have the clients wait about 10 feet from the screening spot, walk one at a time in a straight line and stop with their feet in a marked outline on a ramped platform on the floor.²³ The screener stands to the side of the client's path and holds the handle angled downward in front of the client so that the PRD is at shin level. As soon as the client stops, the screener scans the PRD up the front of the client and over their head, allowing the client to pass under the handle and walk away. The same screener can scan the PRD down the back of the client before the client is told to go, but the operation is much faster if the scan down the client's back is performed by a second screener while the first screener scans the client's front. Either version of this method (whether using one or two screeners) can detect 22 μCi (0.8 MBq) of Cs-137 contamination, even if it is spread out over the client's body. The two-screener version for second-stage prescreening is illustrated in [Figure 5-3](#).



Figure 5-3 Second-stage prescreening by two screeners using PRDs on long handles

If sufficient personnel are available,

- Perform second-stage prescreening using the two-screener version of the method for scanning the front and back of clients ([Figure 5-3](#)).

²³ See section 5.5.3.



- To maintain the required sensitivity, screeners should be trained to wait until both of a client's feet have stopped in the marked position and to take at least a full second to perform each scan.
- To avoid PRD alarms caused by contamination on those who are waiting to go through second-stage prescreening, the front of the line for second-stage prescreening should be 10 feet (3 m) from the marked position.

Using the two-screener version, scanning a client, including the client's walking time, can be completed in less than 4.5 seconds and the method can screen up to 800 people per hour if there are few alarms and the screeners are not fatigued. [20] If both personnel and PRDs are critically limited, one screener can scan both the front and back of each client, but that will take about 6.5 seconds, limiting throughput to no more than 550 people per hour.

- The handle for the PRD should be similar to a broom or mop handle: about 4 feet (1.2 m) long.

The PRD can be mounted on the handle in many different ways. Some suitable methods are described in [Appendix D](#). The orientation of the PRD influences the sensitivity of the screening method.

- Mount the PRD so that its long dimension is parallel to the handle. The PRD and any mounting devices at the end of the handle should be protected from potential contamination by covering them with a small plastic bag. The mounted PRD should have no material thicker than a plastic bag covering or obscuring the PRD's detector.
- Scan with the detector side facing the client.

Facing the detector side of the PRD toward the client with no intervening material optimizes screening sensitivity. This is especially important if the event involves a radionuclide such as Am-241 that emits low-energy photon radiation or one such as Sr-90 that emits only beta-particle radiation.

5.5.3 DETECTING CONTAMINATION ON SHOES

Radioactive contamination on clients' shoes could be tracked into the CRC and contaminate the facility's floor covering, which could shut down CRC operations until the contamination is removed.

- Do not have people remove and carry their shoes, because they might contaminate their hands and clothing in the process and because walking through the CRC without shoes increases the chance of injuries.

Instead:

- Prescreen clients' shoes during second-stage prescreening by having the clients stand on a small, raised platform with a PRD under it.
- The platform should have gently sloped ramps leading to and from it so it will not be a trip hazard.
- To protect it from possible contamination, cover the ramped platform with removable nonslip material like that used on the portal approach lanes.
- Place the PRD under the ramped platform with its detector side up (as shown in [Figure 3-10](#)).
- Mark the center of the platform to show clients where to place their feet; the feet should be close together so both feet will be close to the PRD underneath.



NUSTL used a wheelchair ramp for a commercial cable protection system²⁴, but other ramps and platforms are acceptable. The platform needs to have space underneath it for the PRD but not be much higher than the PRD and must not pose a trip hazard. To avoid blocking radiation, the material over the PRD should be relatively thin and light (low density) such as plywood, fiberboard, plastic less than ½ inch (12 mm) thick, or thin aluminum.

The PRD under the ramped platform can detect and alarm in 1 second for less than 2 µCi (74 kBq) of Cs-137 or other gamma-emitting radionuclides on a person's shoe soles. If second-stage prescreening is done while clients stand over a PRD on the floor, the clients' shoes can be screened without slowing the prescreening process at all.

If there are insufficient resources to do second-stage prescreening, consider finding another spot outside the CRC where clients can momentarily stop for shoe prescreening or consider another solution. Some CRCs rely on sticky pads that clients step on to remove contamination from the soles of their shoes before entering the CRC. This solution, however, is less than ideal for the NYC CRCs because it does not detect remaining contamination on shoes, and it may be impractical because the high throughput would quickly degrade each layer of the pads, requiring staff to continually monitor and maintain the pads.

5.5.3.1 REMOTE AUDIBLE ALARM ACCESSORY

Because the PRD used to prescreen shoes is hidden beneath the platform, the PRD's alarm light cannot be seen and prescreening personnel must rely on the PRD's audible alarm. Unfortunately, the ramp muffles the alarm sound, and the use of HazMat personal protective equipment can make it even harder to hear the alarm sound and impractical to use headphones. At the request of FDNY, NUSTL developed a remote audible alarm accessory to amplify the alarm sound from the PRD underneath the ramp.

- If it is difficult to hear the alarm from the PRD used to screen clients' shoes, use the remote alarm accessory.

The remote alarm accessory box would be placed on the ground just outside the ramp and connected to the PRD's audio output jack with an audio cable. The accessory provides a loud alarm sound that can be easily heard, and it does so without the use of batteries or external power, so it can be stored indefinitely and always be ready for use. A detailed description of the remote audible alarm accessory is given in [Appendix B](#).

Because the display of the PRD cannot be seen while it is under the ramp,

- Regularly test the operation of the shoe-screening PRD with a radiation check source and/or remove the PRD from under the ramp to examine the display and battery charge level.

5.6 WAITING AND PRESCREENING LOCATIONS

5.6.1 WAITING LINE

To be sufficiently far from the portals, the line of people waiting to go through prescreening might need to be outdoors outside the CRC building.

²⁴ Ultra-Sidewinder Large and Ultra-Sidewinder Ramp, large; <https://www.spillcontainment.com/products/sidewinders-cable-protection/>.



Buildings other than the CRC building can also provide shielding to reduce radiation levels at the prescreening stations and portal area caused by radioactivity on clients in the waiting line.

- In built-up urban areas, if the waiting line is outdoors and long, consider bending it around a street corner so buildings provide radiation shielding.

5.6.2 PRESCREENING STATIONS

Based on calculations benchmarked by measurements, NUSTL determined values for four minimum distances from prescreening stations that are necessary to avoid misattributed alarms for our design-case scenario:

1. From the portals to first-stage prescreening
2. From the portals to second-stage prescreening
3. Between the first-stage and second-stage prescreening stations
4. From first-stage prescreening to the front of the line of people waiting to be prescreened and to the decontamination area

These distances are shown schematically in [Figure 5-4](#).

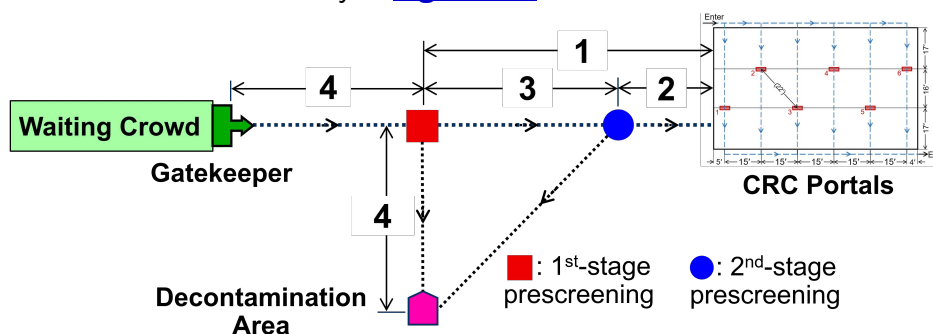



Figure 5-4 Distances calculated in order to avoid misattributed alarms

The values for distances 1, 3, and 4 given in sections [5.6.3](#) through [5.6.6](#) below are for our design-case scenario of an explosive RDD made with 2000 Ci of Cs-137 and a relatively small amount of explosive.

5.6.3 DISTANCE FROM PRESCREENING STATIONS TO PORTAL MONITORS

To avoid multiple misattributed portal alarms or the false appearance that there is contamination inside the CRC:

- Locate the first-stage prescreening station outside the CRC building at a considerable distance from the portal monitors (distance 1 in [Figure 5-4](#)).
- Distance 1 depends on shielding provided by the building materials: from 80 feet (24 m) for a building with brick exterior walls and a concrete roof to 250 feet (76 m) if there is no building at all. Values for distances 1–4 for these and other building types are shown in the figures in section [5.6.6](#).
- The second-stage prescreening station can be located inside the CRC building. The distance from second-stage prescreening to the nearest portal (distance 2 in [Figure 5-4](#)) should be at least 35 feet (11 m) if there are no intervening walls or 25 feet (8 m) if there is an intervening masonry or



brick wall. Distance 2 depends on the sensitivity of first-stage screening, not on the activity released in the incident.

5.6.4 DISTANCE TO FIRST-STAGE PRESCREENING AND BETWEEN PRESCREENING STATIONS

Misattributed alarms can occur during prescreening as well as during whole-body screening. NUSTL performed calculations for our design-case incident to determine the minimum distance from the front of the line of unscreened people waiting to enter the CRC to the first-stage prescreening station (distance 4) and between the first-stage and second-stage prescreening stations (distance 3) that will avoid misattributed PRD alarms during prescreening:

- Locate the first-stage prescreening station 80 feet (24 m) from the front of the line of people waiting to enter the CRC (distance 4 in [Figure 5-4](#)).
- Locate the second-stage prescreening station the same distance of 80 feet away from the first-stage prescreening station— (distance 3 in [Figure 5-4](#)).

5.6.5 DECONTAMINATION AREAS

Highly contaminated people and accumulated radioactive waste at the decontamination area could cause misattributed alarms and elevated background radiation levels unless the area is sufficiently far from all the screening stations.

- Locate the prescreening decontamination area at least as far from the portals as the first-stage prescreening area (distance 4 in [Figure 5-4](#)) and at least 80 feet (24 m) from both prescreening stations.

It may not be possible within the prescreening decontamination area to perform scans to determine if a person has been sufficiently decontaminated to proceed to whole-body screening, especially if other contaminated people are nearby or there is contaminated material in the area.

- Consider having two decontamination areas: one for people who trigger an alarm during prescreening and another for those who did not trigger a prescreening alarm but do trigger a portal alarm during whole-body screening. The second decontamination area can be located inside the CRC fairly close to the portals.
- Send people who have been decontaminated in the prescreening decontamination area back through first-stage prescreening (without waiting in line) before they proceed to whole-body screening.
- If people are being sent to the prescreening decontamination area faster than they can be decontaminated, establish a decontamination waiting area 80 feet (24 m) from the decontamination area and the prescreening stations.

5.6.6 DIAGRAMS OF PRESCREENING LOCATIONS

Below are diagrams showing recommended distances and examples of where prescreening stations should be located to avoid misattributed portal and PRD alarms for CRCs in three types of buildings and outdoors on open ground. As previously stated, these distances are starting values for our design-case RDD scenario and should be adjusted according to the nature of the event.



5.6.6.1 BUILDING WITH BRICK EXTERIOR WALLS

- [Figure 5-5](#) shows the distances between screening stations for a CRC in a building such as a NYC high school with structural brick exterior walls and a concrete-block interior wall around the gymnasium with the portal monitors.

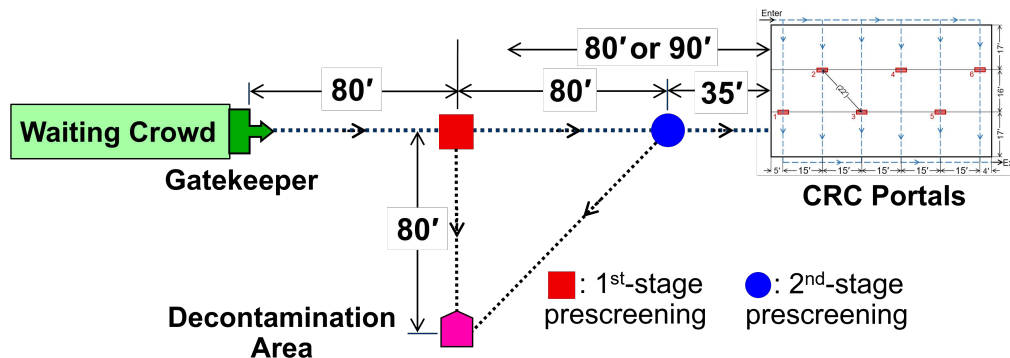


Figure 5-5 Distances between screening stations for a CRC in a building with brick walls

Distances are given in feet. The red square represents the first-stage prescreening station and the blue dot represents the second-stage prescreening station. The decontamination area in the figure is the prescreening decontamination area. If the building has a concrete roof, the distance from the portals to first-stage prescreening (distance 1 in [Figure 5-4](#)) can be 80 feet (24 m). Without the radiation shielding provided by a concrete roof or additional building floors above, the minimum distance should be 90 feet (27 m). If there is a second-stage prescreening station between first-stage prescreening and the portal area, the 10-foot difference will not matter because the sum of the recommended distances from first-stage prescreening to second-stage prescreening and from second-stage prescreening to the portals (distances 3 and 2 in [Figure 5-4](#)) is greater than 90 feet.

- [Figure 5-6](#) shows example locations of the screening stations on city streets for a CRC in a large school with brick exterior walls on three sides.

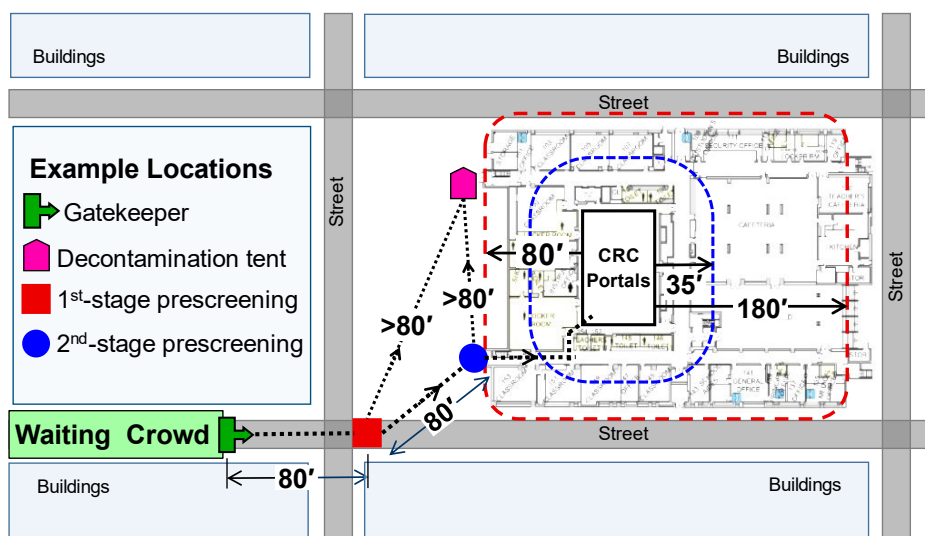


Figure 5-6 Locations of screening stations on city streets for a CRC in a brick building



The first-stage prescreening station must be outside the dashed red line outside the building, and the second-stage prescreening station must be outside the blue dashed line 35 feet from the area with the portals. The decontamination area is shown as a tent.²⁵ In this example, the gymnasium is near the center of the school, so almost any location outside the building would be at least 80 feet (24 m) from the portal monitors inside the gymnasium. In such a case, First-stage prescreening could be closer than the location shown without causing portal alarms. However, second-stage prescreening is also located outside the building (in order to provide a direct path to decontamination), and first-stage prescreening must be 80 feet away from there.

5.6.6.2 BUILDING WITH 4-INCH-THICK CONCRETE-BLOCK WALLS

- [Figure 5-7](#) shows the distances between screening stations for a CRC in a building such as a warehouse with a 4-inch-thick concrete-block exterior wall, no interior walls, and a thin roof.

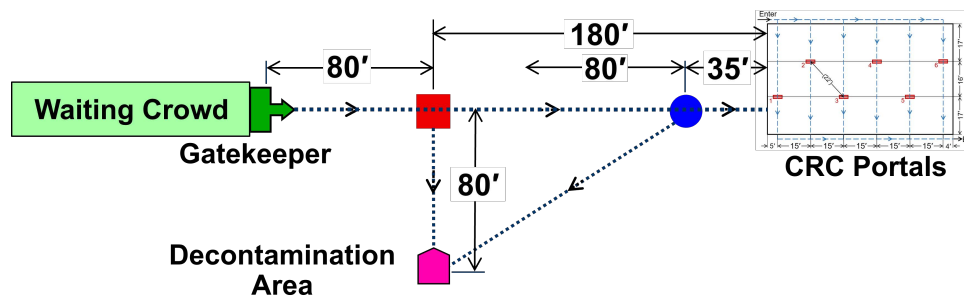


Figure 5-7 Distances between screening stations for a CRC in a warehouse-like building

As in the previous two figures, the red square is the first-stage prescreening station and the blue dot is the second-stage prescreening station. For this thin-walled building, the first-stage prescreening station should be 180 feet (55 m) from the nearest portal monitor and the decontamination area should be at least that far from the portals.

- [Figure 5-8](#) shows example locations of the screening stations on city streets for a CRC in a building like the one considered above: a warehouse with a 4-inch thick concrete block wall.

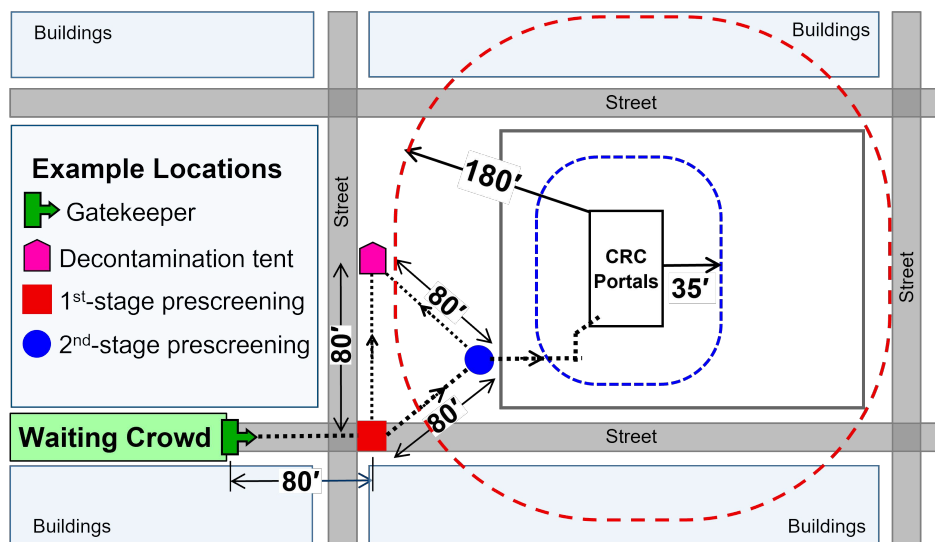


Figure 5-8 Locations of screening stations on city streets for a CRC in a warehouse-like building

²⁵ One of the tents that FDNY would use as decontamination areas is shown in the cover photograph.



The first-stage prescreening station must be outside the dashed red line outside the building, and the second-stage prescreening station must be outside the blue dashed line at 35 feet from the portals. With very little shielding provided by the building wall, the first-stage prescreening station and decontamination area have to be at least 180 feet from the portal monitors inside.

5.6.6.3 OPEN GROUND

- [Figure 5-9](#) shows the spacing distances between screening stations for a CRC set up on open ground such as a field or large parking lot.

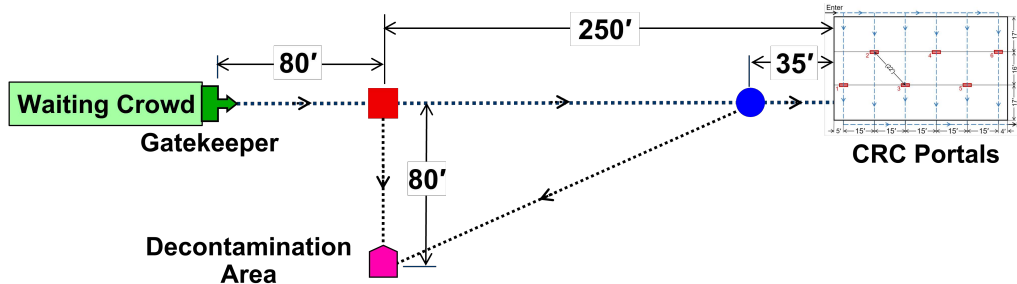


Figure 5-9 Distances between screening stations for a CRC on open ground

With no building to provide shielding, the first-stage prescreening station and decontamination tent must be 250 feet (76 m) away from the portal monitors. The distance from the first-stage prescreening station to the decontamination tent and the front of the waiting crowd can be the same as for prescreening on a city sidewalk—80 feet.

5.6.7 ADJUSTMENTS TO PRESCREENING DISTANCES

The values given above for distances 1, 3, and 4 in [Figure 5-4](#) are for our design-case scenario of an explosive RDD made with 2000 Ci of Cs 137 and a relatively small amount of explosive.

- Those distances should be taken as starting values and adjusted according to the nature of the event and the layout of the area around the CRC.
- If the most practical locations for prescreening are at larger distances, use those locations.
- If the activity released in the incident is known to be much greater than 2000 Ci, use larger distances.
- If the activity of an exploded RDD or similar accidental release is known to be less than 200 curies (7.4 TBq), the starting values for distances 1, 3, and 4 in [Figure 5-4](#) can be cut in half without increasing misattributed alarms.
- If no misattributed alarms or elevated background rates are observed during CRC operations, the prescreening distances can be decreased if it is convenient and useful to do so.
- Do not decrease the portal approach-lane spacing or the distance from the second-stage prescreening station to the nearest portal (distance 2 in [Figure 5-4](#)). These two distances depend only on prescreening sensitivity, not the activity released in the incident.

5.7 PRESCREENING FLOW CONTROL AND COMMUNICATION BETWEEN SCREENING STATIONS

To avoid pile-ups of clients at any of the screening stations, warn downstream stations when highly contaminated clients arrive and tell upstream stations to pause client traffic when alarms and other delays occur,



- Establish and maintain communication between personnel at all the screening stations: gatekeeping, prescreening, decontamination area, whole-body portal screening, and follow-up handheld screening.

Even with the large separation distances we recommend, there can still be misattributed PRD and portal alarms from heavily contaminated RDD victims, such as those who do not change clothes and shower before going to a CRC, or if certain nuclear medicine patients go to a CRC. When such people reach the front of the waiting line, the PRD at first-stage screening and instruments at the decontamination area will alarm. If such people reach the first-stage prescreening station, and when they reach the decontamination area, the portals' background count rate will rise and the PRD at second-stage prescreening and possibly the portal monitors will alarm. Good communication between the screening stations can explain what happened, pause client traffic, and restore normal client flow with minimal delay.

5.8 NUCLEAR MEDICINE PATIENTS

Many people are given radioactive materials internally to treat or diagnose a medical condition, and radiation detection instruments used by first responders frequently alarm when encountering nuclear medicine patients. Nuclear medicine patients who come to a CRC following a radiological dispersal incident could be confused with people contaminated by the incident, and some could cause misattributed alarms. Most of the radionuclides used medically have short half-lives or are given in small amounts, so most nuclear medicine patients will not cause misattributed alarms. One exception is I-131, used to treat cancer of the thyroid gland and frequently used to treat hyperthyroidism. NUSTL found that the amount of I-131 typically remaining in the thyroid 10 days after a patient is treated for hyperthyroidism [\[21\]](#) could cause a PRD to alarm 80 feet away. That is, up to 10 days after treatment, these nuclear medicine patients may emit more radiation than our design-case RDD victim, and such patients could cause misattributed portal alarms at even larger distances. Other nuclear medicine procedures can also leave patients with sufficiently radioactivity to trigger alarms at a CRC that can be confused with alarms from contamination.

- Have radionuclide identification devices (also called radioisotope identification devices or RIIDs) at the decontamination area and the handheld screening area to recognize nuclear medicine patients and determine whether they might also be contaminated by the radiological incident.

5.9 RADIONUCLIDES OTHER THAN CESIUM-137

NUSTL performed measurements and calculations to determine if radionuclides emitting different kinds of radiation would require different procedures, a larger portal separation distance, or larger prescreening station separation distances than those required for an RDD made with Cs-137. We considered Sr-90, which emits beta particles, Co-60, which emits two high-energy gamma rays, and Am-241 and Ba-131 which emit low- and medium-energy gamma rays. In all cases, we found that:

- No changes to CRC screening are necessary for an RDD made with other radionuclides that emit energetic gamma-rays or beta particles. A CRC designed to avoid misattributed alarms for an RDD made with 2000 Ci of Cs-137 will also avoid misattributed alarms from an RDD made with similar activities of other radionuclides.

This is an important finding: there is no need to plan different screening procedures or locations for incidents involving different radionuclides.



6.0 SUMMARY

If there is a radiological release, whether from an accident or from a terrorist act, local response agencies can set up community reception centers (CRCs) to screen the public for radioactive contamination. This “Optimizing Radioactive Contamination Screening at Community Reception Centers Report” provides the Fire Department of the City of New York (FDNY) and other emergency response organizations with technical guidance for deploying CRC radiation detection equipment to optimize screening efficiency. The report provides specific recommendations based on the results of NUSTL’s measurements and calculations, including where to position the pedestrian radiation portal monitors used for sensitive whole-body screening and how and where to do prescreening with personal radiation detectors to avoid mistaken alarms and maximize CRC contamination screening throughput. The report includes an introduction to CRCs, describes FDNY’s CRC radiation detection equipment, and describes the methods NUSTL used to determine how and where to best use the equipment. Appendices provide full details of NUSTL’s measurements and radiation transport calculations and a remote audible alarm accessory device to aid in screening people’s shoes.



7.0 REFERENCES

- [1] Centers for Disease Control and Prevention, "Population Monitoring in Radiation Emergencies: A Guide for State and Local Public Health Planners, second edition," April 2014. [Online]. Available: <http://emergency.cdc.gov/radiation/pdf/population-monitoring-guide.pdf>. [Accessed 21 November 2019].
- [2] Centers for Disease Control and Prevention, "Population Monitoring and Community Reception Center (CRC) Resources," U.S. Centers for Disease Control and Prevention, 4 April 2018. [Online]. Available: <https://www.cdc.gov/nceh/radiation/emergencies/populationmonitoring.htm>. [Accessed 21 November 2019].
- [3] Centers for Disease Control and Prevention, "Radiation Dictionary," [Online]. Available: <https://www.cdc.gov/nceh/radiation/emergencies/glossary.htm>. [Accessed 2022].
- [4] G. H. Kramer, K. Capello, B. M. Hauck and J. T. Brown, "Sensitivity of portable personnel portal monitors: potential problems when dealing with contaminated persons," *Health Physics*, vol. 9, no. 4, pp. 367-372, 2006.
- [5] G. H. Kramer, K. Capello, B. Hauck, G. Moodie, A. DiNardo, L. Burns, A. Chaing, L. Marro and J. Brown, "A methodology for improving throughput using portal monitors," *Radiation Protection Dosimetry*, vol. 134, no. 3-4, pp. 152-158, 2009.
- [6] Interagency Scenario Working Group, "National Planning Scenario #11," Homeland Security Council and U.S. Department of Homeland Security, 2005. [Online]. Available: <https://www.phe.gov/Preparedness/planning/playbooks/rdd/Pages/scenario.aspx>. [Accessed 22 January 2020].
- [7] International Atomic Energy Agency, "The Radiological Accident in Goiania," 1988. [Online]. Available: https://www-pub.iaea.org/MTCD/publications/PDF/Pub815_web.pdf. [Accessed 15 December 2017].
- [8] J. M. Smith, A. Ansari and F. T. Harper, "Hospital management of mass radiological casualties: reassessing exposures from contaminated victims of an exploded radiological dispersal device," *Health Physics*, vol. 89, no. 5, pp. 513-520, 2005.
- [9] Armed Forces Radiobiology Research Institute, "Medical Management of Radiological Casualties, Fourth Edition," July 2013. [Online]. Available: <https://afrrri.usuhs.edu/sites/default/files/2020-07/4edmmrhandbook.pdf>. [Accessed 26 January 2022].
- [10] Thermo Scientific, Operating Instructions, RadEye PRD-ER, DB-066 E, Erlangen, Germany: Thermo Fisher Scientific Messtechnik, 2014.
- [11] Thermo Fisher Scientific Inc., "RadEye PRD and SPRD Personal Radiation Detectors Brochure," December 2020. [Online]. Available: <https://www.thermofisher.com/document->



connect/document-connect.html?url=https://assets.thermofisher.com/TFS-Assets%2FCAD%2Fbrochures%2FRadEye-PRD-SPRD-Brochure.pdf. [Accessed 1 June 2022].

- [12] Ludlum Measurements, Inc., "Ludlum Model 52-1, 52-5, and 52-6 Series Portable Scintillation Portal Monitors Technical Manual," February 2021. [Online]. Available: https://ludlums.com/images/product_manuals/M52-1_&_M52-4_&_M52-5_&_M52-6_Series.pdf. [Accessed April 2021].
- [13] Federal Emergency Management Agency, "FEMA-REP-21, Contamination monitoring standard for a portal monitor used for radiological emergency response," 1995. [Online]. Available: <https://remm.hhs.gov/FEMA-REP-21.pdf>. [Accessed 9 January 2020].
- [14] Ludlum Measurements, Inc., "Ludlum Model 26-2 Frisker User Manual," [Online]. Available: https://ludlums.com/images/product_manuals/M26-2.pdf. [Accessed 11 February 2020].
- [15] Ludlum Measurements, Inc., "Model 44-9 Alpha-Beta-Gamma Detector," [Online]. Available: <https://ludlums.com/products/all-products/product/model-44-9>. [Accessed 1 June 2022].
- [16] Fire department of the City of New York, "Community Reception Center Operations Manual, Version 2," New York, 2014.
- [17] American National Standards Institute, "N42.35-2016 - American National Standard for Evaluation and Performance of Radiation Detection Portal Monitors for Use in Homeland Security," IEEE, [Online]. Available: <https://ieeexplore.ieee.org/document/7551097>.
- [18] S. Chu, L. Ekström and R. Firestone, "The Lund/LBNL Nuclear Data Search," February 1999. [Online]. Available: <http://nucldata.nuclear.lu.se/toi/index.asp>. [Accessed 2017-2021].
- [19] A. R. Tilley and Henry Dreyfuss Associates, "Chapter 1, Anthropometry," in *The Measure of Man and Woman: Human Factors in Design, Revised Edition*, Wiley, 2001, pp. 10-32.
- [20] L. Finklea, A. Salame-Alfie and A. Ansari, "Time Motion Studies for Conduct of Population Monitoring During Functional Radiological Exercises at Community Reception Centers," *Disaster Medicine and Public Health Preparedness*, vol. 17, no. e237, pp. 1-8, 2023.
- [21] F. A. Mettler and M. J. Guiberteau, "4. Thyroid, Parathyroid, and Salivary Glands," in *Essentials of Nuclear Medicine and Molecular Imaging, 7th Edition*, Philadelphia, PA, Elsevier Health Sciences, 2018, pp. 85-115.
- [22] L. Lucas, L. Pibida, M. Unterweger and L. Karam, "Gamma-ray emitting test sources for portal monitors used for homeland security," *Radiation Protection Dosimetry*, vol. 113, no. 1, pp. 108-111, 2005.
- [23] Centers for Disease Control and Prevention, "Segment 1 of 4: Screening People for External Contamination: How to use Hand-held Radiation Survey Equipment," 4 April 2018. [Online]. Available: <https://www.cdc.gov/nceh/radiation/emergencies/screeningvideos/script1.htm>. [Accessed 29 May 2020].
- [24] Los Alamos National Laboratory, "MCNP Home," [Online]. Available: <https://mcnp.lanl.gov/index.html>. [Accessed February 2023].



- [25] C. J. Werner (editor), "MCNP User's Manual - Code Version 6.2, LA-UR-17-29981," (2017). [Online]. Available: https://mcnp.lanl.gov/pdf_files/TechReport_2017_LANL_LA-UR-17-29981_WernerArmstrongEtAl.pdf. [Accessed February 2023].
- [26] D. Krstic and D. Nikezic, "Debugging of ORNL Series of Mathematical Phantoms of Human Body," *Acta Physica Polonica A*, vol. 119, no. 3, pp. 279-281, 2011, [Online]. Available: <http://przyrbwn.icm.edu.pl/APP/PDF/119/a119z3p01.pdf>. [Accessed April 2019].
- [27] D. Krstic and D. Nikezic, "Input files with ORNL-mathematical phantoms of the human body for MCNP-4B," 2008. [Online]. Available: <https://www.pmf.kg.ac.rs/radijacionafizika/InputFiles.html>. [Accessed April 2019].
- [28] T. Booth, K. Kelly and S. McCready, "Monte Carlo Variance Reduction Using Nested DXTRAN Spheres," *Nuclear Technology*, vol. 168, no. 3, pp. 765-767, December 2009.



APPENDIX A. DETAILED DESCRIPTION OF MEASUREMENTS OF PORTAL EXTERNAL SENSITIVITY

This appendix gives a more detailed description of the measurements of the portal monitor count-rate sensitivity to external radiation sources that are summarized in section [3.1](#).

A.1 MATERIALS AND METHODS

Laboratory measurements of the count rate sensitivity of the portals to radiation from external sources and the angular dependence of the sensitivity were done by placing a portal in a long open space and placing a radioactive source of known activity at five measured distances from the center of the portal at nine different angles. Rather than move the source to the different angles, the source was kept in place at each distance and the portal was rotated. At first, we tried to do the measurements on the roof of the building where NUSTL is located so there would be minimal scattered radiation, but the background count rate varied too much during the day,²⁶ so the measurements were moved indoors to the loading dock of NUSTL's vehicle bay. The loading dock was chosen because it was the largest empty indoor space available, 38 feet x 15.3 feet (11.6 m x 4.7 m) with a 13.7-foot (4.2-m) high ceiling, minimizing scattering of radiation from the ceiling and walls. The center of the portal and the source were positioned 10 feet (3 m) from a brick wall with large wooden sliding doors along one side of the loading dock. [Figure 7-1](#) (identical to [Figure 3-1](#)) is a photograph of the setup for the measurements. The source was positioned with its active element 1 m above the floor by inserting it into a slot in a plastic-foam block mounted on an adjustable-height stand made from a 1.25-inch diameter acrylic plastic rod inserted into a three-legged base.

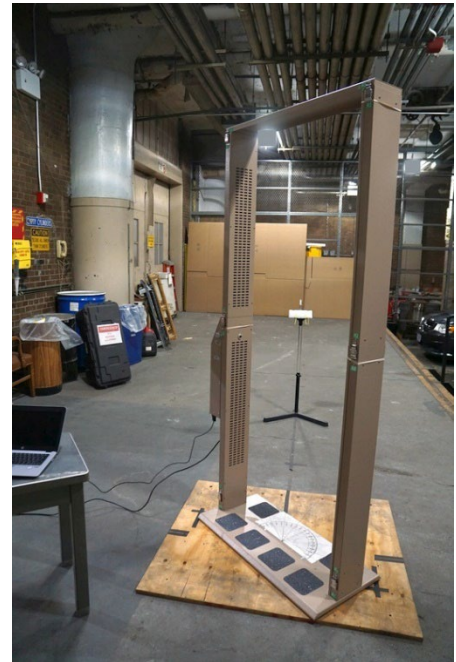


Figure 7-1 Setup for measurements of portal external sensitivity and angular dependence

The selection of radionuclides, vertical positioning of radioactive test sources and the standard laboratory conditions including radiation background levels were consistent with ANSI N42.35 American National Standard for Evaluation and Performance of Radiation Detection Portal Monitors for Use in Homeland Security. [\[17\]](#)

Two different radionuclide sources were used: Cs-137 and Am-241. Cs-137 was used because an RDD using it could produce high levels of contamination [\[8\]](#) and for consistency with the FEMA-REP-21 standard [\[13\]](#), which cited its "widespread availability, long half-life, and common use as a standard reference source of beta and gamma radiation." Cs-137 decays by beta-particle emission to either stable or metastable barium-137. The latter quickly decays, usually emitting a gamma-ray photon with an energy of 661.7 keV. A total of 85.1% of Cs-137 decays lead to this gamma ray emission. The encapsulation of the Cs-137 source used for these tests blocks the beta particles, so the measurements are for gamma radiation only. Since radiation detector efficiency can vary with photon energy, Am-241 was used to test the low energy photon response. Am-241 decays by

²⁶ Caused by diurnal and precipitation-related variations in the concentration of radon and its progeny in the air.



alpha-particle emission (the alpha particles are blocked by the source encapsulation), but 36% of decays also emit a gamma ray with an energy of 59.54 keV. (Both radionuclides also emit lower energy gamma rays and x rays in a few percent of their decays.) The Cs-137 source was an Eckert & Ziegler Isotope Products model GF-137-R2 plastic rod source with a diameter of 0.5 inches (12.7 mm) and an activity of 127 μCi (4.7 MBq) $\pm 3.0\%$ (99% confidence) on the date of the measurements. The Am-241 source was a NIST portal monitor test source [22] with a NIST-calibrated activity of 505 μCi (18.7 MBq) $\pm 4.0\%$ (95% confidence) on the date of the Am-241 measurements. The Am-241 material in the source is deposited in glass-fiber filter paper and encapsulated between two stainless steel discs, each 0.01 inch (0.25 mm) thick and 1.5 inches (38.1 mm) in diameter. The discs are welded together and mounted in an aluminum holder.

For these measurements, the output of the portal's RS-232 serial port was connected to a laptop computer where software written by NUSTL (in LabVIEW and Python programming languages) was used to collect count-rate data every 6 seconds from each of the four detectors in the portal for each position of the radioactive source. Background counts were collected separately without the source present. With standard firmware, the portal monitor outputs data only during an alarm condition. The portal manufacturer provided custom firmware that output data continuously.

A cylindrical coordinate system centered at the midline inside the portal was used to specify the source positions in terms of distance and angle (r , θ). The angle $\theta = 90$ degrees aligns with the direction of transit through the portal, 0 degrees corresponds to the side of the portal with the attached electronics module, and 180 degrees is the other jamb of the portal. The relative position of the radionuclide was varied by rotating the portal (θ) and moving the source (r). After verifying front-to-back symmetry, the angle was varied in 22.5-degree increments from 0 to 180 degrees, the distance was varied in 1-m increments from 1 to 5 m, and a constant height of 1 m was maintained, resulting in 45 positions (Figure 7-2).

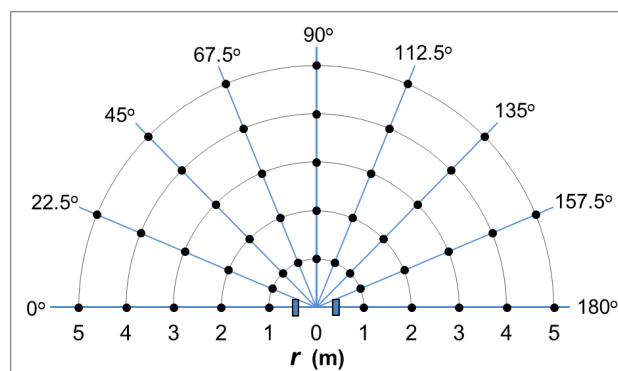


Figure 7-2 Source positions around the portal

The height of 1 meter was chosen for consistency with ANSI N42.35, but it complicated the analysis. One meter is below the 1.105-m height of the midpoint between the two detectors in each jamb of the Model 52-1-1 portal monitor, so the source was always slightly closer to the lower detectors of the portal than it was to the upper detectors and the lower detectors tended to have higher count rates, especially at $r = 1$ or 2 m. The net count rate from the detector having the maximum net count rate was used for analysis to be consistent with the portal parameter setting used for NYC CRCs, which allows any individual detector to trigger an alarm.

Typically, 300 seconds of data were collected and totaled to determine the gross count rate in each detector at each position. The procedure was repeated for each of the two radionuclides. Data were collected for all positions in a single day for each radionuclide. Cs-137 and Am-241 tests were conducted on November 21st and October 18th, 2016, respectively. The background count rate (averaged for the 4 detectors) was 1247 cps and 1408 cps on those dates. For the total background collection time on each date, the 1-sigma percentage statistical uncertainties in the background



rates were 0.15% and 0.16%. The net count rate (source minus background) in the detector having the maximum net count rate for the Cs-137 source ranged from 395 ± 0.8 cps at $r = 5$ m and 90 degrees to $12,650 \pm 20$ cps at $r = 1$ m and 180 degrees (1 sigma statistical uncertainties). The net count rate in the detector having the maximum net count rate for the Am-241 source ranged from 200 ± 0.4 cps at $r = 5$ m and 90 degrees to $12,578 \pm 19$ cps at $r = 1$ m and 180 degrees.

A.2 ANALYSIS AND RESULTS

A.2.1 ANGULAR DEPENDENCE OF PORTAL SENSITIVITY

For each fixed distance r , the net count rate in the highest-rate detector measured at each angle was divided by that at 90 degrees. The data normalized in this way for each distance are shown in [Figure 7-3](#) for Cs-137. The angular position of the Cs-137 source is plotted on the horizontal axis, where 90 degrees corresponds to the direction of pedestrian transit through the portal and 0 degrees is the side with the electronics module. The vertical axis shows the count rate relative to that at 90 degrees, expressed as a percentage increase. The data points are connected by lines for ease of viewing. Using this representation, if the portal were equally sensitive in all directions the graph would be all flat horizontal lines at 0%.

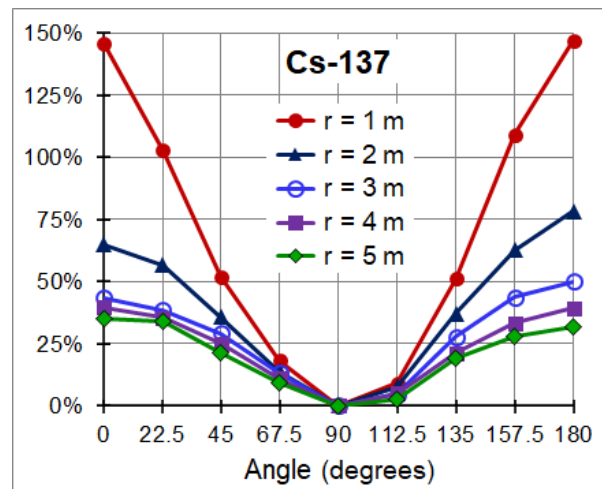


Figure 7-3 Angular dependence of portal monitor net count rate for Cs-137

The graph of the measurement data shows that the portal is more sensitive to external sources oriented to either side, away from the direction of transit. There are two reasons for this. As the portal is rotated away from 90 degrees, one jamb of the portal moves closer to the source, so the scintillation detectors in that jamb will have higher count rates. This is the most significant effect at distances close to the center of the portal and explains the almost 150% increase in count rate for 0 and 180 degrees at $r = 1$ m. The other reason is that the scintillation material in each detector is 4 inches (10.16 cm) wide facing toward and away from the portal center (0 and 180 degrees) and only 1.5 inches (3.81 cm) wide facing 90 degrees.

Consequently, as the portal is rotated away from 90 degrees, the area of the detectors facing the source increases, intercepting more gamma rays. This effect happens at all distances, so even at a distance of 5 m (16.4 ft) the portal is 32% to 35% more sensitive to either side than it is at 90 degrees.

Similar effects are observed for the normalized data for Am-241 shown in [Figure 7-4](#), though the data at 1 m show a large asymmetry between corresponding angles on either side of 90 degrees that is not seen for Cs-137. The asymmetry for the Am-241 source is caused by the electronics box located at $\theta = 0$ degrees shielding the bottom detector on that side. The low energy 60-keV photons from Am-241 are

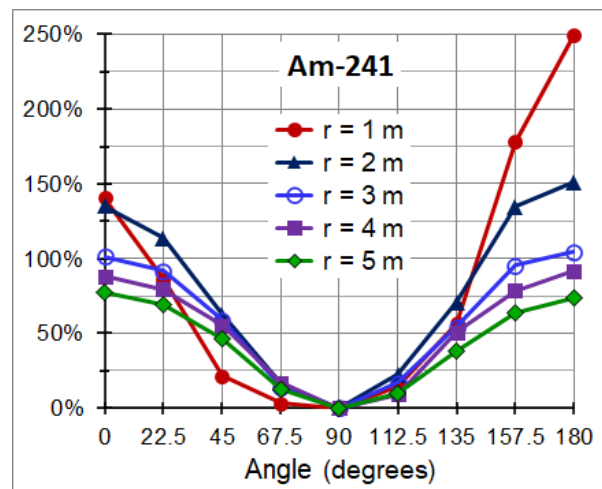


Figure 7-4 Angular dependence of portal monitor net count rate for Am-241



absorbed by materials more strongly than the 662-keV photons from the Cs-137 source, so many of the photons from Am-241 are absorbed by the box while almost all of the photons from the Cs-137 source penetrate through it. The Am-241 results are more symmetric for distances at larger values of r , where the distance from the source at 1 m height to the unshielded upper detector is not so much greater than its distance to the lower detector. For Am-241 at a distance of 5 m, the portal is 76% more sensitive to the side than it is on the central axis. The portal shows more angular dependence for the Am-241 photons than the photons from the Cs-137 source because the target surface area geometry is more significant for shorter range 60 keV photons than 662 keV photons, which can penetrate deeper into the detector when incident from a smaller area side.

The measurement results show that the portal monitor sensitivity to external gamma-ray sources is highest directly to the side of the portal. That position is also where people approaching or leaving a portal pass closest to the portals in adjacent approach lanes. This result means that CRC designs need to be especially careful of someone who has not been effectively prescreened walking beside the portal on transit paths that pass by the sides of portals. While a misattributed alarm would only occur when the presence of an external source is coincident with a portal occupancy, avoidance through pedestrian traffic control and timing may be difficult to achieve with multiple portals and large populations with people walking at different speeds and sometimes being delayed at a portal.

For optimal throughput, it would be best to identify people who have enough radioactivity on or in them to cause an alarm as they walked past portals in adjacent lanes and divert them for decontamination before they enter the CRC portal area. That can be done if prescreening outside the CRC building is sensitive enough. How sensitive the prescreening needs to be depends on how sensitive the portals are to radioactivity on people walking past them and how far apart the portal approach lanes are. Looked at another way, the minimum portal approach-lane spacing that will avoid misattributed alarms depends on both the portal sensitivity and the prescreening sensitivity.

A.2.2 EXTERNAL SOURCE ACTIVITY THAT COULD CAUSE A MISATTRIBUTED ALARM

The same measurement data were analyzed in a different way to obtain an estimate of the source activity that could cause a misattributed portal alarm at a particular distance and angle, which we denote as $A_{al}(r, \theta)$. This is the activity that would cause the portal's net count rate, N , to reach its alarm threshold rate, N_{al} . Note that the actual number of counts in a measurement is randomly spread around its average value. In a series of real measurements, if the average count rate is N_{al} , the portal will alarm in about half of the measurements, because the actual count rate will be above the average half of the time and below the average half of the time. If the average count rate is higher than N_{al} , the probability of an alarm will be greater than 0.5, and if the average count rate is less than N_{al} , the probability of an alarm will be less than 0.5, but there will always be some chance of an alarm and some chance of no alarm.

The portal's sensitivity to a source at a given position is the net count rate per unit source activity, $S(r, \theta) \equiv N/A$, where $S(r, \theta)$ is the sensitivity and A is the source activity. The measurements determined $S(r, \theta)$ for Cs-137 and Am-241. The activity that would produce count rate N at a given position is

$$\text{A-1} \quad A(r, \theta) = N/S(r, \theta).$$



The activity that would produce the alarm threshold count rate is

$$A_{al}(r, \theta) = N_{al}/S(r, \theta).$$

The next step is to determine what count rate causes an alarm. The Ludlum portal monitor's microprocessor continually samples the count rate in each detector every 0.2 s. In walk-through mode with the NYC values of the portal setup parameters, the alarm algorithm combines the 0.2-second sample measurements in pairs and tallies the counts in six overlapping 0.4-second measurements over 1.4 s. In each of those 0.4-second measurements, if the net counts in any detector (or the sum in the upper pair or lower pair of detectors) exceeds 4.5 times the square root of the expected background counts, the portal alarms. NUSTL was initially unaware of the complexity of the portal alarm algorithm, and for analysis of the static laboratory measurements, we approximated the alarm condition using a single measurement 1 second long.

If alarms were determined from single measurements 1 second long, the alarm threshold would be

$$A_{al} = 4.5\sqrt{B},$$

where B is the rate of background counts per second.

For the portal's four detectors, the alarm threshold net count rates were 155 to 161 cps for the Cs-137 measurements and 165 to 171 cps for the higher-background Am-241 measurements. Combining equations A-2 and A-3, we have

$$A_{al}(r, \theta) = 4.5\sqrt{B}/S(r, \theta).$$

The points plotted in [Figure 7-5](#) (top) show the $A_{al}(r, \theta)$ in microcuries determined from the Cs-137 measurements. For each fixed angle from 0 to 90 degrees, a line connects the discrete data points for $r = 1, 2, 3, 4,$ and 5 m. These results show the expected consistency with the analysis in [Figure 7-3](#) in that the portal is more sensitive towards the side, i.e., it would alarm to a weaker source. For example, at a distance of 5 m (16.4 ft), a 38 μCi (1.4 MBq) source to the side could cause an alarm vs. 51 μCi (1.9 MBq) in the direction of transit. The dashed line shows the best-fit quadratic function for the most sensitive orientation ($\theta = 0$ degrees). Similar results for Am-241 source activities expected to cause an alarm at various positions are shown in [Figure 7-5](#) (bottom).

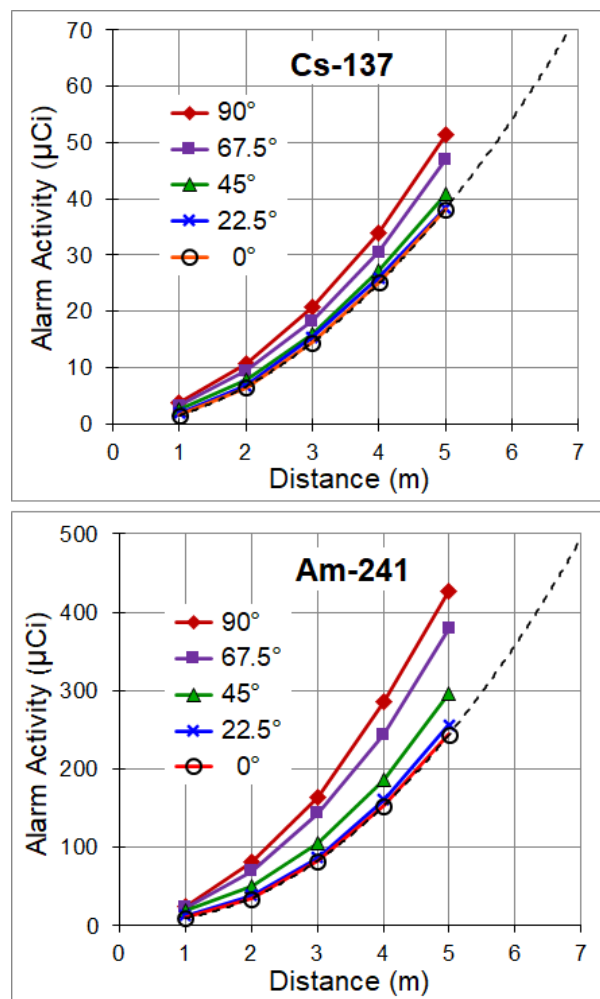


Figure 7-5 Activity of an external source that could cause a misattributed alarm at various distances and angles
Top—Cs-137, Bottom—Am-241
The dashed lines are fits to the 0° data.



The best-fit quadratic expressions for the two radionuclides at $\theta = 0$ degrees with A_{al} in μCi and r in meters are:

A-5 Cs-137: $A_{al}(r, 0) = 1.349r^2 + 1.083r - 0.943$

A-6 Am-241: $A_{al}(r, 0) = 11.08r^2 - 7.84r + 6.53$

These expressions fit the data almost perfectly—the calculated goodness of fit (coefficients of determination) for these functions are greater than 0.9999. The fits provide values of the external source activity that could cause an alarm for distances between the measurements. For example, a 23 μCi (0.85 MBq) Cs 137 source could cause a misattributed alarm half of the time at a distance of 12.5 feet (3.8 m) to the side of a portal that is screening someone. The fits can also be used to extrapolate beyond the distances and sources used in the measurements, though with increasing uncertainty as the distance increases. As a rough approximation, if the portal screening area of a CRC is 90 feet (27 m) long, a person entering the CRC with 1 millicurie (37 MBq) of Cs-137 contamination on them could cause every portal in use in that CRC to alarm.

The measurements with stationary sources have limited usefulness because they differ in several important ways from the situation in a CRC when a contaminated person walks near a portal while another person is being screened in that portal. In the laboratory measurements, the radioactivity was in an isolated point source; the portal was empty; the radiation was constant and measured with high precision; the background rate had a particular value; and the analysis was done for single 1-second-long measurements. In the real case, the radioactivity is likely to be spread out on the body of the contaminated person and their body back-scatters some radiation toward the portal; there is also a person in or near the portal scattering some radiation into the detectors and blocking some background radiation; both people are moving, so the radiation changes throughout the 1.4-second screening window; the background rate can have different values; and the portal alarms if any of six 0.4-second measurements in any of the four detectors reaches the alarm threshold. Nevertheless, the measurements with stationary sources provided valuable target values for the amount of radioactivity that prescreening must be able to detect to avoid misattributed alarms from people passing a given distance from the portals. The static measurements also provided starting values for source strengths and distances to use for the more realistic walk-beside measurements described in section [3.2](#).



APPENDIX B. REMOTE AUDIBLE ALARM ACCESSORY

To avoid contaminating the floor of the CRC facility, it is best to screen people's shoes for possible radioactivity before they enter the CRC building. NUSTL developed a way to prescreen shoes during second-stage prescreening, so it takes no additional time. This is done by performing second-stage prescreening while people stand on a small, raised platform with a PRD under it. (Gently sloped ramps lead to and from the platform, as shown in [Figure 7-6](#)). The PRD can detect and alarm on less than 2 μCi (74 kBq) of Cs-137 or other gamma-emitting radionuclide on the shoes of a person, which is a very small amount of radioactivity. However, because the PRD is hidden beneath the platform, the PRD's alarm light cannot be seen and CRC personnel must rely on the PRD's audible alarm. Unfortunately, the platform muffles the alarm sound, and the use of HazMat personal protective equipment can make it even harder to hear the alarm sound. At the request of FDNY, NUSTL developed a remote audible alarm accessory to amplify the alarm sound from the PRD underneath the ramped platform. The remote alarm accessory box is placed on the ground just outside the ramped platform and connected to the PRD's audio output jack with an audio adapter cable. The remote alarm accessory provides a loud alarm sound that can be easily heard even through the headgear of HazMat personal protective equipment. This appendix gives a detailed description of the remote audible alarm accessory developed by NUSTL.



Figure 7-6 Prescreening a person standing on the ramped platform

The remote alarm accessory is a relatively simple device containing a circuit that feeds the audio output signal from a RadEye PRD-ER to two piezoelectric audio transducers: one that responds to alternating current (AC) signals and one that responds to direct current (DC). The audio output signal of the PRD-ER is a square wave with a frequency that alternates between 1.0 kHz and 2.35 kHz and an amplitude of -2.75 V to $+2.75\text{ V}$. The signal is connected directly to the AC transducer and connected to the DC transducer through a step-up transformer and a rectifier bridge. With a specific choice of components, this simple circuit allows the transducers to produce a loud alarm signal without the need for powered amplification. No batteries are used; no maintenance is required, and the device is always ready for use even after long periods of storage.

Another important feature for its intended use is that the diecast aluminum box housing the circuit is strong enough to withstand being stepped on or kicked multiple times during use. [Figure 7-7](#) shows a photograph of the top of a remote alarm box on the left and an opened box on the right. Since the box must have holes in it to allow the sounds from the transducers out, the alarm accessory should be placed inside a plastic bag to protect it from water and the possibility of radioactive contamination when in use at a CRC.

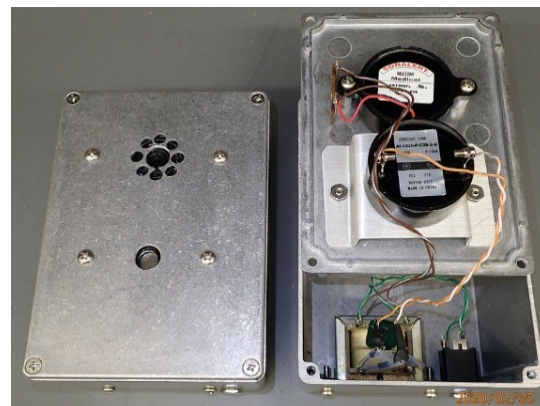
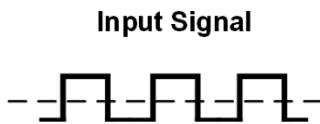
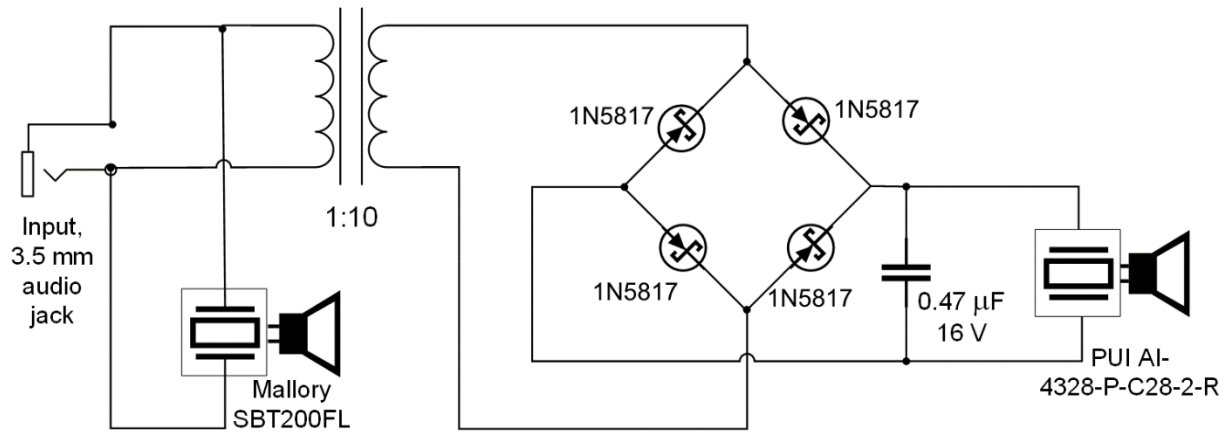


Figure 7-7 Assembled remote alarm accessory box (left) and an opened box (right)



The circuit diagram and parts list are shown in [Figure 7-8](#). All the parts are available from major suppliers of electronic components. In small quantities, the total cost of the parts for each remote alarm accessory was approximately \$65 in 2022.



| PARTS LIST | | |
|---|--|-----|
| Description | | QTY |
| Box, diecast aluminum (Hammond Mfg. 1550W K) | | 1 |
| Transformer (Signal Transformer 241-4-12) | | 1 |
| Schottky rectifier diode (1N5817) | | 4 |
| Capacitor (0.47 µF 16V) | | 1 |
| Audio jack, 3.5 mm | | 1 |
| Piezoelectric alarm (PUI Audio Inc. AI- 4328-P-C28-2-R) | | 1 |
| Piezoelectric alarm (Mallory Sonalert SBT200FL) | | 1 |
| Audio adapter cable, 2.5 mm male to 3.5 mm male | | 1 |

Figure 7-8 Remote audible alarm accessory circuit diagram and parts list

The alarm accessory was designed to work with the RadEye PRD-ER. We performed a brief test of the device with the successor model to the PRD-ER, the RadEye PRD-ER4, and the accessory worked equally well.

DHS has patented this device: U.S. patent 11,140,476, Remote Audible Alarm Accessory for Detection Instruments with Audio Outputs. State, local, tribal, and territorial emergency response agencies may exercise the patent for noncommercial purposes, including making these accessories for their own use. To apply for a commercial use license, email the DHS Technology Transfer and Commercialization Branch at T2C@hq.dhs.gov. Please reference DHS-0213 in the subject line. For additional information about how to make the device, email NUSTL@hq.dhs.gov.



APPENDIX C. DETAILED DESCRIPTION OF RADIATION TRANSPORT AND ASSOCIATED CALCULATIONS

This appendix gives a more detailed description of the radiation transport computer calculations described generally in section 4.0. In particular, we include descriptions of parameters, tallies, and features of MCNP used in the calculations, including the variance reduction methods we used that make it possible to perform the calculations in a reasonable length of time. We also include details of the purpose-written Monte Carlo code simulating the Ludlum portal monitor alarm algorithm. This appendix is intended for readers having some familiarity with radiation transport calculations and especially those who might want to perform their own calculations for the response of other radiation detection instruments to radiation sources at a distance—for example, the response of other models of portal monitors or PRDs used in CRCs.

To avoid having to frequently refer back to section 4.0, figures and much of the text from section 4.0 are reproduced in the appendix, with additional details inserted.

We performed calculations to determine minimum distances to and between screening stations required to avoid misattributed portal and PRD alarms that could be caused by radioactivity on clients waiting to be prescreened. We calculated values for four distances:

1. From the portals to first-stage prescreening
2. From the portals to second-stage prescreening
3. Between the first-stage and second-stage prescreening stations
4. From first-stage prescreening to the front of the line of people waiting to be prescreened

These distances are diagrammed in Figure 7-9. Increasing distances 1 and 2 reduces misattributed portal alarms during whole-body screening. Increasing distance 3 reduces misattributed PRD alarms at second-stage prescreening. Increasing distance 4

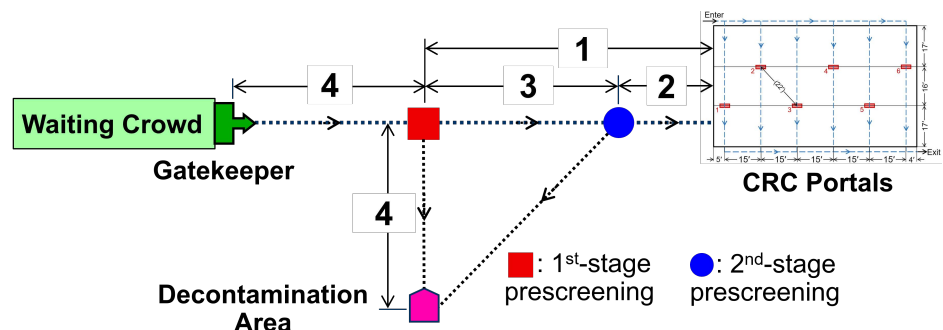


Figure 7-9 Distances calculated in order to avoid misattributed alarms

reduces misattributed PRD alarms at first-stage prescreening. The distance from the decontamination area to first-stage prescreening should be at least as large as distance 4.

Minimum values for these distances depend on the count-rate sensitivity and alarm threshold of the portals and PRDs, how much radioactivity might be on people who come to a CRC, and what fraction of the emitted radiation reaches the instrument detectors and produces a count. The instrument count-rate sensitivities were determined from the measurements described in sections 3.2 and 3.4. We estimated how much radioactivity might be on RDD victims and nuclear medicine patients from published papers and books. [8] [21] We determined how much radiation reaches the instruments in various situations and the count rates it produces using the Monte Carlo radiation transport



computer code MCNP. [24] [25] We determined the probability that a portal monitor will alarm at a given count-rate by writing a computer code simulating the portal's alarm algorithm.

To perform an MCNP calculation of the count rate in a detector exposed to a radiation source, the user creates an input file that describes the radiation source; the dimensions and locations of the source, detector, and other relevant material objects; the atomic composition and density of the materials in the objects; how detailed the physics calculation will be; techniques used to reduce the statistical variance of the answer; and what is to be calculated in the detector (the MCNP "tally"). An example of one of the input files we used for the calculations is given in C.3. The code performs the calculation by simulating what happens to each radiation particle step-by-step as it is emitted from the source, interacts with materials that it hits, perhaps generating secondary particles, and is eventually either absorbed or exits the geometric space of interest. The code contains the known physics of how each type of particle interacts with every type of atom. At each step, the code decides what happens to the particle, for example a gamma-ray photon being scattered from a carbon atom at a particular angle, by generating a random number weighted according to the probability of that process happening. Then the code generates another particle and calculates what happens to that particle. The answer for the count rate in the detector is determined by calculating what happens on average to a large number of particles. The precision of the answer generally depends on the square root of the number of particle histories that are followed. Our calculations typically followed the histories of 100 million to 2 billion particles to reduce the statistical uncertainty in the calculated count rate to less than 1%.

We used MCNP6.2, the latest version of MCNP available in 2018 through 2022. For most of our calculations we used "mode p," which transports only photons, because "mode p e," which transports electrons as well, caused our calculations to run 7 times slower and one of the variance-reduction methods we used cannot be used with charged particles. In "mode p," photon interactions can still produce electrons, but the electrons don't move; they immediately deposit their kinetic energy where they are created or produce bremsstrahlung and other x-ray photons. This is often an acceptable approximation because the range of secondary electrons is relatively short. When we did sample calculations with electron transport turned on, calculated count rates in the portal monitor detectors increased by 1%. For most of our calculations, we used the MCNP6.2 default physics parameters, which enable detailed photon interactions including bremsstrahlung production and tracking of photons with energies down to 1 keV. The MCNP calculations were run in parallel on 20 to 64 processor cores of computers running Windows 10, and most of the calculations took 10 minutes to 12 hours to run.

C.1 DISTANCE FROM PRESCREENING STATIONS TO PORTAL MONITORS

Before we calculated how far away from the portals the first-stage and second-stage prescreening stations need to be to avoid misattributed portal alarms (distances 1 and 2 in Figure 7-9), we verified that we could calculate correct portal monitor count rates for a known situation with a portal exposed to external radiation—the count rates we measured during the portal walk-beside tests. The walk-beside tests described in section 3.2 were performed primarily to determine what source activity at what distance to the side of a portal would cause the portal to alarm. However, the count rate in each of the portal's scintillators was recorded for each trial, providing measured count rates for known sources at known distances that we used to test our MCNP simulations. Comparing



calculated count-rates with the measured count rates of the walk-beside tests with different radionuclides also enabled us to determine the portal's low-energy counting efficiency.

C.1.1 SIMULATION OF WALK-BESIDE TESTS

The calculated count rate in a portal monitor detector exposed to a gamma-ray source is the product of the source activity in decays per second times the number of photons emitted per decay of the radionuclide times the calculated fraction of emitted photons that hit the detector and produce a count. For the walk-beside portal sensitivity measurements, we know the activities and the number of photons emitted per decay of each of the sources we used. We calculated the fraction of photons reaching the portal scintillators and the energy each photon deposits by simulating the portal walk-beside measurements using MCNP.

[Figure 7-10](#) is a diagram showing our MCNP model of the walk-beside tests that were done with single sources of Cs-137, Am-241, and Ba-133. The diagram was produced by the geometry plotting feature of MCNP, which displays cross-sectional slices of the three-dimensional geometry. The MCNP simulation includes the

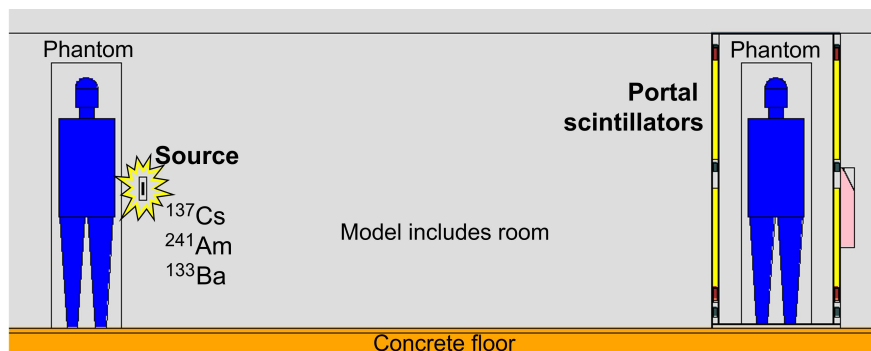


Figure 7-10 MCNP model of the walk-beside tests

dimensions and materials of the source encapsulation and holder, the portal monitor, and the room. The objects labeled “phantom” are simple geometric stand-ins for the bodies of the person walking through the portal and the person carrying the source. Radiation that is initially going away from the portal can scatter toward the portal when it hits the phantoms and the floor, ceiling, and walls of the room, so they are significant parts of the calculation.

The phantoms we used in the walk-beside simulations were based on the overall dimensions of the 1960s MIRD phantom [26] [27] (see [Figure 7-18](#)) but had separated legs and consisted entirely of material with the average atomic composition and density of human soft tissue (no bones or lungs). The torso is the largest and most important part of the phantom for scattering radiation and influencing the calculated count rates. The torso and arms of the MIRD phantom, and ours, are combined and represented by an elliptical cylinder 20 cm thick, 40 cm from side to side, and 70 cm from crotch to shoulder. The MIRD phantom was intended to represent an average-size person, male or female. Without bones, our phantom weighs 163 pounds (73.9 kg), which is lighter than the weight of the personnel who performed the tests. When we did a test calculation for the walk-beside tests with Cs-137 using phantoms with torsos 22 cm thick, which increased the phantom's mass to 173 pounds (78.5 kg), the calculated count rates increased by only 0.4% ±0.3%. Likewise, there was no significant difference in the calculated count rates when we tried several calculations with the legs of the phantoms bent forward and backward as if walking.

For visual clarity, [Figure 7-10](#) shows the phantoms centered in the portal and directly to the side of the portal, but that is not the situation that gave the highest count rate in the portal's four detectors. We found that we got the highest calculated count rates and the best agreement with the measured count rates when the phantoms were at least a foot (30 cm) from the portal, representing the



position of a person just after walking through the portal. This is consistent with the portal firmware recording walk-through count rates for a 0.4-second measurement interval after the occupancy sensor IR beam is no longer blocked. When the phantom is centered in the portal, it shields the two detectors more distant from the source, lowering the calculated count rates in those detectors by about 50% relative to the off-center positions and making them 40% to 60% lower than the measured count rates.

Gamma-ray and x-ray emission energies and probabilities for the source nuclides were taken from the *WWW Table of Radioactive Isotopes*. [18] In addition to gamma rays, we included x rays with energies above 25 keV and emission probabilities greater than 0.1% in the MCNP source definition.

The sources used for the walk-beside measurements were NIST portal monitor test sources [12] with encapsulation as described in A.1 and NIST-calibrated activities of 23.3 μCi^{27} (862 kBq) of Cs-137, 103.8 μCi (3.84 MBq) of Am-241, or 15.5 μCi (574 kBq) of Ba-133. NIST calibrates the activity of these sources by their gamma-ray emission rate measured using high purity germanium (HPGe) detectors and notes that “the measured gamma-ray emission rate is reduced due to the attenuation in the stainless steel disc.” [22] This means that the contained activity in the sources is higher than the calibrated activity. To determine the contained activity to use in the MCNP simulations of our measurements, we performed separate MCNP calculations simulating the NIST HPGe calibration measurements. We determined the ratio of the contained activity to the emission-calibrated activity from the ratio of the calculated HPGe count rates at the energies of the prominent gamma-ray lines without and with the encapsulation present. The calculated contained activity was 2.0% higher than the calibrated activity for the 661.7-keV gamma ray from the Cs-137 source and 29.4% \pm 0.5% higher than the calibrated activity for the 59.54-keV gamma from the Am-241 source. As seen in Table 3-1, Ba-133 has five significant gamma-ray lines from 81 keV to 384 keV, with 78% of the emission in the two prominent lines at 81 and 356 keV. Depending on whether NIST used all five lines or just the most prominent two, the calculated contained activity was 7% or 8% higher than the calibrated activity, so we used 7.5% for the Ba-133 source. We used these same corrections for the contained activity in the NIST sources when we did MCNP simulations of the PRD-ER sensitivity measurements with Cs-137 and Ba-133 (C.2.1).

We modeled the portal monitor using dimensions we measured from the Ludlum 52-1-1 portal monitor that NUSTL bought to perform the measurements for this work. We modeled the photomultiplier tubes, tube bases, magnetic shields, and wiring connector blocks as well as the scintillators and the aluminum structure surrounding them. Including a realistic model of the aluminum structure was important for matching the calculated count rates to the measured ones for some of the measurements. The photomultiplier assemblies of the Ludlum portal are at the top and bottom; including them had negligible effect on the calculated count rates.

The room was NUSTL’s first-floor warehouse, which is 84 feet long, 44 feet wide and 13.6 feet from floor to ceiling (25.6 m x 13.4 m x 4.1 m). We also modeled some of the larger objects in the room near the portals or source, though that added less than 0.5% to the calculated count rates.

Gamma-ray and x-ray photons cause counts in a scintillator when they transfer some or all of their energy to electrons in the atoms of the scintillator, and energetic electrons can generate bremsstrahlung photons which can generate more electrons. MCNP has several general types of

²⁷ Rounded to 23 μCi in the descriptions of the measurements in section 3 and Appendix A.



“tallies” that keep track of various kinds of radiation quantities in an object. For photon or electron radiation, MCNP tally type f8, the pulse-height tally, totals the energy deposited in an object by all the photons and electrons produced by each source particle and can count the number of pulses with deposited energies in user-specified energy bins.

In our MCNP calculations, we used the f8 pulse-height tally to determine the fraction of photons emitted by the source that produce pulses that deposit energy in each energy-deposition bin. For the walk-beside simulations and other calculations for the portal monitors, we used 2-keV-wide energy bins ranging from zero deposited energy to above the maximum energy of photons emitted by the source radionuclide. The number of counts registered by the detector in each energy bin is the number of pulses in that energy bin times the detector’s counting efficiency for that energy. The fraction of emitted photons that produce a count is the sum of the number of counts for all the energy bins. To determine the statistical uncertainty in the calculated count rates, we used a separate f8 tally that included a bin for all pulses above an approximate low-energy counting efficiency cut-off.

To determine if a photon that deposits a certain energy in a portal scintillator produces a count, it is necessary to know the portal’s counting efficiency at that energy. Initially, we did not know the portal’s counting efficiency at low energies. All we knew to start with was that the efficiency was likely to be near 100% for deposited energies above about 30 keV and 0% below some lower energy. We determined the portal’s low-energy response by using MCNP to simulate the walk-beside tests and comparing the calculated count rates with the measured count rates, adjusting the portal’s low-energy response to get the best agreement.

We could not get good agreement for all the measurements using any one energy as a sharp cut-off from full efficiency to zero efficiency. We would have needed cut-off energies of 14 keV for the measurements with Cs-137 and Ba-133, and 11.9 keV for Am-241. We got very good agreement using a portal counting efficiency that gradually decreased from 100% for energy deposits above 30 keV to 0% below 5 keV. [Figure 7-11](#) shows a graph of the values we determined for the portal monitor counting efficiency as a function of the energy deposited in its scintillators that gave the best agreement of the calculated count rates with the measured count rates. The solid line is the efficiency curve that gave the best agreement; the dashed lines are limits for possible curves within estimated uncertainties.

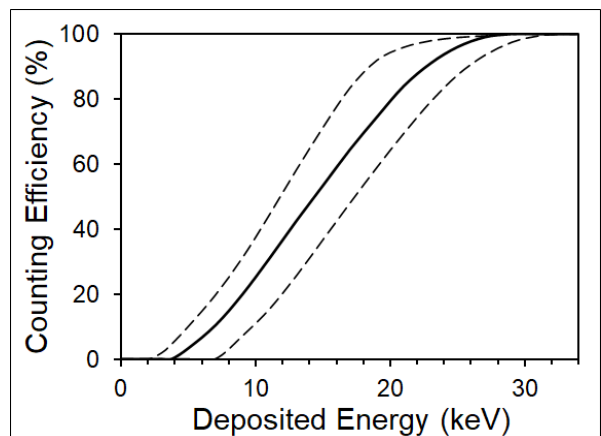


Figure 7-11 Portal monitor counting efficiency vs. energy deposited in a scintillator

Using the portal counting efficiency that gave the best agreement, the calculated count rates averaged for the portal’s four detectors were within 1% of the measured count rates for the walk-beside measurements with Cs-137 and Am-241, and within 2% for Ba-133. This agreement means we have modeled the portal monitor’s count-rate response correctly and gives us confidence in our calculations of the count rates in a portal in a CRC with a contaminated person at a prescreening station outside.



The technical manual for the Ludlum Model 52 series portal monitors [12], gives the energy response range of the portal as 30 keV to 3 MeV, but these values are for the energies of photons that the portal is specified to efficiently detect. The low-energy counting efficiency curve we determined is for the energy deposited in the scintillators.

Calculations simulating the walk-beside tests were useful in another way. We wanted to do portal and PRD measurements with Co-60, which emits high-energy gamma rays, because we were concerned that the count-rate sensitivity of the portal monitors might decrease for high-energy gamma rays less than the sensitivity of the PRDs used for prescreening decreases. If that were so, the 15-foot separation of the portal approach lanes that is sufficient to avoid misattributed portal alarms for Cs-137 contamination would not be sufficient for Co-60. However, we did not perform portal sensitivity measurements or walk-beside tests with Co-60 because we did not have a suitable Co-60 source. As a substitute for measurements, we did calculations. To determine the relative sensitivity of the portal monitors to photons from the two radionuclides, we performed MCNP calculations simulating a contaminated person walking beside a person going through a portal, first with Cs-137 contamination and then with Co-60. The phantoms representing the two people are 15 feet (4.6 m) apart—the recommended portal approach-lane spacing. The most difficult distribution of contamination on the body of a person for second-stage prescreening to detect is spread along the side of the person (see 3.3.2), so our MCNP simulation used a vertical line source along the side of the torso of the phantom representing the contaminated person. The result is that the portal is 88% as sensitive to Co-60 gamma rays as it is to Cs-137 photons. Fortunately, when we calculated the relative sensitivity of the PRDs to photons from Co-60 and Cs-137, the result was a similar decrease (see last paragraph of C.2.1), so a portal approach-lane spacing that works for Cs-137 will also work for Co-60.

C.1.2 DISTANCE FROM FIRST-STAGE PRESCREENING STATION TO PORTAL MONITORS

The first-stage prescreening station is the place where unscreened people who might be highly contaminated would get closest to the portal monitors in a CRC. To calculate how far the first-stage prescreening station needs to be from the portal monitors inside a CRC to avoid misattributed portal alarms (distance 1 in Figure 7-9), we estimated how much radioactivity might be on the most contaminated RDD victims who might come to a CRC and calculated the count rates in the portal's detectors used using MCNP to model a portal monitor in a CRC building with such a contaminated person outside (C.1.2.2). We modeled different kinds of buildings that may house CRCs and tried various distances to the contaminated person, looking for the distance that resulted in calculated count rates that would produce a portal alarm probability of about 0.5. We determined what count rates in the portal's four detectors would cause the portal to alarm by writing a short Monte Carlo computer code that simulates the portal's alarm algorithm (C.1.2.3). Results for the recommended distances from the first-stage prescreening station to the CRC portal monitors in four types of buildings are given in C.1.2.4.

C.1.2.1 RADIOACTIVITY ON RDD VICTIMS

The count rate in the portal monitors from contamination on people waiting to be prescreened depends on how much radioactivity is on people who come to a CRC. Section 4.1.2.1 describes how we used information in Smith et al. [8] to estimate the activity on the most-contaminated victims likely to come to a CRC following the 2000 Ci (74,000 GBq) Cs-137 RDD used as the design-case incident in our work—about 7 mCi (0.25 GBq). We performed our calculations of the minimum



distance to keep people waiting to be prescreened from the CRC portal monitors and prescreening stations using this activity as our design case.

C.1.2.2 PORTAL COUNT RATE FROM RADIOACTIVITY ON PEOPLE OUTSIDE A CRC

Since many potential NYC CRC locations are high schools, our basic MCNP input file describes the materials in a portal monitor in a high school basketball court in a gymnasium inside a notional high school building. [Figure 7-12](#) is a pair of diagrams showing top and front views of our MCNP model. The person with radioactivity on them and a person being screened inside a portal are represented by simple phantoms, as they were in the simulation of the walk-beside tests. The diagrams are to scale, so the phantoms and the portal appear tiny in the main diagrams—practically just points in the top view. A jagged halo emphasizes the location of the phantom representing the person with radioactivity outside the building. The outdoor phantom is directly to the side of the portal—the direction of the portal’s highest sensitivity. Magnified insets show details of the phantom with the radioactive source and the portal monitor and the phantoms in and near it. We used a single point source 1 m above the ground on the surface of the outdoor phantom. We added a third phantom representing the portal operator reading the display. The legs of the phantoms shown in profile are not visible in the figure because the view shown is a cross-section slice down the middle between their legs. The portal inset shows the screened phantom centered in the portal, but the calculations were performed with the screened phantom 1 foot (30 cm) past the portal’s center because that situation gave the highest count rate in the portal’s four detectors. The circles and arcs around the portal scintillator and building are spherical surfaces used for variance reduction to reduce the calculation time.

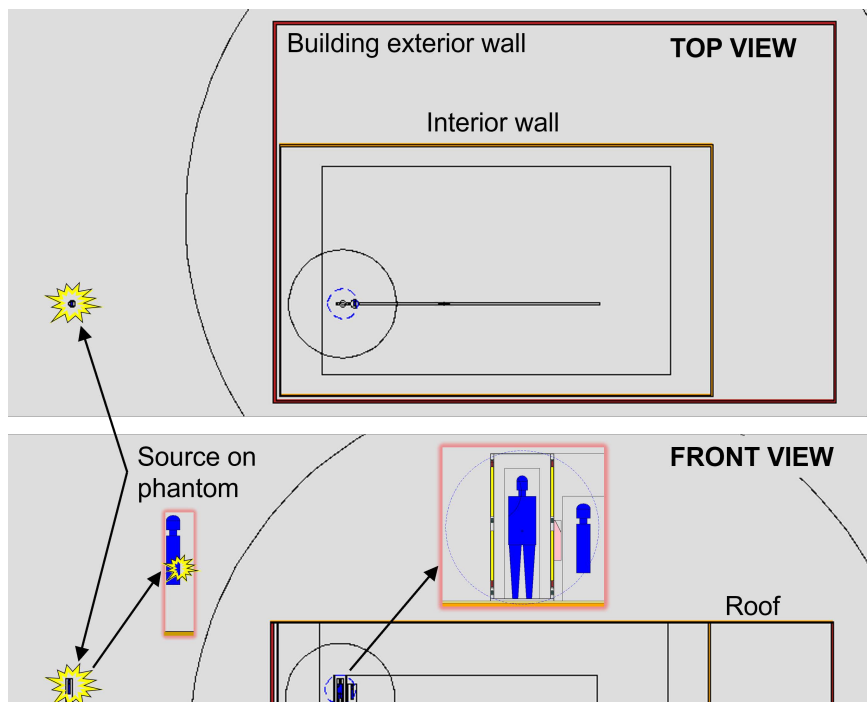


Figure 7-12 MCNP model of CRC building and person with radioactivity outside

The outdoor phantom is directly to the side of the portal—the direction of the portal’s highest sensitivity. Magnified insets show details of the phantom with the radioactive source and the portal monitor and the phantoms in and near it. We used a single point source 1 m above the ground on the surface of the outdoor phantom. We added a third phantom representing the portal operator reading the display. The legs of the phantoms shown in profile are not visible in the figure because the view shown is a cross-section slice down the middle between their legs. The portal inset shows the screened phantom centered in the portal, but the calculations were performed with the screened phantom 1 foot (30 cm) past the portal’s center because that situation gave the highest count rate in the portal’s four detectors. The circles and arcs around the portal scintillator and building are spherical surfaces used for variance reduction to reduce the calculation time.

We modeled four basic kinds of potential CRC buildings:

1. No building—an open field, parking lot, or outdoor stadium
2. A warehouse with a 4-inch (10cm) thick concrete-block exterior wall and an insubstantial roof²⁸
3. A building representing a NYC school, with an 8-inch (20-cm) thick brick exterior wall, one 4-inch (10-cm) thick concrete-block interior wall surrounding the gymnasium, and an insubstantial roof
4. The same brick school building, but with a 3-inch (8-cm) thick concrete roof

²⁸ Thin enough so that it does not significantly attenuate gamma rays—modeled as no roof.



The “ground” was modeled as concrete for all four building options, including no building. Concrete scatters gamma rays at least as much as soil, so a distance that avoids misattributed alarms for a paved area will also work for an open field. We used the pulse-height tally in each of the four portal scintillators with the low-energy response determined from the simulations of the walk-beside measurements. We made several trial calculations for each type of building, putting the phantom with the radioactive source at different distances to find the distance that would cause the portal to alarm with 50% probability. The input file for the building with a brick wall and a concrete roof when a Cs-137 source on a phantom is 22 m (72.18 ft) from the center of the portal is given in [C.3](#).

The amount of radioactive contamination on some victims of a major RDD can potentially be large, so the distance from the first-stage prescreening station to the nearest portal in a CRC required to avoid misattributed alarms needs to be large. Because the source and the portal detectors are far apart and the building shields some of the radiation, only a small fraction of the emitted radiation hits the detectors. Without employing variance reduction methods, each MCNP calculation would have to track about 2×10^{10} particles and would take about 10 hours to collect enough hits to reach statistical precision of about 1% for the calculated count rates. Because we needed to do many trial calculations to see the effect of various geometries and then to find the correct distance for each building type, we looked for variance reduction methods to speed up the calculations.

MCNP has a variety of variance reduction methods that can be used to increase the number of particle tracks in objects of interest, in this case the portal detectors and nearby objects that can scatter radiation toward them. When the number of particle tracks is increased, the “weight” of each such track is reduced proportionally, so the tallied answer is unchanged while the statistical uncertainty is decreased. We used two variance reduction methods: cell “importance” with geometry splitting, and deterministic transport spheres. These two are among the subset of variance reduction methods that work with the f8 pulse-height tally.

“Importance” (imp) is a parameter assigned to each geometric object (cell). When a particle track goes from a cell with $\text{imp}=1$ to a cell with, say, $\text{imp}=4$, the track is split into 4 identical tracks with $\frac{1}{4}$ the weight of the original track. When a particle track goes from a cell with $\text{imp}=4$ to a cell with $\text{imp}=1$, the code randomly kills the track with probability of $\frac{3}{4}$ of surviving and increases the weight of a surviving track by a factor of 4. This variance reduction method is very commonly used and relatively gentle in the sense that it usually works without distorting the answer or causing other variance problems. The solid circles and arcs in [Figure 7-12](#) are cross sections of spherical surfaces where the importance is increased inside. We increased the importance a factor of 2 or 4 at each such surface and tried setting the importance of the cells representing the portal and nearby objects as high as 512. This method generally works well when materials attenuate radiation before it reaches a detector. It sped up the calculations for the school building by a factor of 6 but did not speed up the calculations for open ground.

Deterministic transport spheres are a more extreme variance reduction method that can significantly speed up calculations when a detector subtends a small solid angle (a small detector at a large distance from the source) and there is not too much absorption by intervening material. The user defines a “dxt” sphere around the detector and materials near it that can scatter radiation into it. Whenever a particle is emitted from the source or scatters, the code calculates the probability that the particle will head toward and reach the dxt sphere and sends a “pseudo-particle” to the surface of the sphere with weight reduced by that probability. The code kills real particles reaching the dxt sphere and makes other corrections to assure that the tallied answer is not biased. This method



must be used with caution because in some situations relatively rare high-weight tracks cause fluctuations that prevent the answer from converging. The blue dashed circles in [Figures 4-4, 4-9, 4-10, 7-12, 7-17, and 7-18](#) are cross sections of dxt spheres. Using a dxt sphere around the portal sped up the calculation for open ground by a factor of 30 and for the school building by a factor of 7. Using a dxt sphere around the portal combined with increasing the importance of cells near the portal sometimes dramatically sped up a CRC building calculation but, depending on the particular cell importances and dxt parameter settings used, often caused tally fluctuations that made the answer unreliable. MCNP performs 10 statistical checks on tally fluctuations to warn of such problems when they occur.

The main output of the MCNP calculations is the net count rate in each of the four detectors for a given activity of the radionuclide on the source phantom outside the CRC. We performed calculations with Cs-137 as the source for all four building types, and for Co-60 and I-131 for no building and for the brick building with a concrete roof. The count rate in the two detectors closer to the source was 13% to 27% higher than in the other two detectors. The count rate in the top detectors was 5% to 14% higher than in the bottom detectors on the same side for the three types of actual buildings and about equal for no building.

C.1.2.3 PORTAL COUNT RATE ALARM THRESHOLD

Using MCNP, we can calculate the average count rate in each of a portal's four scintillator detectors at a given distance from a radioactive source, but to determine the minimum distance that will avoid misattributed portal alarms, we need to know what count rate in the detectors will cause a portal to alarm. Or, rather, we need to know the probability that the portal will alarm at a given count rate in each detector. Whether a portal alarms when someone walks through it depends on the count rate in its detectors, the background count rate, and the alarm algorithm of the portal's microprocessor.

The Ludlum portal monitor alarm algorithm involves multiple short measurements, and descriptions of it in versions of the technical manual before the current one [\[12\]](#) were incomplete. The portal monitor's microprocessor continually samples the count rate in each detector every 0.2 s. The portal setup parameters that most affect the alarm response and the FDNY settings for them are “# of Samples” = 2 and “Sigma” (sigma multiplier) = 4.5. In walk-through mode with those parameter values, the alarm algorithm combines the 0.2-second sample measurements in pairs and tallies the counts in 0.4-second measurement intervals starting with the 0.2-second sample period before the first sample period when the occupancy sensor infrared (IR) beam is blocked and advancing by 0.2 s until 0.8 s after the end of the last sample period when the IR beam is blocked. At a typical walking speed of 1.4 m/s (3.1 miles/h), a person will block the IR beam for roughly 0.2 s starting at a random time within one of the sample periods, so people being screened will generally block the beam during two sample periods. The result is six 0.4-second measurements over 1.4 s. In each of those six measurements, if the net counts in any detector or the sum in the upper pair or lower pair of detectors exceeds 4.5 times the square root of the expected background counts, the portal alarms.

NUSTL was initially unaware of the details of the portal alarm algorithm, and for our analysis of the static laboratory measurements, we approximated the alarm condition using a single measurement 1 second long. We wanted a more realistic and accurate alarm condition to determine when a portal monitor will alarm given the count rates in its scintillators.



Since the alarm criterion depends on the background-radiation count rate, we need to choose a background rate for our analysis. Average background rates in each scintillator of NUSTL's portal monitor ranged from 1053 to 1164 cps during the walk-beside tests and from 1183 to 1444 cps during the portal sensitivity measurements on our loading dock. Average background rates in the FDNY portal monitor we used when we did walk-beside measurements at the NYC CRC training facility ranged from 988 to 1099 cps. Since a portal will alarm at lower net count rates for lower background rates, we want to use a low, but not unusual, background rate for our alarm analysis to make sure we put the prescreening stations far enough from the portals. We chose a background rate of 1000 cps.

With a background count rate of 1000 counts per second in each detector, the average number of background counts in a 0.4-second measurement is 400 counts, the alarm threshold for the net counts is $4.5\sqrt{400} = 90$ counts, and the alarm condition for the gross counts (background plus signal) is 490 counts in a 0.4-second measurement. The net-count-rate alarm threshold for each 0.4 second measurement in each detector is $90/400 = 22.5\%$ of the background rate. The net-count-rate alarm threshold for the paired detectors is $1/\sqrt{2}$ times lower than the threshold for a single detector. For a pair of detectors summed together, the background count rate is 2000 counts per second, the average number of background counts in a 0.4-second measurement is 800 counts, the alarm threshold for the net counts is $4.5\sqrt{800}=127.3$ counts, and the alarm condition for the gross counts (background plus signal) is 927.3 counts in a 0.4 second measurement. The net-count-rate alarm threshold for each 0.4 second measurement in a pair of detectors is $127.3/800 = 15.9\%$ of the background rate.

We assume that the average count rate in each detector is constant during the 1.4-second alarm test window. The mean net count rates in a portal at large distances from a stationary or slowly moving source (i.e., radioactivity on a person waiting to be prescreened) should be constant except for the effect of shielding by the body of the person walking through the portal. The net count rates in the two portal detectors farther from the source are actually lower when a person is inside the portal, but ignoring that variation vastly simplifies the analysis and yields an only slightly larger minimum distance to avoid misattributed alarms.

Radiation emission and detection are random processes. We can know the mean count rate in a detector, but the number of counts in a particular measurement is likely to be somewhat lower or higher than predicted from the average, and we can predict only the probability that it will have a particular value. Given the mean number of counts in a measurement interval, the probability of a particular number of counts is given by the Poisson probability distribution for that mean value.

If the six 0.4 second measurements in each detector did not overlap, so they were statistically independent of each other, we could have used standard statistical formulas to determine the alarm probability as a function of the count rate in each of the detectors. But the measurements do overlap, and in addition, we need a way to account for alarms in the upper and lower pairs of detectors as well as in any of the four detectors of a portal.

The solution was to write a Monte Carlo computer program that duplicates the alarm test algorithm of the portal monitor's microprocessor, substituting code-generated pseudo-random numbers for the number of counts in each of the four detectors. The program was written in the computer language R. The inputs to the code are the background rate in the detectors, the number of trials to run (we used 100,000), the ratio of the count rate in each detector to the count rate in the detector with the



highest count rate, and the range of net count rates in the highest-rate detector (0 to 200 cps). At a background rate of 1000 cps, the mean number of background counts in each 0.2-second sample period is 200. To simulate the fluctuations in the background counts in the 0.4-second portal alarm-test measurements for each detector, the code creates 100,000 (i.e., 10^5) sets of six numbers that are sums of pairs of seven random numbers drawn from a Poisson distribution with a mean of 200. The pairs of numbers are created just as the portal's alarm algorithm makes them, using one of the numbers from the first pair in the second pair, the other number from the second pair in the third pair, and so on. To simulate the fluctuations in the net counts in the 0.4-second alarm-test measurements, the code performs a similar procedure for each detector. Let m be the mean net count rate for the highest-rate detector. Then the mean number of counts in each 0.2-second sample period is $0.2m$. For each value of m , the code creates 10^5 sets of six numbers that are sums of pairs of seven random numbers drawn from a Poisson distribution with a mean of $0.2m$. The pairs of numbers are created just as the pairs were created for the background fluctuations. The background and net counts are summed to get the gross counts for each of the 10^5 sets of six measurements. This process is repeated for the other three detectors, but with the value of the mean net count rate reduced by the ratio of the net count rate in that detector to the rate in the highest-rate detector. The code sums the gross counts in the top two detectors and the bottom two detectors to create 10^5 sets of six measurements for the paired detectors.

The 10^5 sets of six numbers for each detector and the paired upper and lower detectors are tested to see how many contain a number that is larger than the alarm criterion, 490 counts for the individual detectors and 927.3 counts for the paired detectors. The fraction of the sets of six numbers with one or more numbers that is larger than the alarm criterion is the alarm probability for net count rate m . The program repeats the calculation for each half-integer value of m from zero to 200.

[Figure 7-13](#) shows a graph of the output of the alarm algorithm simulation code: the probability for a portal to alarm as a function of the mean net count rate in the detector with the highest count rate when the background count rate is 1000 cps. The graph shows plots for the ratios of detector net count rates from the MCNP calculations with a Cs-137 source for the four building types. The four curves are so similar that some are visually almost indistinguishable. The count rate in the highest-rate detector that gives an alarm probability of 0.5 is 114 cps for open ground, 116 cps for the brick building with a concrete roof, and 113 cps for the other two building types.

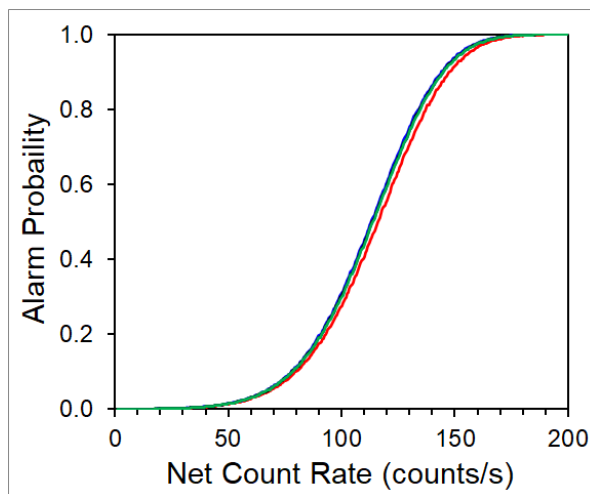


Figure 7-13 Probability for a portal monitor to alarm vs. net count rate in highest-rate detector

The alarm probability code also gives the probability of a portal false alarm just from random fluctuations in the background. For a background rate of 1000 cps, setting the net count rate to zero gives an alarm probability of 2×10^{-4} , or 2 portal false alarms in 10,000 screenings. In a CRC with six or more portals screening people as fast as they arrive from prescreening—800 people per hour—there will be about 1 false alarm every 6 hours. Screeners should be made aware that there will be occasional false alarms as well as misattributed alarms, and procedures should include methods to deal with them.



C.1.2.4 RESULTS OF CALCULATIONS FOR THE FOUR BUILDING TYPES

[Table 4-1](#) gives the results of our calculations of the minimum distance from the first-stage prescreening station to the nearest portal in a CRC that will avoid most misattributed alarms when our design-case RDD victim is prescreened outside each of the four types of CRC building. The distances in that table are rounded up to the nearest 10 ft. [Table 7-1](#) gives the actual calculated distances for a portal alarm probability of 0.5 for the Cs-137 activity on our design-case RDD victim, 7 mCi (0.25 GBq), as well as the rounded-up distances and the alarm probability for the rounded distances.

Table 7-1 First-stage Prescreening Distance from Portals and Portal Alarm Probabilities

| CRC building type | Distance for 0.5 alarm probability | Rounded-up distance | Alarm probability for rounded-up distance |
|---|------------------------------------|---------------------|---|
| No building (open field, parking lot, stadium) | 241 feet (73 m) | 250 feet (76 m) | 0.37 |
| 4" concrete-block exterior wall, thin roof (warehouse) | 172 feet (52 m) | 180 feet (55 m) | 0.37 |
| Brick exterior wall, 4" concrete-block interior wall, thin roof | 83 feet (25 m) | 90 feet (27 m) | 0.27 |
| Brick exterior wall, 4" concrete-block interior wall, concrete roof | 72 feet (22 m) | 80 feet (24 m) | 0.20 |

The distances for 0.5 alarm probability in [Table 7-1](#) were calculated using the portal counting efficiency curve that gave the best agreement with the walk-beside measurement results (solid line in [Figure 7-11](#)). If we use the maximum portal counting efficiency curve within the uncertainty (upper dashed line in [Figure 7-11](#)), the calculated distances increase 2% to 3% and are still less than the rounded-up distances.

Many people are given radioactive materials internally to treat or diagnose a medical condition, and nuclear medicine patients might come to a CRC following a radiological dispersal incident. Most of the radionuclides used medically have short half-lives or are given in small amounts, so most nuclear medicine patients will not cause misattributed alarms. One exception is I-131, used to treat cancer of the thyroid gland and frequently used to treat hyperthyroidism. While few patients recently given therapeutic doses of I-131 are likely to come to CRCs, we performed calculations to see if those who do might cause misattributed alarms. We repeated the MCNP simulation calculation for open ground and the brick building, replacing the Cs-137 source on the surface of the torso of the distant phantom with an I-131 source inside the phantom at the location of a person's thyroid gland. Because 91% of the photons emitted by I-131 have lower energy than the Cs-137 gamma ray, the walls of the brick building provide sufficient shielding so that I-131 nuclear medicine patients are unlikely to cause misattributed portal alarms. However, for open ground, the amount of I-131 typically remaining in the thyroid up to about 10 days after a patient is treated for hyperthyroidism [\[20\]](#) can cause the portals to alarm as far away as our design-case RDD victim. The same is true for misattributed PRD alarms during prescreening. Since people emitting relatively high levels of radiation will be detected at first-stage prescreening, details of the calculations for I-131 are given below in [C.2.2](#).



C.1.3 DISTANCE FROM SECOND-STAGE PRESCREENING TO PORTAL MONITORS

The second-stage prescreening station is the place where people who have had only first-stage prescreening would come closest to the portal monitors in a CRC. NUSTL did MCNP calculations to determine how far the second-stage prescreening station should be from the portal monitors to avoid misattributed portal alarms (distance 2 in [Figure 7-9](#)). The source we used in the calculations was the maximum activity that could be on people who reach the second-stage prescreening station, which is the largest activity that might be missed by first-stage prescreening. We modeled the portal and source with phantoms as we did in the calculations for the minimum distance to the first-stage prescreening station, but we allowed the second-stage prescreening station to be inside the building, with no intervening walls to provide shielding. For the maximum activity that could be missed by first-stage prescreening, the distance that results in a 50% probability of causing a portal alarm is 30 feet (9 m). Allowing an extra 5 feet for a client to possibly walk closer to the portal before turning to go to decontamination, the second-stage prescreening station should be located at least 35 feet (11 m) from the nearest portal. The 30-foot distance with no shielding can be decreased to 20 feet (6 m) if there is an intervening masonry or brick wall, in which case the second-stage prescreening station can be located as close as 25 feet (8 m) from the nearest portal.

C.2 DISTANCE BETWEEN PRESCREENING STATIONS

Misattributed alarms can occur during prescreening as well as during whole-body screening. NUSTL performed calculations to determine the minimum distance from the front of the line of unscreened people waiting to enter the CRC to the first-stage prescreening station and between the first-stage and second-stage prescreening stations that will avoid misattributed PRD alarms during prescreening (distances 4 and 3 in [Figure 7-9](#)). To test and calibrate the prescreening station distance calculations, we simulated the count-rate sensitivity measurements of the RadEye PRD-ER that we made for this purpose—see section [3.4](#).

C.2.1 SIMULATION OF PRD SENSITIVITY MEASUREMENTS

A diagram of our MCNP model of the PRD sensitivity measurements is shown in [Figure 7-14](#), which may be compared with the photograph of the measurement setup shown in [Figure 3-11](#). In addition to the PRD-ER, gamma-ray source, and water phantoms, the model of the measurements includes the wire-shelf cart supporting the water phantoms and the floor, walls, and ceiling of the large room where the measurements were made.

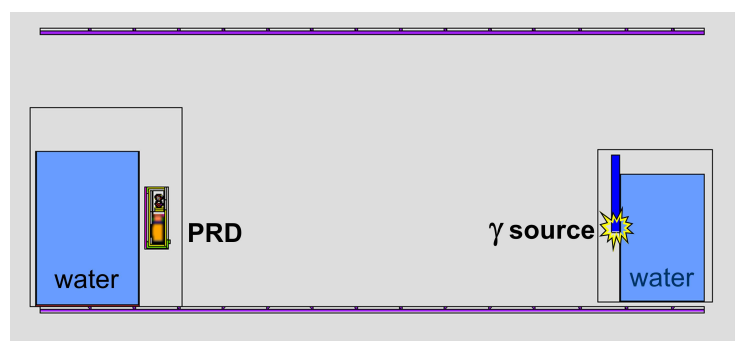


Figure 7-14 MCNP model of PRD-ER sensitivity measurements

The most important part of modeling the PRD sensitivity measurements is modeling the PRD-ER itself. We determined the dimensions of the significant components of the PRD by taking apart a damaged RadEye PRD and measuring each component. To calculate the counting sensitivity of the PRD, it is essential to know the dimensions of the sodium iodide crystal scintillator, which is unpublished sensitive proprietary information. We measured the sodium iodide crystal of the



damaged RadEye PRD by opening the sealed aluminum cylinder containing it. The manufacturer informed us that the dimensions of the crystal of the PRD-ER are the same as those of the RadEye PRD we measured. [Figure 7-15](#) shows cross-sectional diagrams of our MCNP model of the PRD-ER viewed from the top, front, and side. Details of the PRD's crystal have been blurred in the figure to obscure proprietary information. The PRD model included the protective rubber sleeve and part of the holster that was used to attach the PRD to the water-filled recycling container used as the phantom behind it during the sensitivity measurements.

The purpose of making the PRD sensitivity measurements with different radionuclides (Cs-137 and Ba-133) and with phantoms behind the source and PRD and then simulating the measurements with MCNP was to determine if the simulation could reproduce the measured count rate over a range of photon energies, especially low energies. Low energies are important because many of the photons reaching the PRD from distant sources have scattered down to low energy.

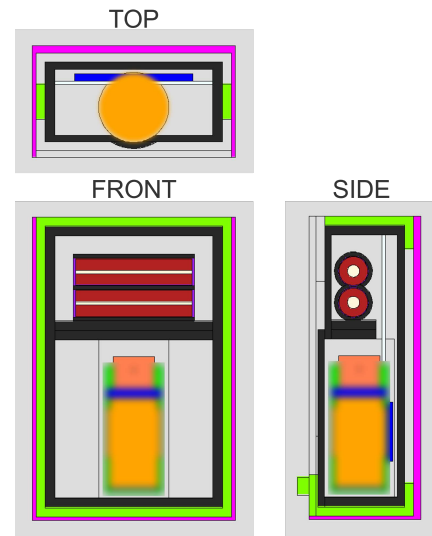


Figure 7-15 MCNP model of PRD-ER

To determine if a photon that deposits a certain energy in the PRD's crystal produces a count, it is necessary to know the PRD's counting efficiency at that energy. In the operating instructions book that comes with the PRD-ER [\[10\]](#), diagram 11-3 shows a graph of the relative count-rate response of the PRD-ER as a function of incident photon energy. We converted values of relative response versus photon energy taken from that graph to counting efficiency versus energy deposited in the crystal by performing MCNP simulations of the type of measurements the manufacturer made to obtain the data used to make the graph. [Figure 7-16](#) shows a graph of the resulting counting efficiency as a function of deposited energy.

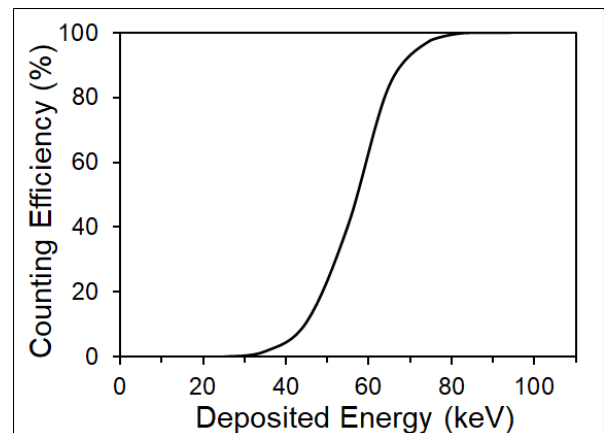


Figure 7-16 PRD-ER counting efficiency vs. energy deposited in its scintillator

In our simulations of the PRD sensitivity measurements and the calculations described in section [C.2.2](#) below, we used the f8 pulse-height tally and binned the calculated pulses according to their energy deposit using 10-keV wide energy bins. The calculated number of counts is the sum of the number of pulses in each deposited-energy bin times the counting efficiency for that energy.

The MCNP simulations of our PRD count-rate sensitivity measurements with a Cs-137 source and with Ba-133 sources with and without filters to remove the low-energy x-rays gave calculated count rates that matched the three measured count rates to within 0.2%, 3%, and 2% respectively. This agreement means NUSTL modeled the PRD-ER and its low-energy response correctly and gives us confidence in the results of our calculations of the count rate in a PRD-ER from radioactivity on a contaminated person at a given distance.



As mentioned in the last paragraph of [C.1.1](#), we did not have a suitable Co-60 source to do measurements but were concerned that the count-rate sensitivity of the PRDs might decrease for high-energy Co-60 gamma rays more than the sensitivity of the portal monitors would decrease. If that were so, the 15-foot (4.6-m) separation of the portal approach lanes that is sufficient to avoid misattributed portal alarms for Cs 137 contamination would not be sufficient for Co-60. To determine the relative sensitivity of the PRD-ER to photons from the two radionuclides, we performed MCNP calculations simulating second-stage prescreening for Cs-137 and Co-60 contamination. We placed the PRD 9 inches (23 cm) in front of the torso of the phantom representing the person being screened and used a vertical line source along the side of the torso of the phantom. The result showed that the PRD is 89% as sensitive to Co-60 gamma rays as it is to Cs-137 photons. When we calculated the relative sensitivity of the portal monitors to external sources of the two radionuclides, we found that the portal is 88% as sensitive to Co-60 gamma rays as it is to Cs-137 photons—almost the same—so the portal approach-lane spacing that avoids misattributed alarms for Cs-137 contamination will also work for Co-60.

C.2.2 DISTANCES TO FIRST-STAGE PRESCREENING

There are two places where unscreened people who might be highly contaminated would come closest to PRDs being used to prescreen someone else and, thus, might cause a misattributed prescreening alarm: at the front of the line of people waiting to be prescreened, where they stand some distance from the first-stage prescreening station just before their turn to approach it, and at the first-stage prescreening station, where they need to be a similar distance away from the second-stage prescreening station. These are distances 4 and 3 in [Figure 7-9](#). Using MCNP, we calculated minimum values of these two distances that will avoid a disruptive number of misattributed PRD alarms from contamination on our design-case RDD victims and from I-131 possibly remaining in certain nuclear medicine patients.

To determine if a calculated count rate would cause an alarm, we used the same alarm threshold settings that FDNY uses.²⁹

Our MCNP model for calculating both distances is similar: a phantom representing an RDD victim or a nuclear medicine patient with radioactivity on or in them standing on a sidewalk near city buildings and a second phantom at some distance representing either a screener wearing a PRD (first-stage prescreening) or a client with the PRD about 9 inches (23 cm) from them (second-stage prescreening). We made trial calculations at different distances to find the distance that produced a PRD count rate at the alarm threshold, using $1/(\text{distance})^2$ scaling to choose the distance for the next calculation.

²⁹ For more information, contact NUSTL@hq.dhs.gov.



[Figure 7-17](#) is a pair of diagrams showing two views of our MCNP model for calculating the minimum distance to the first-stage prescreening station. The diagrams are to scale, so the phantoms appear tiny, and the PRD is invisible. The circles centered around the PRD are spherical surfaces used for variance reduction to reduce the calculation time. As indicated in

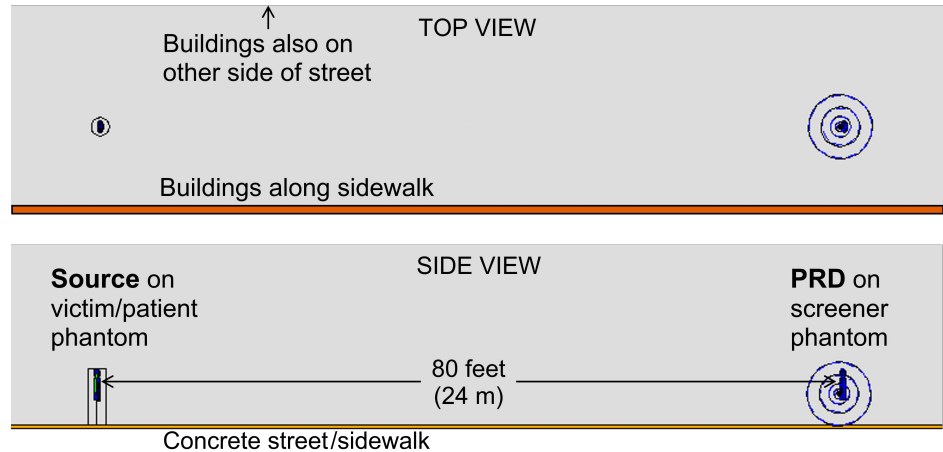


Figure 7-17 MCNP model for calculating distance to first-stage prescreening

[Figures 7-17](#) and [7-18](#), the answer for the distance required to avoid misattributed PRD alarms from the design-case contaminated RDD victim is 80 feet (24 m) from the first-stage screener.

[Figure 7-18](#) shows close-up side views of the phantom with the source and the phantom representing the screener with the PRD. The phantom with the source (left) is now more detailed and is shown with two possible sources. This phantom was developed in the 1960s for the Medical Internal Radiation Dose (MIRD) Committee. We used it because it includes a model of the thyroid gland, the MCNP input for it is available, [\[27\]](#) [\[26\]](#) and we wanted to calculate how far away nuclear medicine patients might cause misattributed alarms. The screener phantom (right) is the same one we used for the portal calculations. (The legs of the phantoms are not visible in the figure because the profile view shown is a slice down the middle, between their legs.)

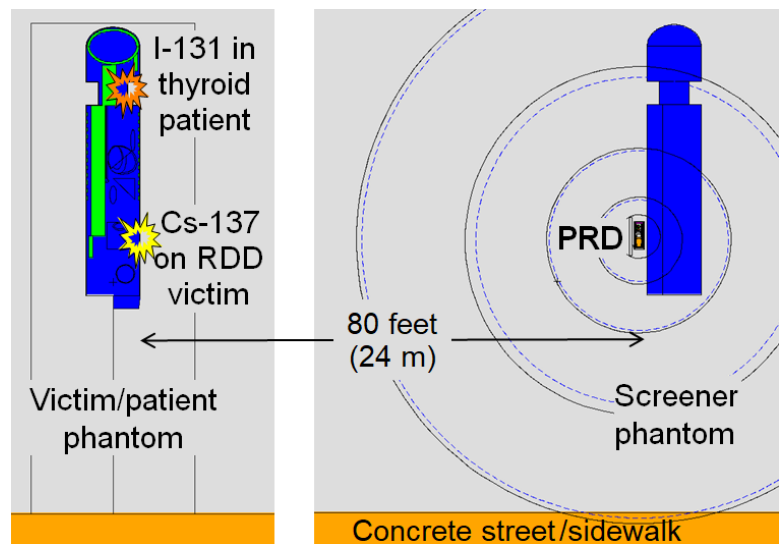


Figure 7-18 Details of MCNP model for calculating distance to first-stage prescreening

For the radioactive source on an RDD victim, we used the same design-case activity of Cs-137 that we used to calculate the distance from the first-stage prescreening station to the nearest portal ([C.1.2.1](#)). We used a single point source 1 m above the ground on the surface of the torso of the phantom.

For a medical patient who might cause misattributed alarms at large distances, we repeated the MCNP prescreening simulation calculation at a distance of 80 ft, replacing the Cs-137 source on the surface of the torso of the MIRD phantom with an I-131 source inside the thyroid gland of the phantom. We looked in the medical literature for how much I-131 could be in the thyroid gland of someone after receiving a therapeutic dose of I-131. [\[21\]](#) We found that the amount of I-131



typically remaining in the thyroid 10 days after a patient is treated for hyperthyroidism could cause a PRD-ER to alarm 80 feet away.

As in the calculations for the distance from first-stage prescreening to the portal monitors, we used the f8 pulse-height tally to determine the fraction of photons emitted by the source that produce pulses that deposit energy in each energy-deposition bin. The number of counts registered by the detector in each energy bin is the number of pulses in that energy bin times the detector's counting efficiency for that energy. The fraction of emitted photons that produce a count is the sum of the number of counts for all the energy bins. To determine the statistical uncertainty in the calculated PRD count rates, we used a separate f8 tally that included a bin for all pulses with a deposited energy above a low-energy cutoff of 57 keV, which gave approximately the same number of counts.

The sodium iodide crystal that is the radiation detector of the PRD is smaller than a person's thumb. Consequently, the detector subtends a tiny solid angle from the source, very few of the photons emitted by the source hit the detector, and the calculation would take a very long time to run without using variance reduction. The situation is significantly worse than for the calculation of the minimum required distance from first-stage prescreening to the portal monitors. Without employing variance reduction methods, each MCNP calculation of the PRD count rate would have to track about 1×10^{11} (100 billion) particles and would take up to 6 days to collect enough hits to reach statistical precision of about 1%.

Because the problem is solid angle rather than absorption by shielding, we used deterministic transport spheres. However, when we used a single dxt sphere, large tally fluctuations made the answer unreliable. We eventually found a paper that explains the cause of the fluctuations and reduces the fluctuations by using multiple nested dxt spheres. [28] Using several dxt spheres nested within one another allows many possible configurations, and it took us many tries to find some that caused the f8 pulse-height tally for the PRD count rate to converge properly. Calculations using the four nested dxt spheres shown by the dashed circles around the PRD in [Figure 7-18](#) converged properly and, according to the MCNP tally figure of merit, ran over 900 times faster than the calculation without variance reduction for the same statistical uncertainty. The practical speed advantage was more like 50 times faster because the calculation had to be run until the statistical uncertainty was 0.2% in order to be sure that it converged.

Using nested dxt spheres has another potential issue, but we showed it was not a problem. The MCNP6 output files for our calculations warn that "f8 variance reduction has not been verified for more than one dxtran sphere". Once we found the correct distance using calculations with nested dxt spheres, we ran a calculation for the same 80-foot distance without variance reduction to verify that using nested dxt spheres does not give a wrong answer for the f8 tally. The count rate from a calculation without variance reduction that took 88 hours and tracked 6.2×10^{10} source particles agreed with the count rate from the calculation using nested dxt spheres within the 1.2% 1-sigma statistical uncertainty of the slow calculation.

While an MCNP input file for the MIRD phantom is available on the internet [27] [26], using it was more difficult than expected. The input file has a small geometry error that must be corrected to avoid losing many particles and halting execution. The file also uses some geometric surfaces that MCNP cannot rotate, so we had to rotate the surfaces of our PRD model to face the MIRD phantom. The MIRD phantom also has its own coordinate rotations that are not quite orthogonal and models the ribs as toroids. A torus is a fourth order surface, which does not have an exact closed solution, so



at large distances from a source there can be small position errors that cause a few particles to be lost. We used the MCNP “lost” statement to allow more than 10 lost particles during calculations with the MIRD phantom. For our thyroid-patient calculations, we would have been better off if we had used just the head, neck, and clavicle of the MIRD phantom incorporated into our simpler soft-tissue phantom.

The 80-foot (24-m) calculated distance required to avoid misattributed first-stage prescreening PRD alarms from the design-case contaminated RDD victim is significantly larger than simpler calculations would have predicted. We did calculations with various simpler models to see if we really needed to include the air, ground, phantoms, and buildings. When we did the calculation for just the source and sodium iodide crystal in empty space without any other materials, the answer was 33 feet (10 m). [Table 7-2](#) shows the effect of various objects on the calculated PRD count rate and the distance at which the amount of Cs-137 on our design-case RDD victim would cause the PRD to alarm. The reason for the differences is that the materials surrounding the source and detector scatter the radiation, so that photons that would have missed the detector can bounce toward it. Just including air (in a 50-m radius sphere) increased the calculated count rate by 22% and increased the alarm distance to 36 feet (11 m). When we include everything except buildings along the sidewalk, the answer is 72 feet (22 m), and this is the required distance if prescreening is done on open ground rather than on a city sidewalk. However, we recommend using 80 feet so there is just one value for the distance to first-stage prescreening.

Table 7-2 Effect of Scattering Material on Calculated PRD Count Rate and Alarm Distance

↓
Increasing
realism

| Configuration | Relative count rate | Alarm distance | |
|--|---------------------|----------------|--------|
| | | Feet | Meters |
| Source & NaI crystal in vacuum | 1.00 | 33 | 10 |
| Source & NaI crystal in air | 1.22 | 36 | 11 |
| Source & PRD in air | 1.36 | 38 | 12 |
| Source & NaI crystal, air over ground | 1.7 | 43 | 13 |
| Source & PRD, air over ground | 1.9 | 45 | 14 |
| PRD on phantom, source in air /ground | 2.7 | 54 | 16 |
| Source on phantom, PRD in air /ground | 3.4 | 61 | 19 |
| Source & PRD on phantoms, open ground | 4.7 | 72 | 22 |
| Source & PRD on phantoms, near buildings | 6.0 | 80 | 24 |

C.2.3 DISTANCE BETWEEN FIRST-STAGE AND SECOND-STAGE PRESCREENING

For calculating the distance between the first-stage and second-stage prescreening stations (distance number 3 in [Figure 7-9](#)), the only difference is that the PRD in second-stage prescreening is about 9 inches (23 cm) away from a person undergoing second-stage prescreening rather than being worn by the first-stage screener. The calculated distance at which the contamination on the design-case RDD victim would cause a PRD to alarm during second-stage prescreening on a city sidewalk is 75 feet (23 m). For operational simplicity, we recommend that the distance between the



two prescreening stations be the same as the distance from the front of the line of people waiting to be prescreened to the first-stage prescreening station: 80 feet.

C.3 EXAMPLE OF MCNP INPUT

As an example of an MCNP input file for one of our calculations, below is the input for calculating the energy-deposit distribution in the four scintillators of a Ludlum 52-1-1 portal monitor in a CRC building with a brick wall and a concrete roof when a Cs-137 source on a phantom is 22 m (72.18 feet) from the center of the portal.

```
CRC11a,Cs137,72ft,b,: CRC, brick wall,concrete roof, 3 phantoms, Cs-137 @22.0 m
c Source is 22.0 meters (72.18 ft) **+y** from center of portal
c Tally all 4 portal monitor scintillators,
c Source on torso of one soft tissue phantom
c Another phantom in (30 cm past) portal
c Third phantom sitting on far side of portal
C
C CELLS
11 3 -1.032 -11 imp:p=1 $ -x lower scintillator 1
12 3 -1.032 -12 imp:p=1 $ -x lower scintillator 2
C
21 3 -1.032 -21 imp:p=1 $ -x upper scintillator 1
22 3 -1.032 -22 imp:p=1 $ -x upper scintillator 2
C
c base of portal 17.5" x 36" x ~1" = 44.45 x 91.44 x 2.54 cm
c Assume base sheet aluminum is .126"= 0.32 cm thick to homogenize bracing
13 1 -1.1278e-3 -13 imp:p=1 $ air inside portal base
14 6 -2.68 13 -14 imp:p=1 $ portal base
15 6 -2.68 15 -16 -18 imp:p=1 $ electronics enclosure
16 6 -2.68 -16 18 -19 imp:p=1 $ top of electronics enclosure
17 14 -0.132 -15 -18 imp:p=1 $ electronics
18 6 -2.68 -17 imp:p=1 $ portal top piece
19 1 -1.1278e-3 -16 19 imp:p=1 $ air above electronics slanted top
7 6 -2.68 -7 imp:p=1 $ upright 1 -x cover strip
8 6 -2.68 -8 imp:p=1 $ upright 1 +x cover strip
9 6 -2.68 -9 -189 imp:p=1 $ upright 2 -x cover strip hi imp
209 6 -2.68 -9 189 imp:p=1 $ upright 2 -x cover strip low imp
10 6 -2.68 -10 -189 imp:p=1 $ upright 2 +x cover strip hi imp
210 6 -2.68 -10 189 imp:p=1 $ upright 2 +x cover strip low imp
C
23 1 -1.1278e-3 -24 14 16 17 7 8 9 10 30 50 25 26 -189 imp:p=1 $ -x portal uprights slab
24 1 -1.1278e-3 -24 14 16 17 7 8 9 10 30 50 25 26 189 -190 imp:p=1 $ -x portal uprights slab
224 1 -1.1278e-3 -24 14 16 17 7 8 9 10 30 25 26 190 imp:p=1 $ -x portal uprights slab
25 6 -2.68 14 -25 27 81 82 83 84 imp:p=1 $ portal upright 1 aluminum
26 6 -2.68 14 -26 28 85 86 87 88 -189 imp:p=1 $ portal upright 2 aluminum
226 6 -2.68 14 -26 28 85 86 87 88 189 imp:p=1 $ portal upright 2 aluminum hi imp
27 1 -1.1278e-3 14 -80 -108 109 imp:p=1 $ lowest air in portal upright low imp 1
29 1 -1.1278e-3 -27 11 80 -89 92 93 imp:p=1 $ air around lower scintillator etc. 1
37 1 -1.1278e-3 -27 89 -98 -110 111 imp:p=1 $ middle air in portal upright 1
38 1 -1.1278e-3 -27 21 98 -99 102 103 imp:p=1 $ air around upper scintillator etc. 1
39 1 -1.1278e-3 -27 99 imp:p=1 $ highest air in portal upright 1
c Go to cells 116 -120 for upright 2 air cells
C
30 1 -1.1278e-3 14 -30 31 32 33 34 35 36 189 imp:p=1 $ container for portal phantom, hi imp
230 1 -1.1278e-3 14 -30 31 32 33 34 35 36 -189 imp:p=1 $container for portal phantom, low imp
31 11 -1.04 -31 189 imp:p=1 $ torso of phantom in portal
231 11 -1.04 -31 -189 imp:p=1 $ torso of phantom in portal
32 11 -1.04 -32 189 imp:p=1 $ neck of phantom in portal
232 11 -1.04 -32 -189 imp:p=1 $ neck of phantom in portal
33 11 -1.04 -33 189 imp:p=1 $ lower head of phantom in portal
233 11 -1.04 -33 -189 imp:p=1 $ lower head of phantom in portal
34 11 -1.04 33 -34 189 imp:p=1 $ upper head of phantom in portal
234 11 -1.04 33 -34 -189 imp:p=1 $ upper head of phantom in portal
35 11 -1.04 14 -35 31 61 imp:p=1 $ left leg of phantom in portal
36 11 -1.04 14 -36 31 61 imp:p=1 $ right leg of phantom in portal
C
40 1 -1.1278e-3 -40 41 42 43 44 45 46 imp:p=1 $ container for phantom with source
41 11 -1.04 -41 imp:p=1 $ torso of source phantom
42 11 -1.04 -42 imp:p=1 $ neck of phantom
43 11 -1.04 -43 imp:p=1 $ lower head of phantom
```



```

44 11 -1.04          43 -44          imp:p=1 $ upper head of phantom
45 11 -1.04          -45 41 61       imp:p=1 $ left leg of phantom
46 11 -1.04          -46 41 61       imp:p=1 $ right leg of phantom
C
50 1 -1.1278e-3 5 61 -50 51 52 53 54 55 56 imp:p=1 $ container for sitting phantom
51 11 -1.04          -51          imp:p=1 $ torso of sitting phantom
52 11 -1.04          -52          imp:p=1 $ neck of phantom
53 11 -1.04          -53          imp:p=1 $ lower head of phantom
54 11 -1.04          -53 -54        imp:p=1 $ upper head of phantom
55 11 -1.04          5 61 -55 51 61  imp:p=1 $ left leg of phantom
56 11 -1.04          5 61 -56 51 61  imp:p=1 $ right leg of phantom
C
58 1 -1.1278e-3 24 30 -60 -189          imp:p=1 $BB court air really near portal 1
59 1 -1.1278e-3 14 24 30 50 -60 189 -190 imp:p=1 $BB court air near portal 1
60 1 -1.1278e-3 2 3 4 14 24 30 50 -60 190 imp:p=1 $ Basketball court air
61 1 -1.1278e-3 60 -62 61 190 imp:p=1 $ Gym air outside of bb court
261 1 -1.1278e-3 60 -62 61 -190 imp:p=1 $ Gym air outside of bb court near portal 1
62 4 -0.689          -61 190          imp:p=1 $ gym floor, maple wood
262 4 -0.689          -61 -190         imp:p=1 $ gym floor near portal 1
c Areal density of 4" thick block+tile wall is 17.2 g/cm2; sg = -17.2/10.16= -1.693
63 8 -1.693          62 -63          imp:p=1 $ concrete block+tile wall around gym
64 1 -1.1278e-3 63 -64          imp:p=1 $ air in school outside gym
65 10 -1.84          64 -65          imp:p=1 $ brick wall of school
67 8 -2.35          -68          imp:p=1 $ concrete roof on gym
68 8 -2.35          -67 68          imp:p=1 $ concrete school roof outside gym
C
70 8 -2.35          -5 6 -63.1 -63.2 -63.3 -63.4 imp:p=1 $ concrete foundation in gym
71 8 -2.35          -5 6 (63.1:63.2:63.3:63.4) -65.1 -65.2 -65.3 -65.4 imp:p=1 $
concrete foundation in school outside gym
C
72 8 -2.35          -5 6 (65.1:65.2:65.3:65.4) -191 imp:p=1 $ paving inside shell 1
73 8 -2.35          -5 6 191 -999          imp:p=1 $ paving outside shell 1
C
190 1 -1.1278e-3 5 65 67 -191 imp:p=1 $ air outside school inside imp shell 1
190 1 -1.1278e-3 5 40 191 -999 imp:p=1 $ air outside imp shell 1
C
81 1 -1.1278e-3 -81          imp:p=1 $ air in -x lower slot in portal upright 1
82 1 -1.1278e-3 -82          imp:p=1 $ air in +x lower slot in portal upright 1
83 1 -1.1278e-3 -83          imp:p=1 $ air in -x upper slot in portal upright 1
84 1 -1.1278e-3 -84          imp:p=1 $ air in +x upper slot in portal upright 1
85 1 -1.1278e-3 -85          imp:p=1 $ air in -x lower slot in portal upright 2
86 1 -1.1278e-3 -86          imp:p=1 $ air in +x lower slot in portal upright 2
87 1 -1.1278e-3 -87          imp:p=1 $ air in -x upper slot in portal upright 2
88 1 -1.1278e-3 -88          imp:p=1 $ air in +x upper slot in portal upright 2
C
90 2 -1.0          -90          imp:p=1 $ inside lower PM tube 1 (LB) low density Cu
91 15 -2.23          90 -91          imp:p=1 $ glass of lower PM tube 1 (LB)
92 16 -8.7          91 -92          imp:p=1 $ mag shield of lower PM tube 1 (LB)
93 17 -1.0          -93          imp:p=1 $ base of lower PM tube 1 (LB)
94 2 -1.0          -94          imp:p=1 $ inside lower PM tube 2 (RB) low density Cu
95 15 -2.23          94 -95          imp:p=1 $ glass of lower PM tube 2 (RB)
96 16 -8.7          95 -96          imp:p=1 $ mag shield of lower PM tube 2 (RB)
97 17 -1.0          -97          imp:p=1 $ base of lower PM tube 2 (RB)
100 2 -1.0          -100         imp:p=1 $ inside upper PM tube 1 (LT) low density Cu
101 15 -2.23          100 -101        imp:p=1 $ glass of upper PM tube 1 (LT)
102 16 -8.7          101 -102        imp:p=1 $ mag shield of upper PM tube 1 (LT)
103 17 -1.0          -103         imp:p=1 $ base of upper PM tube 1 (LT)
104 2 -1.0          -104 189        imp:p=1 $ inside upper PM tube 2 (RT low density Cu
204 2 -1.0          -104 -189       imp:p=1 $ inside upper PM tube 2 (RT low density Cu
105 15 -2.23 104 -105 189 imp:p=1 $ glass of upper PM tube 2 (RT)
205 15 -2.23 104 -105 -189 imp:p=1 $ glass of upper PM tube 2 (RT)
106 16 -8.7 105 -106 189 imp:p=1 $ mag shield of upper PM tube 2 (RT)
206 16 -8.7 105 -106 -189 imp:p=1 $ mag shield of upper PM tube 2 (RT)
107 17 -1.0          -107         imp:p=1 $ base of upper PM tube 2 (RT)
C
108 6 -2.68          14 -27 108 -80 imp:p=1 $ lower reinforcing of portal upright 1
109 17 -1.26          -109         imp:p=1 $ lower connector block, upright 1
110 6 -2.68          -27 89 -98 110 imp:p=1 $ middle reinforcing of portal upright 1
111 17 -1.26          -111         imp:p=1 $ middle connector block, upright 1
112 6 -2.68          14 -28 118 -80 imp:p=1 $ lower reinforcing of portal upright 2
113 17 -1.26          -119         imp:p=1 $ lower connector block, upright 2
114 6 -2.68          -28 89 -98 120 -189 imp:p=1 $ middle reinforcing of portal upright 2
214 6 -2.68          -28 89 -98 120 189 imp:p=1 $ middle reinforcing of portal upright 2
115 17 -1.26          -121         -189 imp:p=1 $ middle connector block, upright 2
215 17 -1.26          -121         189 imp:p=1 $ middle connector block, upright 2

```




C
116 1 -1.1278e-3 14 -80 -118 119 imp:p=1 \$ lowest air in portal upright 2
117 1 -1.1278e-3 -28 12 80 -89 96 97 imp:p=1 \$ air around lower scintillator etc. 2
118 1 -1.1278e-3 -28 89 -98 -120 121 -189 imp:p=1 \$ middle air in portal upright 2
119 1 -1.1278e-3 -28 89 -98 -120 121 189 imp:p=1 \$ middle air in portal upright 2
120 1 -1.1278e-3 -28 22 98 -99 106 107 -189 imp:p=1 \$ air around upper scintillator etc. 2
121 1 -1.1278e-3 -28 22 98 -99 106 107 189 imp:p=1 \$ air around upper scintillator etc. 2
122 1 -1.1278e-3 -28 99 imp:p=1 \$ highest air in portal upright 2
C
998 0 -6 -999 imp:p=0 \$ below paved ground
999 0 999 imp:p=0 \$ rest of universe
C
C Blank line below ends cells.

C Blank line above ends cells and starts surfaces.
C
C SURFACES
C
C Ludlum 52-1-1 has 4 scintillators.
C Each scintillator is 1.5"(3.81 cm) thick, 4"(10.16 cm) wide, 28"(71.12cm) tall
C Scintillator if centered at origin:
C rpp -5.08 5.08 -1.905 1.905 -35.56 35.56 \$ scintillator if at origin
C Center-to center distance between scintillators is 34"
C Center of portal to outside of scintillator is 17.75"= 45.085 cm
C -+Y ends of rpp containing scintillators are
C 7.5'+15'+17.75"= 287.75"= 730.885 cm. 287.75"+15'=467.75"= 1188.085 cm.
C Scintillators start 11.5"=29.21cm above floor; end 75.5"=191.77cm above floor
C Top of lower scintillators 29.21+71.12=100.33 cm above floor, z=103.33
C Bottom of upper scintillators 191.77-71.12=120.65 cm above floor, z=123.65
C
C Slab containing -x lower portal scintillators:
2 1 rpp -248.92 -238.76 -730.885 -100 32.21 103.33 \$ -x lower scint slab
3 1 rpp -248.92 -238.76 -730.885 -100 123.65 191.77 \$ -x upper scint slab
4 1 rpp -248.92 -238.76 -730.885 -100 103.33 123.65 \$ between-x scint slabs
5 pz 0.0 \$ plane of paved ground
6 pz -14.78 \$ bottom of concrete, below is imp=0 (should be 7" - 3cm = 14.78cm thick)
C
11 rpp -248.92 -238.76 -730.885 -727.075 32.21 103.33 \$ -x lower scint 1
12 2 rpp -248.92 -238.76 -730.885 -727.075 32.21 103.33 \$ -x lower scint 2
C
21 rpp -248.92 -238.76 -730.885 -727.075 123.65 194.77 \$ -x upper scint 1
22 2 rpp -248.92 -238.76 -730.885 -727.075 123.65 194.77 \$ -x upper scint 2
C
C X center of portal is -243.84.
C base of portal 17.5" x 36" x 1.25" = 44.45 x 91.44 x 3.175 cm
C Assume base sheet aluminum is .126"= 0.32 cm thick to homogenize bracing
13 rpp -265.74 -221.94 -731.20 -640.40 3 5.855 \$ inside of portal base
14 rpp -266.06 -221.62 -731.52 -640.08 3 6.175 \$ outside of portal base
C
C Electronics box on Left side of left portal upright near cell 11
C same x width as upright, y thickness= 4"= 10.16 cm
C top near midpoint between scintillators, z= 118.25 (measured);
C height= 22.56"= 57.3 cm including angled part (measured)
15 rpp -251.94 -235.74 -741.52 -731.68 61.11 118.09 \$ inside of electronics enclosure
16 rpp -252.10 -235.58 -741.68 -731.52 60.95 118.25 \$ outside of electronics enclosure
C slanted top piece bottom at 6.6875"=17.0 cm below top; top end 1.5 cm -y from upright
C => bottom inside y= -731.52 z= 118.09-17.0= 101.09 ; top y= -733.02 z= 118.09
C 3-point plane for inside of top of electronics enclosure
18 p -252.10 -741.68 101.09 -235.58 -741.68 101.09 -243.84 -733.02 118.09 \$ plane
C for inside of top of electronics enclosure
C 3-point plane for outside of top of electronics enclosure
19 p -252.10 -741.68 101.41 -235.58 -741.68 101.42 -243.84 -733.10 118.25 \$ plane
C for outside of top of electronics enclosure
C
17 rpp -252.10 -235.58 -731.52 -640.08 213.66 213.90 \$ portal top piece, 0.093"=0.236cm thk
C
C Aluminum enclosing scintillators is 0.067"=0.170 cm with paint
C Outside dimensions of portal uprights: x width=6.5"=16.51cm -> 16.52cm,
C y width=2"=5.08cm, z height=83"=210.82cm above floor.
C 16/2=8 ft = 243.84 cm. 243.84+8.26= 252.10 cm. 243.84-8.26= 235.58 cm.
C Outside width of portal uprights is 36"
C Outside of slab containing -x portal uprights
7 rpp -252.27 -252.10 -727.71 -726.44 6.175 213.66 \$ upright 1 -x cover strip
8 rpp -235.58 -235.41 -727.71 -726.44 6.175 213.66 \$ upright 1 +x cover strip

```

9 2 rpp -252.27 -252.10 -731.52 -730.25 6.175 213.66 $ upright 2 -x cover strip
10 2 rpp -235.58 -235.41 -731.52 -730.25 6.175 213.66 $ upright 2 +x cover strip
c
24 rpp -252.27 -235.41 -2570 -640 3.0 213.90 $ -x portal slab - expanded
25 rpp -252.10 -235.58 -731.52 -726.44 3.0 213.66 $ -x portal upright 1 outside
26 2 rpp -252.10 -235.58 -731.52 -726.44 3.0 213.66 $ -x upright 2 outside
27 rpp -251.93 -235.75 -731.35 -726.61 3.16 213.50 $ -x inside of portal upright 1
28 2 rpp -251.93 -235.75 -731.35 -726.61 3.16 213.50 $ -x upright 2 inside
c
c photomultiplier tubes, magnetic shields, bases, reinforcing Al
80 pz 21.41 $ bottom of lower PM base
89 pz 103.33 $ top of lower scintillator
98 pz 123.65 $ bottom of upper scintillator
99 pz 205.57 $ top of upper PM base
c
90 rcc -243.84 -728.98 31.91 0 0 -8.6 1.275 $ inside of lower PM tube 1 (LB)
91 rcc -243.84 -728.98 32.21 0 0 -9.2 1.425 $ outside of lower PM tube 1
92 rcc -243.84 -728.98 32.21 0 0 -9.2 1.625 $ outside of lower mag shield 1
93 rcc -243.84 -728.98 23.01 0 0 -1.6 1.625 $ outside of lower PM base 1 (enlarged)
94 2 rcc -243.84 -728.98 31.91 0 0 -8.6 1.275 $ inside of lower PM tube 2 (RB)
95 2 rcc -243.84 -728.98 32.21 0 0 -9.2 1.425 $ outside of lower PM tube 2
96 2 rcc -243.84 -728.98 32.21 0 0 -9.2 1.625 $ outside of lower mag shield 2
97 2 rcc -243.84 -728.98 23.01 0 0 -1.6 1.625 $ outside of lower PM base 2 (enlarged)
100 rcc -243.84 -728.98 195.07 0 0 8.6 1.275 $ inside of upper PM tube 1 (LT)
101 rcc -243.84 -728.98 194.77 0 0 9.2 1.425 $ outside of upper PM tube 1
102 rcc -243.84 -728.98 194.77 0 0 9.2 1.625 $ outside of upper mag shield 1
103 rcc -243.84 -728.98 203.97 0 0 1.6 1.625 $ outside of upper PM base 1 (enlarged)
104 2 rcc -243.84 -728.98 195.07 0 0 8.6 1.275 $ inside of upper PM tube 2 (RT)
105 2 rcc -243.84 -728.98 194.77 0 0 9.2 1.425 $ outside of upper PM tube 2
106 2 rcc -243.84 -728.98 194.77 0 0 9.2 1.625 $ outside of upper mag shield 2
107 2 rcc -243.84 -728.98 203.97 0 0 1.6 1.625 $ outside of upper PM base 2 (enlarged)
c
-252.10 -235.58 -731.52 -726.44
108 rpp -251.76 -235.90 -731.18 -726.78 6.175 23.01 $ inside of 1 lower reinforcing Al
c measured connector block is 6.2 cm wide (x), 3.1 cm y, ~6.2 cm z
c (On the L side (1) there is another connector (rotated) for the electronics box.)
c visible joint of upright to base is 4.5"= 11.43 cm above top of base
c => z= 6.175+11.43= 17.605
c Top of connector is at part line.
109 rpp -246.94 -240.74 -730.53 -727.43 11.4 17.60 $ 1 lower connector block
110 rpp -251.78 -235.90 -731.18 -726.78 103.33 123.65 $ inside of 1 middle reinforcing Al
111 rpp -246.94 -240.74 -730.53 -727.43 115.15 121.35 $ 1 middle connector block
c
118 2 rpp -251.78 -235.90 -731.18 -726.78 6.175 23.01 $ inside of 2 lower reinforcing Al
119 2 rpp -246.94 -240.74 -730.53 -727.43 11.4 17.60 $ 2 lower connector block
120 2 rpp -251.78 -235.90 -731.18 -726.78 103.33 123.65 $ inside of 2 middle reinforcing Al
121 2 rpp -246.94 -240.74 -730.53 -727.43 115.15 121.35 $ 2 middle connector block
c
c
c phantom representing person in portal
c big cylinder to contain phantom with head and legs
30 3 rcc 0 0 3 0 0 190 25 $ container for phantom
31 3 rec 0 0 83 0 0 70 0 20 0 10 $ torso, MIRD dimensions, vol=43,982.29 cm3
32 3 rcc 0 0 153 0 0 8.4 5.4 $ neck, MIRD dimensions, V=769.51 cm3
33 3 rec 0 0 161.4 0 0 13 10 0 0 8 $ lower head, MIRD dimensions, V=3,267.26 cm3
34 3 ell 0 0 174.4 10 0 0 -8 $ upper head, MIRD dimensions, V=1,340.41 cm3
c My lower thigh above knee is 43 cm circumference, 6.84 cm radius
c 35 3 trc 0 -10 85 15 0 -82 9 3.8 $ left leg, V=? cm3
c 36 3 trc 0 10 85 -15 0 -82 9 3.8 $ right leg, V=? cm3
35 3 trc 0 -10 85 0 0 -82 9 3.8 $ left leg, V=? cm3
36 3 trc 0 10 85 0 0 -82 9 3.8 $ right leg, V=? cm3
c c Volumes of elliptical cells from web calculator,
c Total volume = 72,876.47 cm3; mass = 75791.5 g = 75.792 kg = 167 pounds
c
c phantom representing person with source representing contamination
40 4 rcc 0 0 3 0 0 190 25 $ container for phantom
41 4 rec 0 0 83 0 0 70 0 20 0 10 $ torso, MIRD dimensions, vol=43,982.29 cm3
42 4 rcc 0 0 153 0 0 8.4 5.4 $ neck, MIRD dimensions, V=769.51 cm3
43 4 rec 0 0 161.4 0 0 13 10 0 0 8 $ lower head, MIRD dimensions, V=3,267.26 cm3
44 4 ell 0 0 174.4 10 0 0 -8 $ upper head, MIRD dimensions, V=1,340.41 cm3
45 4 trc 0 -10 85 0 0 -82 9 3.8 $ left leg
46 4 trc 0 10 85 0 0 -82 9 3.8 $ right leg
c
c phantom representing firefighter sitting at portal display panel
50 7 rcc 0 0 3 0 0 190 30 $ container for phantom

```



```
51 7 rec 0 0 83 0 0 70 0 20 0 10 $ torso, MIRD dimensions, Vol=43,982.29 cm3
52 7 rcc 0 0 153 0 0 8.4 5.4 $ neck, MIRD dimensions, V=769.51 cm3
53 7 rec 0 0 161.4 0 0 13 10 0 0 8 $ lower head, MIRD dimensions, V=3,267.26 cm3
54 7 ell 0 0 174.4 10 0 0 -8 $ upper head, MIRD dimensions, V=1,340.41 cm3
55 7 trc -15 -10 95 0 0 -82 9 3.8 $ left leg
56 7 trc -15 10 95 0 0 -82 9 3.8 $ right leg
c
c Gym
60 1 rpp -762 762 -1280 1280 3 603 $ basketball court above floor
61 1 rpp -912 912 -1580 1580 0 3 $ wood floor 3 cm thick
62 1 rpp -912 912 -1580 1580 0 603 $ inside of gym
c interior walls 4"= 10.16 cm thick.
63 1 rpp -922.16 922.16 -1590.16 1590.16 0 603 $ outside of interior wall around gym
c
c 8"(20.3 cm) thick brick wall of school around gym
c inside of brick wall 1 cm -x and 30' (914 cm) +x and +-y, from gym wall
c
64 6 rpp -923.16 1836.16 -1591.16 2504.16 0 603 $inside of brick exterior wall
65 6 rpp -943.46 1856.46 -1611.46 2524.46 0 603 $outside of brick wall
67 6 rpp -943.46 1856.46 -1611.46 2524.46 603 611 $ whole roof slab
68 1 rpp -922.16 922.16 -1590.16 1590.16 603 611 $ roof slab over gym
c
c
c Surfaces for slots in aluminum on inside of portal uprights.
c The slotted area is the same as the scintillator area.
c what fraction of the area should be open?
c In the real portal monitor, an area 2"x0.625" has 2 slots, each 0.75"x0.25".
c So the open area is 2*(.75*.25)= 2*0.1875 in^2 = 0.375 in^2
c and the total area is 2"*0.625"= 1.25 in^2.
c The open fraction is 0.375/1.25 = 0.3 .
c So for a 2" wide space with one slot, the slot should be 0.6" wide = 1.524 cm
c Round up to 1.53 cm and move outer edge inward from +-2" to compensate for
c missing edge of scintillator at 9 degree angle 4.445*(tan a = 0.162)=0.7cm
c So move outer edge of slot inward by 0.7 cm
c Make 2 vertical slots for each scintillator
81 rpp -248.22 -246.69 -726.61 -726.44 32.21 103.33 $ -x slot lower scint 1
82 rpp -240.99 -239.46 -726.61 -726.44 32.21 103.33 $ +x slot lower scint 1
83 rpp -248.22 -246.69 -726.61 -726.44 123.65 194.77 $ -x slot upper scint 1
84 rpp -240.99 -239.46 -726.61 -726.44 123.65 194.77 $ +x slot upper scint 1
85 2 rpp -248.22 -246.69 -731.52 -731.35 32.21 103.33 $ -x slot lower scint 2
86 2 rpp -240.99 -239.46 -731.52 -731.35 32.21 103.33 $ +x slot lower scint 2
87 2 rpp -248.22 -246.69 -731.52 -731.35 123.65 194.77 $ -x slot upper scint 2
88 2 rpp -240.99 -239.46 -731.52 -731.35 123.65 194.77 $ +x slot upper scint 2
c
c Importance shells
189 s -243.84 -642.62 159.21 42 $ importance shell around upper close scint of portal 1
190 s -243.84 -685.8 50 400 $ importance shell around portal 1
191 6 s 430 450 -300 2750 $ importance shell 2
c
999 s 244 0 -1500 6000 $ sphere bounding problem
c 999 s 0 2000 -1500 8000 $ sphere bounding problem for no building
c
c Blank line below ends surfaces.
c
c Blank line above ends surfaces.
c
c TRANSFORMATIONS
c to rotate 90 degrees around z axis
c 0 0 0 cos90 -sin90 0 sin90 cos90 0 0 0 1 = 0 0 0 0 -1 0 1 0 0 0 0 1
c
c Move basketball court, interior (and exterior) walls so
c +y end of basketball court is 5' = 60"= 152.4 cm +y from center of portal.
c That is y= 152.4 -685.8 -1280 = -1813.4
tr1 0 -1813.4 0 $ Move basketball court, interior wall,
c
c The spacing between the centers of scintillators of a portal is 34"= 86.36 cm
c The spacing between portals in the same row is 30'=360"= 914.4 cm
tr2 0 86.36 0 $ scintillator 1 -> 2
tr3 -213.84 -685.8 0 $ move phantom from origin to portal (off center)
tr4 -243.84 1524.2 0 0 -1 0 1 0 0 0 0 1 $ move phantom from origin to source
c want -243.84 (-685.8 + 2200 +10) = -243.84 1524.2
c Note: source should be at -243.84 1514.1 103.0 ,
c but put it at portal center, -243.84 -685.8 103.0, and use tr5 in source
tr5 0 2199.9 0 $ distance from source to portal center ***
```



```
tr6 0 -2727.4 0 $ Move exterior wall, imp shell
tr7 -243.84 -773.8 -40 0 -1 0 1 0 0 0 0 1 $ move phantom to sit at portal display
C
C MATERIALS
C Use default photon cross sections chosen by xsdir
C
C AIR. At 20C and 1013.25 hPa, dry air has a density of 1.2041E-3 g/cm3
C Density depends on pressure, temperature, and humidity
C See https://www.brisbanehotairballooning.com.au/faqs/education/
C 116-calculate-air-density.html
C = How to Calculate Air Density.mht
C Worst case is low density: T=90F=33C, P=1000HPa, Dewpoint=68F=20C
C Moist air density= 1.1278e-3 g/cm3, dry air sg=1.1113, water vap sg=0.0165
C Specific humidity = .0165/1.1278 = 0.01463
C Get composition from file: Isotopic fraction calculator.xls, sheet 2.
m1 1001 -0.001613 $ H in humid air
    6000 -0.000128 $ C (CO2 in humid air)
    7000 -0.744326 $ N (N-14, ignore N-15)
    8000 -0.241236 $ O
    18040 -0.012696 $ Ar
C
C Copper for dynodes of PM tubes
m2 29000 -1.0 $ Cu
C
C PVT plastic scintillator (from NIST STAR database) sg = -1.032
m3 1001 -0.085 $ H in PVT scintillator
    6000 -0.915 $ C
C
C Maple wood for basketball court floor. Sugar Maple sg = -0.689
m4 1001 -0.06 $ H in maple wood
    6000 -0.50 $ C
    8016 -0.44 $ O
C
C Aluminum Alloy, 5052-H32 (Patrick Brand, Ludlum, 2018Jun19)
C sg=-2.68
C Mg .025 Al .9654 (with "other") Si .002 Cr .0025 Mn .0007
C Fe .003 Cu .0007 Zn .0007 $
m6 12000 -.025 $ Mg in 5052 aluminum alloy
    13000 -.9654 $ Al in 5052 aluminum alloy
    14000 -.002 $ Si in 5052 aluminum alloy
    24000 -.0025 $ Cr in 5052 aluminum alloy
    25000 -.0007 $ Mn in 5052 aluminum alloy
    26000 -.003 $ Fe in 5052 aluminum alloy
    29000 -.0007 $ Cu in 5052 aluminum alloy
    30000 -.0007 $ Zn in 5052 aluminum alloy
C
C Concrete, PG Average, see file concrete_compositions,2008.xls
C assume sg= -2.35 from NBS 4 standard concrete
m8 1001 -.0061 $ H in concrete
    6000 -.0055 $ C
    8000 -.5010 $ O
    11000 -.0149 $ Na
    12000 -.0074 $ Mg
    13000 -.0474 $ Al
    14000 -.2872 $ Si
    16000 -.0014 $ S
    19000 -.0127 $ K
    20000 -.1000 $ Ca
    22000 -.0034 $ Ti
    26000 -.0130 $ Fe
C
C Brick walls. (Common brick size is 9 x 4.5 x 2.75 in.)
C Assume mortar is like brick except it has 10% Ca. 20% mortar -> add 2% Ca
C See Brick, CE625-Masonry-Units.pdf;
C density of solid brick = -2.35, but with voids sg = -1.84
C For composition, see Brick clay (Maryland) NBS material 679, SRM certificate.pdf
C and add oxygen for remainder.
C Total water absorption capacity is 12.3%; add 4% water to dry brick composition
C 0.96*brick + 0.04*(-.111894 H, -.888106 O) (NIST Star database)
m10 1000 -.00448 $ H in wetted brick
    8000 -.5095 $ O (.96*.4937 + .04*.888106)
    11020 -.00125 $ Na
    12000 -.00725 $ Mg
    13000 -.1057 $ Al
```




```
14000  -.2337  $ Si
19000  -.02336  $ K
20040  -.0207   $ Ca (.96*.0216)
22000  -.0055   $ Ti
25000  -.00166  $ Mn
26000  -.0869   $ Fe
C
C Interior masonry walls of concrete block+tile -> concrete
C Areal density of 4" thick wall is 17.2 g/cm2; sg = -17.2/10.16= -1.693
C
C Soft Tissue, sg= -1.04
m11  1000 10.454E-02 $ H in soft tissue
      6000 22.663E-02
      7000 2.490E-02
      8000 63.525E-02
      11000 0.112E-02 $ Na
      12000 0.013E-02 $ Mg
      14000 0.030E-02 $ Si
      15000 0.134E-02 $ P
      16000 0.204E-02 $ S
      17000 0.133E-02 $ Cl
      19000 0.208E-02 $ K
      20000 0.024E-02 $ Ca
      26000 0.005E-02 $ Fe
      30000 0.003E-02 $ Zn
      37000 0.001E-02 $ Rb?
      40000 0.001E-02 $ Zr in soft tissue?
C
C portal electronics, epoxy fiberglass, copper, steel, plastic; very rough guess
C sg= -1.0 ?
C FR4 epoxy fiberglass for DUT board sg = -1.82
C H 45.8% C 43.4% O 7.2% + 2.4% = 9.6% Si 1.2%
C look at test outp to get mass fractions:
C H -.0612 C -.6907 O -.2035 Si -.0446
C add 9% copper, 5 % iron, 5% C 1% H (multiply F4 fractions by 0.8)
m14  1000 -0.05896 $ H in electronics
      6000 -0.60256 $ C
      8000 -0.16280 $ O
      14000 -0.03568 $ Si
      26000 -0.05 $ Fe
      29000 -0.09 $ Cu
C
C borosilicate glass for PM tubes
C Pyrex glass from NIST STAR database; sg = -2.23
m15  5000 -0.040064 $ boron in Pyrex glass
      8000 -0.539562 $ O
      11000 -0.028191 $ Na
      13000 -0.011644 $ Al
      14000 -0.377220 $ Si
      19000 -0.003321 $ K
C
C mu metal from mu-metal.com/technical-data.html ; sg= -8.7
m16  14000 -.0025 $ Si in MuMetal
      24000 -.0015 $ Cr
      25000 -.0040 $ Mn
      26000 -.1330 $ Fe
      27000 -.0025 $ Co
      28000 -.8100 $ Ni
      29000 -.0015 $ Cu
      42000 -0.045 $ Mo
C
C black polycarbonate for connector blocks (Use PRD case composition and sg.)
C sg= -1.26
m17  1001 -0.049942 $ H in 10% glass-filled polycarbonate
      6000 -0.680176 $ C
      8000 -0.223139 $ O
      14000 -0.046743 $ Si
C
C
C PARAMETERS
C
C mode p e $ Track photons and electrons
mode p $ Track photons only
C
```



```
rand gen=2 $ use if gen=1 random number period exceeded (gen=2 slower?)
C
dxt:p -243.84 -686 108.21 98 110 1 1e-6 $ dxt sphere around portal
dd 0.05 500 $
C
phys:p 1.5 0 0 0 0 J 0 $ simple physics above 1.5 Mev instead of 100 Mev
cut:p j 0.005 j j j $ E lower cutoff= 5 keV= below minimum detected by portals, PRDs
C *****
C
C SOURCE
C
sdef par=p pos= -243.84 -685.8 103.0 tr=5 erg=d1 $ point source tr5 +y from portal center
C
c Cs-137 x-ray and gamma lines (E > 25 keV)
si1 1 0.031817 0.032194 0.036304 0.0336378 0.037255 0.037349
0.661657 $
sp1 d 0.0204 0.0376 0.00352 0.00680 0.00215 0.00048
0.851 $
c There are 0.92195 photons per decay in above source
C
C
C TALLIES
C
c Use f8:p tallies, which do not allow fm; tally is for 1 source particle.
c For Cs-137 source, there are 0.92195 photons per decay
C
c F8 Photon+electron pulse-height distribution in cells of the 4 scintillators
c cells 12,22= RB,RT = closer to source
c cells 11,21= LB,LT = farther from source
c cells 11,12= LB,RB = lower and 21,22= LT,RT = upper scintillators
C
c Photon+electron coarse pulse-height distribution
c to get uncertainties in counts
f8:p 22 12 21 11 $ for uncertainties, Right Top first for tally fluctuation chart
e8 0 0.013 1.0 $ 3 E bins, 0, 0<E<13keV & E>13keV + total, for tally fluctuation chart
c E bin 3 is pulses >13 keV = counts
tf8 6j 3 j $ tally fluctuation chart for E bin 3 (E>13 keV)
fc8 photon(+electron) pulses, coarse E bins for uncertainties
C
c Photon+electron pulse-height distribution in cells of the 4 scintillators
f18:p 22 12 21 11 $ 4 scintillators, Right Top first for tally fluctuation chart
e18 0.0 1e-6 0.002 333i 0.670 1.0 $
c 335 equal E bins, 0.002 MeV each, 0.670-1 MeV
fc18 photon(+electron) pulse-height distribution in 4 portal scintillators
C
C RUN CONTROL
C
print -10 -30 -50 -70 -85 -110 -130 -140 -170 $
prdmp j 5e7 0 2 5e7
C
nps 1e9
```



APPENDIX D. ATTACHING PRDS TO HANDLES FOR SECOND-STAGE PRESCREENING

This appendix describes three of many suitable ways to mount a PRD on a long handle for second-stage prescreening. The attachment method should have no material thicker than a plastic bag covering or obscuring the PRD's detector. The first method we describe is to buy an adapter and extension handle sold as an accessory by the manufacturer of the PRD, in this case, Thermo Scientific. The second method is to alter a Thermo Scientific PRD adapter so it can be attached to a standard broom/mop handle. The third method uses the holster normally used to carry the PRD on a belt. The first two methods allow the PRD's operating buttons to be used and the display to be seen while the PRD is mounted. The holster method does not, but costs almost nothing, can be used with PRDs from other manufacturers, and is easy to do.

The Thermo Scientific extension handles are intended for other purposes, and most of them are too short, too long, or too heavy to use conveniently for second-stage prescreening. Part number 425067076, "Aluminum extension, length 1.2 m," is the right length. Attaching a PRD to it requires part number 425067078, "RadEye adapter with connector to the handle or extensions." The combination is usable, but the 078 adapter is heavy for something on the end of a stick that must be swung up and down thousands of times per shift.

The 078 adapter or any of several other adapters Thermo sells can be modified to attach a PRD to a broom/mop/extension-pole handle. The actual PRD holder of the adapter can be detached from the heavy unneeded parts and combined with an inexpensive adapter that accepts the standard Acme thread on broom handles using an angle bracket and 1/4-20 screws.³⁰ [Figure 7-19](#) is a pair of photographs showing two views of a PRD-ER mounted in such an assembly that NUSTL made.

The PRD and any mounting devices should be protected from potential radioactive contamination by covering them with a small plastic bag. (The plastic bag is not shown in the figure.)

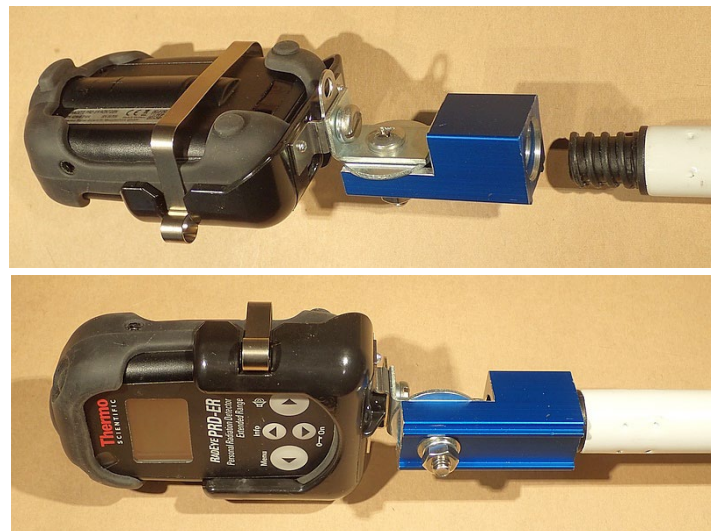


Figure 7-19 Modified commercial adapter used to attach a PRD to a handle with Acme thread

³⁰ www.bontool.com/threaded-brush-adapter-single-ear-82-278



If a different model of PRD is used, or resources are not available to acquire Thermo extension adapters, a simple and inexpensive way to mount the PRD on the handle is to use the PRD's holster. As shown in [Figure 7-20](#), first attach the PRD's holster to the end of the handle and then insert the PRD into the holster. In this example, the holster was attached using two "zip" ties passed through the holster's belt flap and holes drilled in the handle.

- Attach the holster to the handle so that the long dimension of the PRD is parallel to the handle.
- Insert the PRD into the holster with its detector side facing away from the handle.

This orientation in this method for attaching the PRD to the handle optimizes detection sensitivity, but it obscures the PRD's control buttons, so the PRD must be turned on before it is inserted for use. While this mounting method prevents prescreeners from seeing the PRD's display, they can hear the audible alarm, see the alarm light, and feel the alarm vibration through the handle. The PRD can be removed from the holster if it becomes necessary to read its display.



Figure 7-20 Holster method for mounting a PRD on a handle
Top—holster attached to handle with zip ties
Middle and Bottom—PRD in holster